RECLAMATION
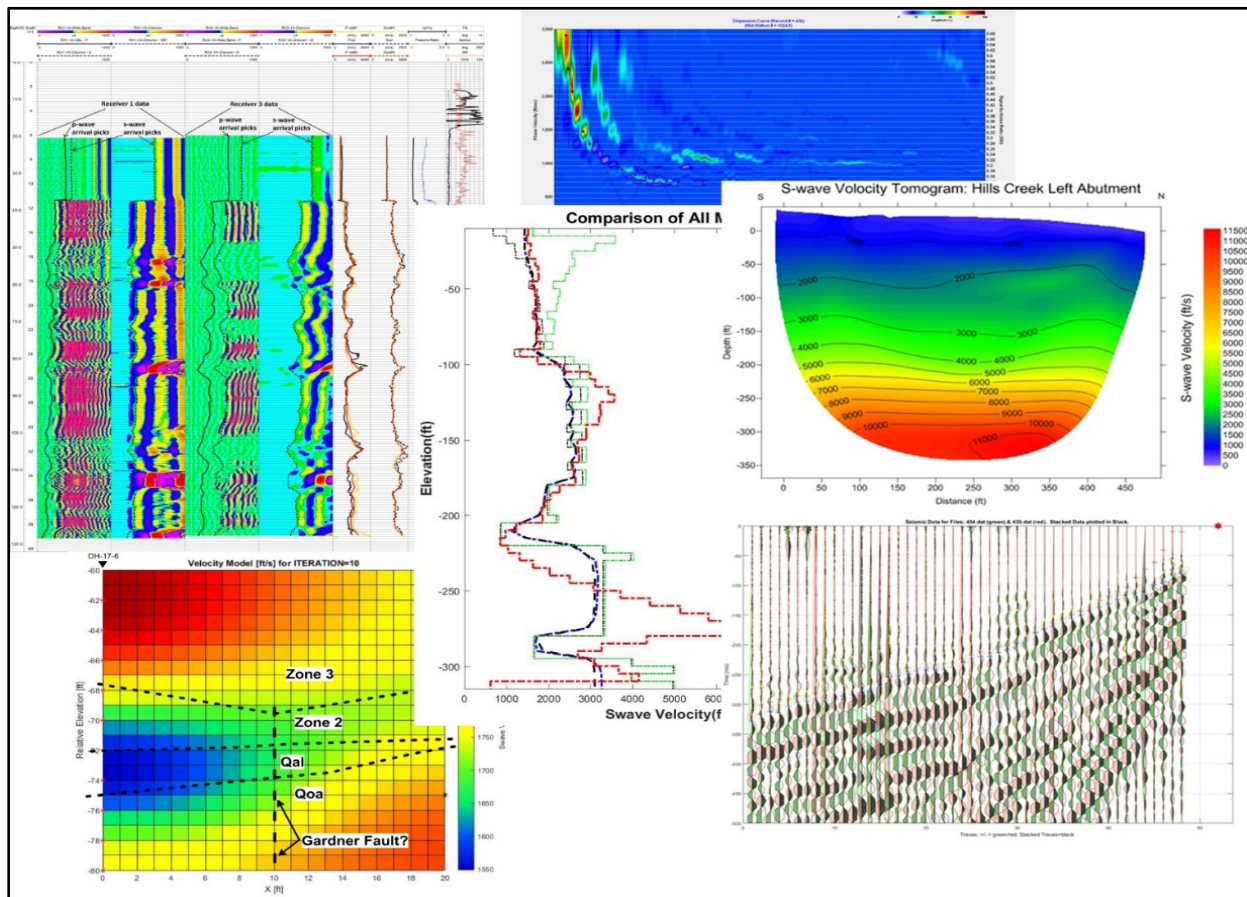*Managing Water in the West*

Technical Memorandum No. TM-85-833000-2019-01

Dam Safety Technology Development Project: Evaluation of Various Approaches to Obtaining Vs30 Values

A Cost-Effective Technique Selection Guideline

Denver, Colorado

United States Department of the Interior

BUREAU OF RECLAMATION
PO Box 25007
Denver, CO 80225-0007

November 23, 2018

MEMORANDUM

To: Program Manager, Dam Safety Office, Denver, CO
          Attn: 84-44000, (Lisa Krosley)

From: Justin B. Rittgers
          Geophysicist, Seismology, Geomorphology, and Geophysics Group (86-68330)

Subject: Transmittal of of Technical Memorandum 85-833000-2019-01 – Evaluation of Various
          Approaches to Obtaining Vs30 Values: A Cost-Effective Technique Selection Guide.

Attached is a copy of the subject final report for the Dam Safety Office Technology Development project Evaluation of Various Approaches to Obtaining Vs30 Values: A Cost-Effective Technique Selection Guide. The report presents an overview and evaluation of all relevant techniques currently available to Reclamation for assessing site-specific Vs30 values. The main objective of the study is to compare and evaluate all indirect Vs30 estimation techniques and all direct Vs30 measurement techniques (surface-based and borehole seismic techniques), in order to better understand the various accuracies, advantages, and limitations of each technique. The study is based upon the quantitative and qualitative comparisons of various co-located seismic surveys and Vs30 estimates conducted at various field sites from 2016 through 2018 at several Reclamation and non-Reclamation embankment dams. Results of these various surveys and corresponding new or otherwise updated Vs30 values are also presented, where applicable.

Finally, these results are utilized to inform and develop a set of practical Vs30 technique selection guidelines that can be used by project managers and engineers in order to optimize the tradeoffs between value of information and cost for future Dam Safety seismic risk analysis planning efforts.

If you have any comments regarding this TM, please contact Geophysicist Justin Rittgers, at 303-445-3010 or via e-mail at jrittgers@usbr.gov.
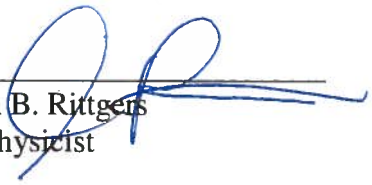
Attachment

cc: Electronic Copy cc recipients (w/ att. to ea)
        DSDaMS@usbr.gov
        OfficialRecordsArchive@usbr.gov
        krosley@usbr.gov -- Dam Safety Program Manager
        kknight@usbr.gov – Director, Security, Safety and Law Enforcement

rwoodruff@usbr.gov – Manager, Embankment Dams & Geotechnical Engineering (8311)
cslaven@usbr.gov – Manager, Embankment Dams & Geotechnical Engineering (8312)
jwormer@usbr.gov – Manager, Embankment Dams & Geotechnical Engineering (8313)
dwittwer@usbr.gov – Manager, Embankment Dams & Geotechnical Engineering (8314)
jgodaire@usbr.gov – Manager, Seismology, Geomorphology, and Geophysics Group
jball@usbr.gov, dliechty@usbr.gov, rmarkiewicz@usbr.gov -- Geophysicist, Seismology, Geomorphology, and Geophysics Group

Technical Memorandum
TM-85-833000-2019-01

Dam Safety Office Technology and Development Project Final Report:
Evaluation of Various Approaches to Obtaining Vs30 Values: A Cost-Effective Technique
Selection Guide
Denver, Colorado

Prepared by:

_____

Justin B. Rittgers
Geophysicist

11/21/18
Date

Peer Review by:

_____

Justin Ball
Geophysicist

11/21/18
Date

of the:
U.S. Department of the Interior
Bureau of Reclamation
Technical Services Center
Seismotectonics & Geophysics Group
Denver, Colorado

Mission Statements

The U.S. Department of the Interior protects America's natural resources and heritage, honors our cultures and tribal communities, and supplies the energy to power our future.

The mission of the Bureau of Reclamation is to manage, develop, and protect water and related resources in an environmentally and economically sound manner in the interest of the American public.

Acronyms and Abbreviations

1D	One-dimensional
2D	Two-dimensional
3D	Three-dimensional
4D	3D time-lapse
AGC	Automatic gain control
BPT	Becker penetration testing
CMS	Conditional mean spectrum
CPT	Cone penetration testing
DEM	Digital elevation model
DMO	Dipping move-out
FDM	Finite-Difference Method
FEM	Finite-Element-Method
FLAC	Fast Lagrangian analysis of continua
FMM	Forward Marching Method
FWS	Full-wave sonic
GMPE	Empirical ground motion prediction equations/Attenuation curves
GPS	Global positioning system
GRM	Generalized reciprocal method
HVSR	Horizontal-vertical spectral ratio
MAD	Median absolute deviation
MASW	Multi-channel analysis of surface waves
MCE	Maximum credible earthquakes
MMSFMM	Multi-Stencil Forward Marching Method
M	Earthquake/seismic magnitude
M_L	Local earthquake/seismic magnitude
M_O	Earthquake/seismic moment
M_w	Earthquake/seismic moment magnitude
NEHRP	National Earthquake Hazards Reduction Program
NGA	Next Generation Attenuation
NMO	Normal move-out
PGA	Peak ground acceleration

PHA	Peak horizontal acceleration
PSHA	Probabilistic seismic hazard analysis
Qal	Quaternary alluvium
ReMi	Refraction micro-tremor analysis
SA	Spectral acceleration
SASW	Spectral analysis of surface waves
SCPT	Seismic cone penetration testing
SPT	Standard penetration testing
s-wave	Shear-wave
TSC	Technical Services Center
UBC	Uniform Building Code
UHS	Uniform-hazard response spectra
USGS	United States Geological Survey
$V\varphi$	Phase-velocities
$V\varphi40$	Phase velocity of a surface-wave frequency component with wavelength of 40m
Vs	S-wave velocity
Vs30	The time-averaged s-wave velocity across a depth interval of 30 meters
VsN	The time-averaged s-wave velocity across a depth interval of N-meters
VSP	Vertical seismic profiling
$Z_{1.5}$	Depth to material exhibiting 1.5 km/s s-wave velocity
$Z_{2.5}$	Depth to material exhibiting 2.5 km/s s-wave velocity

I. Executive Summary

A. Problem

At Reclamation, Vs30 is one of many required input parameters that needs to be either measured or otherwise estimated for a variety of Dam Safety risk analysis studies. At Reclamation, Vs30 has most commonly been calculated using *in-situ* seismic velocity data collected with the use of extremely expensive boreholes installed to a minimum of 100ft (30m) depth, in some cases within hard rock. While boreholes and the data collected within them can serve valuable purposes at Reclamation, these *in-situ* data are not necessary for the sole purpose of obtaining an adequately accurate Vs30 value in most circumstances. Several other candidate techniques/approaches to obtaining a Vs30 each of these techniques have their own set of unique benefits, challenges, and technical limitations.

As a result, we are faced with the challenge of choosing the most cost effective yet sufficiently accurate approach to obtaining a Vs30 value. In order to address this challenge, this project aims to provide a comparison of the various techniques currently available for estimating Vs30, and to offer practical guidelines for selecting an ideal method or set of optional methods based on the project's needs and site conditions and geologic scenarios commonly encountered at Reclamation's Dams.

B. Scope and Approach

This project consisted of four main components:

1) Literature and data review
2) Conducting field investigations and gathering existing data to provide several co-located seismic data types, and associated Vs30 values using both direct and indirect techniques
3) Processing and modeling the acquired seismic data, and evaluating processing alternatives for improving accuracy of results of certain data types
4) Assessing other Dam Safety risk analysis needs beyond a single Vs30 estimate, and the value of information obtained from various approaches to obtaining seismic velocity information to help inform and reduce uncertainties related to specific failure modes commonly investigated by Reclamation.
5) Developing a set of practical guidelines for choosing the optimal approach for measuring or otherwise estimating Vs30, given various typical geologic scenarios, site conditions and typical data needs encountered at Reclamation structures.

Several datasets were collected specifically for this study, and existing datasets were utilized for this study where feasible. The direct Vs30 survey techniques evaluated for this study include: 1D cross-hole s-wave seismic profiling, 2D cross-hole s-wave seismic tomography, 1D spectral analysis of surface waves, 1D/2D multi-channel analysis of surface waves, 1D sonic logging, 1D surface-to-downhole vertical seismic profiling, 2D surface-based s-wave refraction tomography, alternative seismic data collection and analysis techniques. Additionally, the several indirect (non-seismic) techniques for estimating Vs30 were considered in this study, including:

penetration testing data correlations, geologic correlations, topographic slope correlations, and vertical extrapolation techniques for depth-limited datasets.

C.   Results

The main results of this study include the following:

- Quantitative and qualitative evaluations and comparisons of the various techniques are presented in the form of several case studies.
- Verification that any of the various site-specific seismic surveying techniques are valid candidates for obtaining a sufficiently accurate Vs30 value, if appropriate techniques are selected for specific site conditions.
- Several new or otherwise updated Vs30 values are provided for the various Reclamation facilities incorporated in this study, where applicable.
- Development of code to extend and improve the accuracy and reliability of various seismic data processing and modeling techniques applicable to Vs30 estimation. In addition to informing this study, these new data analysis and modeling codes have helped to improve Reclamation's capabilities for site-specific seismic characterization.
- A set of practical guidelines for Vs30 technique selection at soft soil sites, intermediate sites, and at hard rock sites were developed and are presented. These guidelines serve as a starting-point for engineers and project managers during initial project planning, budget estimations, and communications.

Contents

Figures

Tables

Technical Memorandum No. TM-85-833000-2019-01

Dam Safety Technology Development Project: Evaluation of Various Approaches to Obtaining Vs30 Values - A Cost-Effective Technique Selection Guideline

II. Introduction

A. Motivation and Problem

At Reclamation, Vs30 is one of many required input parameters that needs to be either measured or otherwise estimated for a variety of Dam Safety risk analysis studies. Some of the calculations involved in these various risk analyses include probabilistic seismic hazard analysis (PSHA) and the prediction of ground motions that are assumed to be significantly influenced by site-specific geologic conditions and associated response characteristics. The main interest here is to estimate how an embankment and its foundation are going to respond (e.g., linear elastic shaking versus structural failure and nonlinear plastic deformations or liquefaction) to various hypothetical strong motion events (e.g., dynamic loading of an embankment during various earthquake scenarios). In many cases, these estimated seismic loadings are used as dynamic inputs for running Finite-Element-Method (FEM) or Finite-Difference Method (FDM) simulations of earthen embankments, using software such as fast Lagrangian analysis of continua (FLAC) or LS-DYNA[1]. As a result, we are faced with the challenge of choosing the most cost effective yet sufficiently accurate approach to obtaining a Vs30 value.

In order to address this challenge, this study aims to provide a comparison of the various techniques currently available for obtaining a Vs30 value, and to offer practical guidelines for selecting an ideal method or set of optional methods based on a given project's needs and site conditions and geologic scenarios commonly encountered at Reclamation's Dams. This study provides a review of both indirect Vs30 estimation techniques and direct site-specific seismic surveying and Vs30 analysis techniques. These Vs30 techniques are then evaluated based on a series of comparisons of co-located data types and corresponding Vs30 values acquired or otherwise inferred at several earth embankment sites. This is done to gain an understanding of the accuracy and repeatability (and therefore reliability) of the various options for obtaining Vs30 values.

----

[1] Mention of trade names or commercial products does not constitute endorsement or recommendation for use by the U.S. Government.

B.   Scope and Approach

This study involved collecting or otherwise acquiring various co-located seismic surveying data types at several earthen embankment dam sites (e.g., a seismic refraction survey centered on a crosshole seismic triplet) and also utilized existing/historic Reclamation survey data in order to help minimize the cost of obtaining more expensive data types, such as those requiring boreholes. Overall, this project was designed and carried out in a way that would not only utilize existing Reclamation data where possible in order to serve the data needs of the study, but would also provide updated and valuable information for some of Reclamation's recent, current, and ongoing Dam Safety risk studies. Therefore, the results of this Technology Development project have the inherent added value of additional seismic data analysis being performed in support of recent and ongoing Dam Safety risk analysis efforts.

Existing Reclamation seismic data were utilized from previous surveys conducted at Huntington North Dam, Ridgeway Dam, Ochoco Dam, and Boca Dam. Additional seismic data were collected at various Reclamation structures to support this study, including at Prosser Creek Dam, Boca Dam, Granby Dike 3, Nimbus Dam, and Kicking Horse Dam. Various seismic surveys conducted at four USACE earthen embankment structures in Oregon were also utilized in this study, including Hills Creek Dam, Lookout Point Dam, Foster Dam, and Cougar Dam. Specifically, surface-based surveys, cross-hole surveys, downhole VSP surveys, and sonic logging surveys were performed at these USACE structures, helping to inform the comparisons and guidelines presented herein.

The main scope of this project can be summarized as follows:

1) Comparing various approaches to providing a Vs30 value by comparison of co-located seismic data/velocity models and resulting calculated Vs30 values
2) Assessing other Dam Safety risk analysis needs beyond a single Vs30 estimate, and the value of information obtained from various approaches to obtaining seismic velocity information to help inform and reduce uncertainties related to specific failure modes commonly investigated by Reclamation.
3) Developing a set of practical guidelines for choosing the optimal approach for data collection given various typical geologic scenarios, site conditions and typical data needs encountered at Reclamation structures.

This project consisted of four main components: (1) literature and data review, (2) conducting field investigations, (3) processing and modeling the acquired seismic data, (4) and presenting the results and findings in this report. Several datasets collected specifically for this study, and other datasets collected for other projects were utilized for this study. Due to the significant cost of drilling and borehole installations, data collection requiring new borehole installations specifically for this project were not performed. However, several suspension logging (also referred to as sonic logging or full-wave sonic) and downhole and crosshole seismic surveys performed for other projects (both Reclamation projects and inter-agency agreements between Reclamation and the US Army Corps of Engineers) were utilized for this study, in order to evaluate data from these techniques. A comparison of co-located borehole-based seismic surveying techniques (downhole, crosshole and suspension logging) has never been performed specifically for assessing their viability in providing Vs30, mainly because of the elevated costs

associated with borehole installations, and also because crosshole and downhole seismic surveys are typically utilized for cased boreholes installed in unconsolidated materials (e.g., within the embankment materials) while suspension logging surveys are typically utilized for uncased borehole intervals within consolidated materials and hard-rock environments.

The following seismic surveying and analysis techniques applicable to obtaining site-specific Vs30 values that were evaluated as part of this study include:

- 1D cross-hole s-wave seismic profiling
- 2D cross-hole s-wave seismic tomography
- 1D spectral analysis of surface waves
- 1D/2D multi-channel analysis of surface waves
- 1D full-wave sonic profiling
- 1D surface-to-downhole vertical seismic profiling
- 2D surface-based s-wave refraction tomography
- Alternative seismic data collection and analysis techniques

Additionally, the following indirect (non-seismic) techniques for estimating Vs30 were considered in this study:

- Penetration testing data correlations
- Geologic log correlations
- Topographic slope correlations
- Vertical extrapolation techniques for depth-limited datasets

C.   Products

The main products of this study that are presented in this report include the following:

- Evaluation of the above seismic surveying and indirect estimation techniques applicable to obtaining Vs30 values (e.g., difficulty, time/monetary costs, relative accuracy, etc.)
- Additional seismic velocity information and Vs30 results for each selected Reclamation structure incorporated in this study via new data collection and analysis
- A set of guidelines for most appropriate/cost effective Vs30 technique selection for various typical geologic scenarios and site conditions

Additionally, this study involved the extensive development of Matlab codes for processing and modeling various types of seismic survey data, and for calculating Vs30 values from resulting velocity models. Some of these codes developed during and in support of this study include seismic data filtering and pre-processing, automatic and guided first arrival picking, 2D layered crosshole velocity inversion using curved ray-tracing, 2D crosshole refraction tomography modeling, downhole VSP data reduction and analysis, 1D crosshole seismic data profiling analysis, and Vs30 calculations and figure generation. As a result, this study was carried out in a manner that has also helped to develop new Reclamation capabilities in supporting future Dam Safety needs.

III. Background

Characterization of the small-strain shear modulus and the shear wave velocity of soils and rocks is a key component of various seismic analyses, including site classification and site response analysis. The Next Generation Attenuation (NGA) ground motion prediction equations use the shear wave velocity of the top 30 m of the subsurface profile (Vs30) as the primary parameter for characterizing the effects of sediment stiffness on ground motions, as opposed to using more generic geologic descriptions (e.g., hard rock site, soft soil site, or intermediate site). As stated by Wair et al. (2012), "this should not imply that 30m is the key depth range for the site response, but rather that Vs30 is correlated with the entire soil profile. Several of the NGA models incorporate the depth to Vs equal to 1 to 2.5 km/s ($Z_{1.5}$ or $Z_{2.5}$) in addition to Vs30 to distinguish between shallow soil sites, average depth soil sites, and deep soil sites."

S-wave velocity can be either measured directly using site-specific geophysical testing, or by indirect estimation with the use of correlated indicators such as surface geology, topography, and conversion/correlation of penetration testing field data and undrained shear-strength lab measurements of soil and rock samples. Previous reviews of various geophysical methods for measuring the shear wave velocities of soils and rock have been presented by EPRI (1991) and Kramer (1996). Geophysical methods can be divided into two categories: invasive and non-invasive. Wair et al. (2012) present a review of various indirect Vs estimation techniques, and also discuss the use of depth extrapolation for calculating Vs30, where available data doesn't extend to 100ft below ground surface. "Unlike laboratory testing, geophysical tests do not require undisturbed sampling, maintain *in situ* stresses during testing, and measure the response of a large volume of soil," (Wair et al., 2012).

A.   Overview of Reclamation's Dam Safety Risk Analysis Approach

Reclamation and other federal/state dam safety/risk management groups are faced with the challenge of assessing and quantifying risk related to seismic/earthquake hazards at various structures, including earthen and concrete dams. Some of the various scenarios that are considered in these risk analysis efforts include estimating the probability of liquefaction, differential settlement, cracking and slope-stability failures due to large amplitude "shaking" of these structures and their foundations following an earthquake. In some cases, the focus of the analysis is to determine the extent of yield an earth embankment will experience in a strong motion event, in order to assess the impacts, if any, to rigid (i.e., "brittle") appurtenant structures, such as concrete spillway retaining walls or inlet and outlet works features.

Various steps of that risk analysis work-flow require the estimation of site-specific material properties that often control ground motion amplification of earthquake-generated energy (body waves) and the resulting "shaking" at the embankment/foundation contact. Reclamation (2015) provides an overview of the investigation of a dam and its foundation for seismic analysis, and selection of relevant methods for a particular dam. Here, a general order of tasks for evaluation and characterization of embankments and there foundations are provided as the following:

1) File Data review (Reclamation files)
2) Published data review (if relevant Reclamation files are missing or insufficient)
3) Surface-based investigations

       a. Ground-reconnaissance
       b. Topographic/geologic/geotechnical mapping
       c. Surface-based geophysical surveying
4) Subsurface investigations
       a. Test pits/trenches
       b. CPT/SPT/BPT testing
       c. Borehole geophysics
       d. Borehole instrumentation
       e. Vain shear testing
       f. Undisturbed sample shear strength testing

In the case of predicting seismic loading at one of the four locations (points A through D) identified in Figure 1, a Vs30 value is oftentimes required. Most often, this is the case for providing estimated peak horizontal acceleration at the ground surface (PHA, also called PGA), or for estimating other common parameters, such as the spectral acceleration (SA) for a particular response period, or the Arias intensity, which incorporates both the acceleration peaks and the duration of the peaks as an index of seismic energy at the site (Arias, 1970; Kramer and Mitchell, 2006). A more extensive overview of the various workflows, analysis products and applications of seismotectonic studies performed by Reclamation and related Dam Safety stakeholders is provided in Appendix A1 through A9 of Chapter 13 of Reclamation's 2015 *Design Standards No. 13: Embankment Dams* document. These appendices are also provided in Appendix A of this report, for the reader's ease of reference.

The following extensive excerpt taken from Chapter 13 of Reclamation's 2015 *Design Standards No. 13: Embankment Dams* document provides an excellent overview of the overall Dam Safety risk analysis (Reclamation 2015).

Here, Section *13.5.3 Seismic Loading* explains that:

> *Dam-safety practice at the Bureau of Reclamation has changed from the conventional standards-based approach, in which dams are required to withstand the most severe loadings possible at the site without failure, to the use of probabilistic risk analysis to inform dam-safety decisions (Reclamation, 2011). It is therefore necessary to evaluate a dam's performance and its likelihood of failure under both extreme earthquakes and smaller ones. It is not unusual for the greatest contributions to the risk to result from smaller earthquakes because of their much higher probability of occurrence, even if the probability of failure is much smaller in the smaller earthquakes.*
>
> *For higher level analyses, the Reclamation Seismotectonics and Geophysics Group usually provides the analysts with a Probabilistic Seismic Hazard Analysis (PSHA), and earthquake ground motions for selected return periods. The PSHA yields curves indicating the annual probability of exceedance for PHA and spectral acceleration for selected oscillation periods. For simpler seismic geotechnical analyses, this may be all the information that is required, but for more detailed analyses, the hazard curves are used to select ground motions that can be associated with a particular return period. This allows a risk estimating team to estimate the likelihood of dam failure resulting from loadings with various annual probabilities, so that an annual probability of dam failure can be calculated.*

For a given earthquake scenario; i.e., a given combination of fault geometry, area of fault rupture, the values of PHA and spectral acceleration, and the ground motions vary with location relative to the dam and foundation; refer to figure 13.5.3-1. Estimates of peak ground acceleration and/or ground motions are most often provided for a level rock outcropping or the surface of stiff soil, shown at point A in figure 13.5.3-1. However, the widely used Seed-Lee-Idriss simplified method for assessing liquefaction potential (described in later sections) requires as input the peak acceleration of the soil surface, at Point B, which can be slightly lower than to much higher than at Point A. The acceleration of the embankment crest, Point C, can be even higher because the shape of the embankment cross section affects the response. The simplified method was developed from 1D response analyses for level sites, so it is not strictly correct to apply it under a dam embankment. As needed, the Seismotectonics and Geophysics Group can provide hazard curves and earthquake records to represent motion at a soft soil surface (Point B), at the contact between soil and bedrock, or at a greater depth in the foundation, (Point D). One-dimensional response analysis using SHAKE or a similar program can use a record representing Point A, B, or D. FEM or FDM codes like FLAC usually require the ground motion to be put in at the base of the model, Point D. To obtain a record for Point D, usually, a rock-outcrop record (for Point A) is numerically "deconvolved" to account for the response of the material between the base elevation and the surface. Because of these differences, it is important for the engineer to clearly specify to the seismologist the desired location of the earthquake loadings, and for the seismologists to clearly identify the location to the analysts. The intended use of the loadings in analysis, and the nature of the structure being analyzed, should be communicated to the seismologists as early in the process as possible, so that the seismotectonic study can be tailored to the specific needs of the analysis.

Figure 13.5.3-1 referred to in the above passage is presented below in Figure 1.
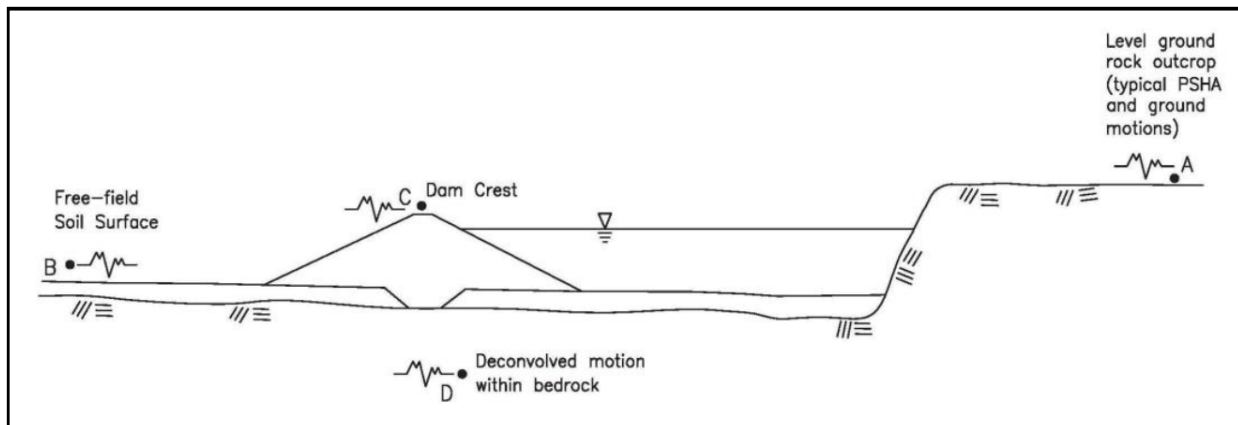
Figure 1 - Locations requiring specific ground-motion records (taken from Reclamation, 2015).

B.   Vs30 Overview

Vs30 is a time-averaged seismic shear-wave velocity within the upper-most 30 meters of the ground surface, and is defined as such regardless of whether the site is considered to be one of the following:

1) A "hard-rock site" (i.e., top of bedrock no more than 10 meters below ground surface)
2) An "intermediate site" (i.e., top of bedrock is more than 10 meters but less than 30 meters below ground surface)
3) A "soft- soil site" (i.e., top of bedrock is greater than 30 meters below ground surface)

Strictly speaking, regardless of the above listed geologic scenarios, the definition of Vs30 is an average of Vs for the uppermost 30m of materials below the ground surface of a given location or test site being characterized for seismic hazard analyses (e.g., to see how much the *ground surface* will shake at a given location in the advent of a hypothetical earthquake event). Therefore, a true Vs30 value calculated for an intermediate site with bedrock within the last few meters of the 30m depth interval will potentially be significantly higher than a similar site exhibiting identical geology, only with slightly deeper bedrock.

Both the National Earthquake Hazards Reduction Program (NEHRP) provisions and the Uniform Building Code (UBC) use Vs30 to classify sites according to type of soil for earthquake engineering design (NEHRP 2003; Martin and Diehl 2004; GEOVision 2018a). In this case, Vs30 is calculated for the depth interval corresponding to the ground surface and down 30m (e.g., the top of the Vs30 depth interval is assigned at point A shown in Figure 2). Accordingly, a "seismic site classification" rating is assigned to given study site based on the associated Vs30 value for sake of determining site-specific building requirements, as shown in Table 1:

Table 1 – List of Seismic Site Classifications A through F and their corresponding Vs30 value ranges and typical material type descriptions.

Seismic Site Class	Typical Material Type Descriptions	Vs30 Ranges
A	Very hard rock	Vs30 > 5,000ft/s
B	Hard rock/Some Weathering	2,500ft/s < Vs30 ≤ 5,000ft/s
C	Very Dense Soil and Soft Rock	1,200ft/s < Vs30 ≤ 2,500ft/s
D	Stiff Soil	600ft/s ≤ Vs30 ≤ 1,200ft/s
E	Soft Soil	Vs30 < 600ft/s
F	Poor Soils Requiring Site-Specific Evaluations	Potentially liquefiable soils, peat, high plasticity/high organic content clays, very thick soft/medium stiff clays

In the case of Reclamation and related Dam Safety stakeholders, the uppermost 30 meters of foundation material below a dam or critical structure is generally of interest, where the Vs30 value for this depth interval is a site-specific input parameter of interest for subsequent risk analysis and modeling efforts. Various predicted site response values and products, (e.g., estimated ground motion time histories, PGA/PHA values, etc.), are used as critical parameters for subsequent modeling of various potential failure modes, so both modeling efforts are directly or indirectly sensitive to the input Vs30 value. In this case, Vs30 is calculated for the depth interval corresponding to the embankment's foundation contact and down 30m (e.g., the top of the Vs30 depth interval is assigned at point B shown in Figure 2). In some cases, the foundation contact coincides with the ground surface immediately downstream of an embankment where Vs30 seismic surveys are most often conducted (e.g., point A coincides with point B in Figure

2), but most typically, there is an engineered backfill layer or berm layer that creates a new ground surface that is above the foundation contact at the downstream toe.
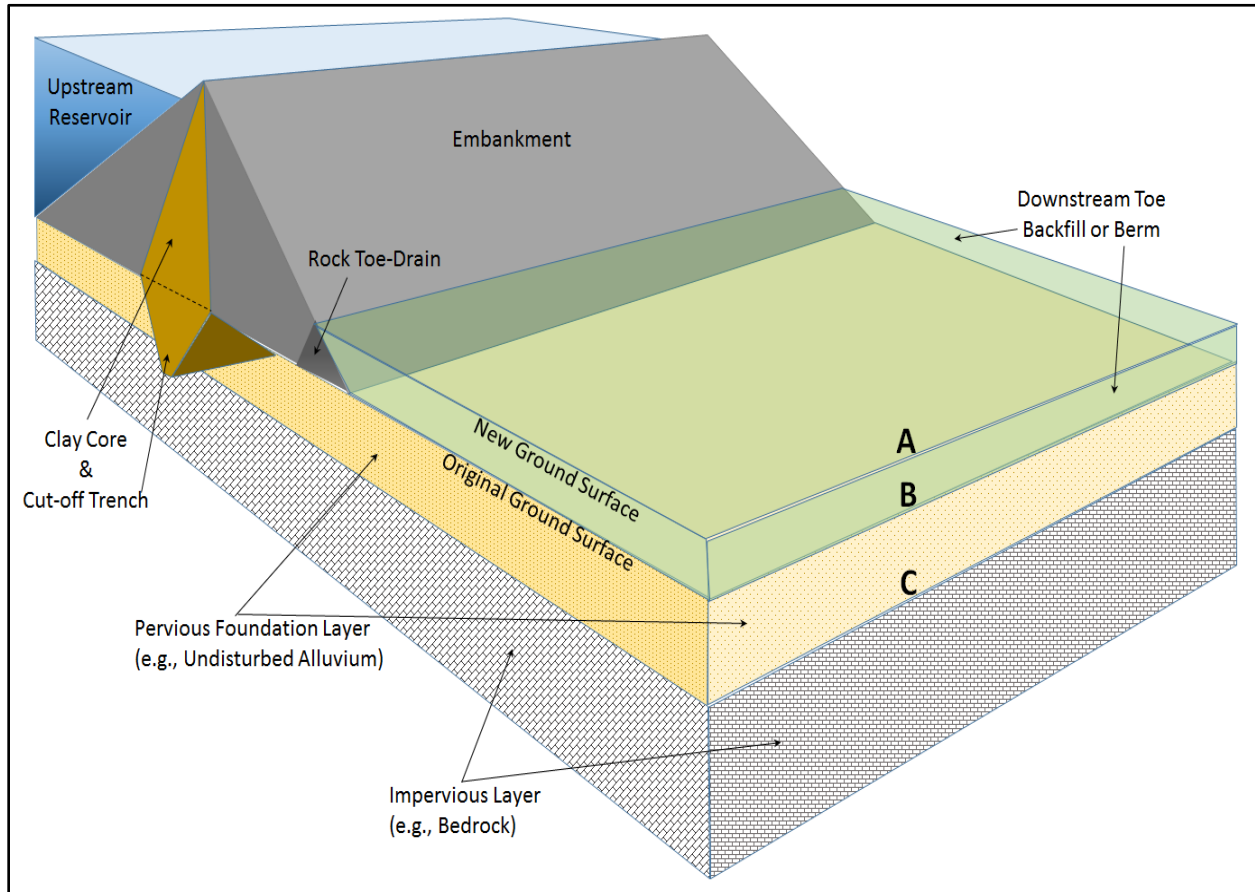
Figure 2 – Diagram showing a zoned earthen embankment schematic, with labels A, B, and C depicting three typical options for the top of a Vs30 depth interval, corresponding to the ground surface, the foundation contact, and the top of bedrock, respectively.

In other certain steps and approaches of the overall risk analysis workflow, moment magnitudes of an earthquake event are needed, which require estimates of the area of an earthquake rupture, the average displacement of the ruptured fault segment, and an estimate of the shear modulus of the rock involved in the rupture event. The shear modulus component requires estimates of both the rock's bulk mass density and shear wave velocity. In this case, a Vs30 value can be calculated for the uppermost 30 meters of bedrock that is assumed to be representative of the earthquake's focus rock, in order to inform an estimate of seismic moment. In this case, Vs30 is calculated for the depth interval corresponding to the top of bedrock and down 30m (e.g., the top of the Vs30 depth interval is assigned at point C shown in Figure 2). In each case of utilizing a Vs30 value, the main difference is the depth interval across which seismic velocity data are averaged.

C.   Vs30 Calculations

Historically, Vs30 has been used as one of the many estimated input parameters for calculation of predicted ground motions (and other required estimated seismic loading parameters) that are subsequently used as a dynamic (time-dependent) input forcing function (upward propagating strain field or particle acceleration time-series) applied to the lower boundary of a FLAC or LS Dyna model domain. Vs30 is calculated using the following equation:

$$Vs30 = \frac{30}{\sum_{i=0}^{n} \frac{h_i}{V_i}}$$ Equation 1

Here, the number 30 represents the total ~30m depth interval across which the Vs30 calculation is made, h_i is the thickness of the ith layer (i.e., depth interval), V_i is the modeled s-wave velocity of the ith layer/interval, and n is the total number of layers across the total ~30m depth interval. This equation can be viewed as 30m divided by the sum of all individually calculated seismic s-wave transmission times for all individual depth intervals (denominator) within the upper-most 30m of bedrock. Here, either one-dimensional (1D) vertical seismic velocity profiles can be used for calculating a Vs30 value, or two-dimensional (2D) or three-dimensional (3D) velocity models can be used. For the sake of calculating average velocities from a given 2D or 3D seismic survey's results, s-wave velocities obtained for each relevant depth can first be averaged using a simple arithmetic average as a function of depth (if needed, such as in the case of utilizing 2D tomographic velocity models). These depth-averaged s-wave velocities, along with the vertical separation (vertical grid node spacing) between recovered tomography parameters can then be used in the Vs30 equation above. The resulting Vs30 value represents an average of a large area of material properties that were imaged (e.g., several hundred feet of data coverage beneath a 2D tomography survey is averaged into a single 1D velocity profile versus depth, and these averaged values are then used to calculate a Vs30 value).

D.   VsN: A New Approach for Providing Averaged Vs values

At Reclamation, Vs30 values have typically been calculated from the top of bedrock and extending down 30 meters. Top of bedrock has generally been used as the top of the Vs30 depth interval, because ground motion prediction equations assume a free-field bedrock outcrop (subsequently deconvolved or simply divided by a factor of two to provide ground motions at the non-free-field condition across the bedrock/soil interface at depth). Furthermore, the associated depth to bedrock is ideally used to define the depth extent of corresponding FLAC/LS Dyna model domains (this bottom boundary of FLAC and Ls Dyna models is required to be within a "rock material" that will presumably only experience linear elastic deformations from input ground motion estimates).

However, in verbal communication with Reclamation seismologists, it was stated that "in the case of very deep bedrock that would result in a large FLAC or Ls Dyna model domain and associated wave propagation computational costs, any velocity equal to or above 2000ft/s is a better choice for defining the top of a Vs30 calculation's depth interval, as s-wave velocities above this nominal value will not make a significant difference in the calculated free-field ground motions and other parameters of interest (e.g., moment). So, we really just need to know

if there is any material with a 2000ft/s (~610 m/s) s-wave velocity or greater beneath the structure, and how deep that 2000ft/s s-wave velocity contour is below the structure. FLAC/LS Dyna models can simply assume this material will only experience linear elastic deformations, and will allow modelers to limit the required depth extent of the model domain and corresponding computational costs without affecting forward modeling results significantly," (Wood, 2018).

Therefore, the process of calculating an average Vs30 value for use in ground motion predictions requires the selection of an appropriate top of the averaging depth interval that may or may not correspond to actual top of bedrock (e.g., according to borehole geologic log data). Based on correspondence with Wood (2018), the following three scenarios exist for top of depth interval selections:

1) A steep vertical gradient in s-wave velocity within a tomography model (or 1D velocity profile) that is known to be associated with the top of bedrock should be used as the top of the averaging depth interval, if located within a "reasonable depth" below a dam's foundation contact.

2) Actual top of bedrock is too deep to be practical for subsequent modeling, and so the 2000ft/s s-wave velocity contour should be selected as the top of the averaging depth interval.

3) Neither bedrock nor the 2000ft/s s-wave velocity contour is within a "reasonable depth" below the foundation contact, and so an arbitrary depth should be agreed upon for the sake of establishing the depth extent of FLAC or Ls Dyna model domains, for average s-wave velocity calculations, and for corresponding ground motion prediction calculations.

Furthermore, despite the fact that ground motion equations still refer to this input parameter as Vs30, it was expressed in recent verbal communication with a Reclamation seismologist that "an actual Vs30 value is really only needed for liquefaction potential studies, and is otherwise an antiquated term that should generally not be used in ground motion prediction equations. A smaller depth interval (i.e., less than 30 meters) would likely be more appropriate for use in calculating free field ground motions," (Wood, 2018). Clearly, this process of selecting an appropriate depth interval for providing time-averaged s-wave velocities for subsequent use in ground motion prediction equations is a subjective process.

Therefore, a new generalized approach has been developed at Reclamation to provide seismologists with a range of time-averaged s-wave velocities to select from, as considered optimal for their use. Here, the range of averaged Vs values corresponds to a range of depth intervals that now extends from only 1 meter to 30 meters below the desired interval top (e.g., from "Vs1" to "Vs30"). The interval top can be placed at points A or B or C, as labeled in Figure 2, depending on subsequent needs by seismologists and engineers. The Vs30 equation from above is still implemented, only now for various depth intervals, such that

$$VsN = \frac{N}{\sum_{i=0}^{n} \frac{h_i}{V_i}}, \ (1 \leq N \leq 30). \qquad \text{Equation 2}$$

Here, N is any depth interval of choice. The same equation can be used to calculate "VsN" from 1D models, where each layer of the MASW model is already defined by a unique thickness and s-wave velocity (no depth-averaging of velocities required). Depending on the nature of the velocity model being used in these VsN calculations, the s-wave velocity model may need to be extrapolated at depth, in order to provide the required model coverage across the maximum depth interval of 30m.

This new approach now provides a curve of time-averaged s-wave velocities as a function of depth interval. An example of this approach taken from Kicking Horse Dam in Montana is presented in Figure 3, were Vs5, Vs10, Vs20 and Vs30 are indicated on the plot, for convenience. In this example, the monotonic increase in VsN values is primarily due to the use of a smooth refraction tomogram that commonly exhibit a smooth vertical gradient in velocities. Different VsN curves would be achieved using different data types and velocity models (e.g., 1D layered crosshole seismic velocity profiles). This approach to providing a range of time-averaged s-wave velocities, as opposed to a single Vs30 value, helps to standardize the data product provided by geophysicists, and will allow seismologists to use their own subjectivity in the selection of a best-suited VsN value for use in ground motion predictions.

When appropriate and feasible, this range of VsN values will be provided for depths corresponding to each of the three scenarios listed above (from top of actual bedrock, from the 2000ft/s s-wave velocity contour, or from the foundation contact). In the case of large lateral variations in tomographic velocity distributions, likely due to complex bedrock topology or otherwise non-horizontal or layered geology, a subsection of velocities will be selected for VsN calculations (in order to avoid unnecessary lateral smoothing and biasing of averaged Vs values).
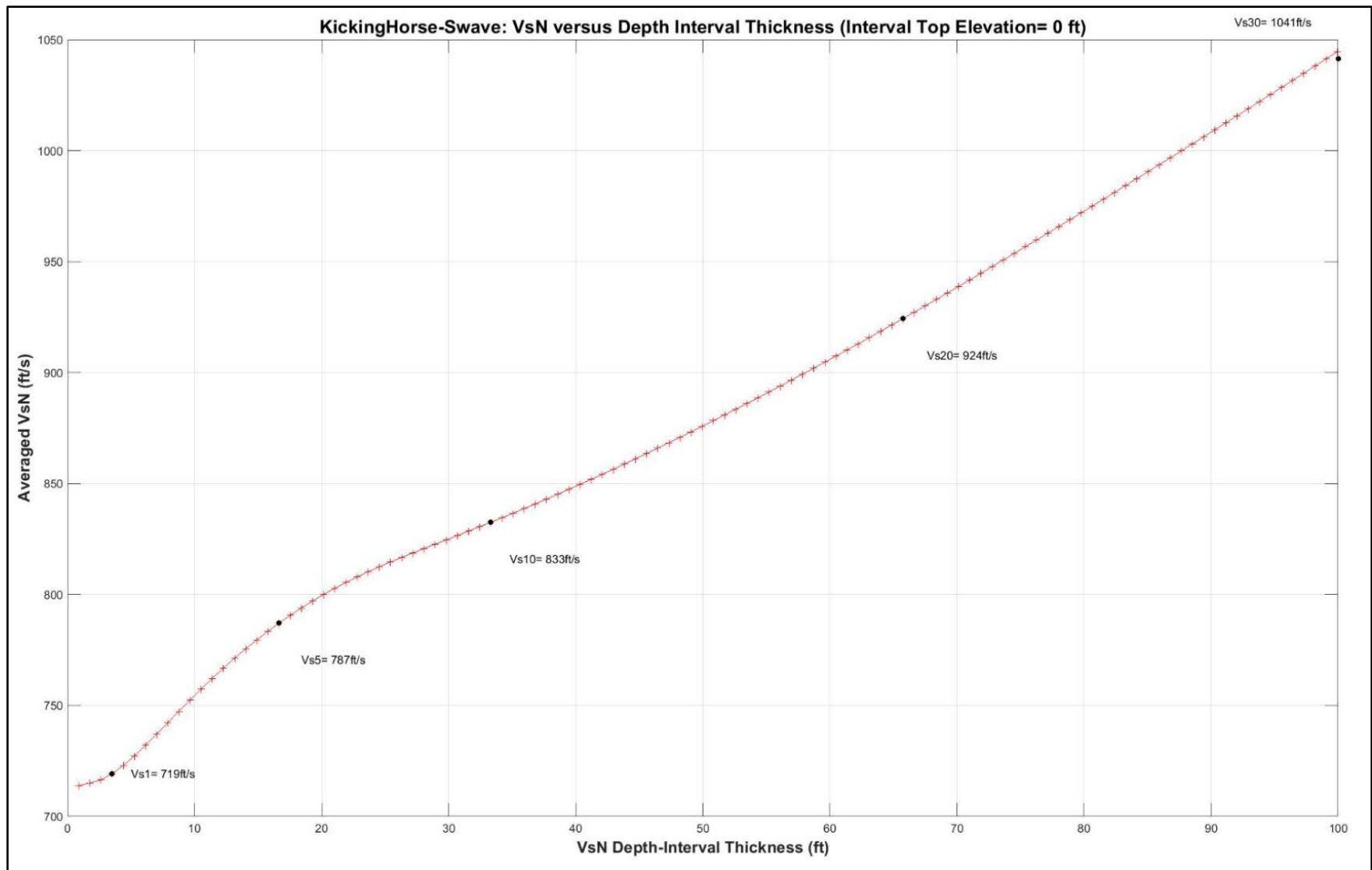
Figure 3 – A plot of VsN values calculated for depth intervals ranging from 1 meter to 30 meters below ground surface at Kicking Horse Dam, MT using seismic s-wave velocity tomography results. Vs1, Vs5, Vs10, Vs20, and Vs30 values are indicated along the curve.

E.   Reclamation Needs beyond a Simple Vs30 Value

It is important to keep in mind that while the various techniques evaluated in this study are indeed demonstrated as being useful for producing a single Vs30 value, there are inherent added values and limitations in the various survey types and corresponding analyses. Specifically, direct measurements of seismic velocities can be utilized to calculate elastic moduli of materials in conjunction with material density information obtained from either downhole logging (e.g., neutron density logging) or as measured on core samples or otherwise estimated. These various elastic modulus values (e.g., bulk and shear moduli) are key input parameters for constructing realistic finite difference models, such as FLAC models of embankments, where each embankment zone or feature may be comprised of vastly different material properties that behave in drastically different ways when excited by seismic loadings.

As a result, the various direct seismic velocity measurement techniques discussed in this study provide different information that may or may not be of added use, depending on the primary failure modes of concern and the corresponding eventual needs for subsequent risk analyses in a given scenario. For example, high-resolution crosshole seismic techniques may provide the needed accuracy at great depths, providing velocity measurements within specific soft layers and thin-beds of concern (e.g., in a liquefaction study, to identify potentially liquefiable layers/failure planes). On the other hand, a 1D crosshole seismic profile will only provide information at one location, and will not help to inform the overall distribution of seismic velocity within complex geologic conditions across an entire study area. In these scenarios, 2D seismic tomography and 2D MASW profiling would offer the benefit of greater spatial data coverage and corresponding velocity information (e.g., imaging lateral variations in velocity associated with stratigraphic structures or related to complex foundation contact at an abutment slope, or across a fault shear zone). This added spatial coverage is obtained at the expense of resolution of thin bedding at depth (tomography results in a smoothed or averaged velocity model that lacks resolution of thin beds/layers otherwise captured in focused downhole and cross-hole surveys).

In either case, any of these techniques are frequently adequate for calculating a Vs30 value, but each technique will provide different information that may affect its value as a survey option for a specific study location.

Assessing liquefaction potential of a soil column or layer is another use for Vs in common Reclamation risk analysis efforts. Measurements of shear-wave velocity involve very small strains, whereas liquefaction is a large-strain phenomenon. Also, Vs is relatively insensitive to changes in relative density, but predicted liquefaction resistance is very sensitive to variation or small measurement errors in VS. Therefore, one should select the most accurate methods for use of Vs in liquefaction studies .The following excerpts taken from Reclamation (2015) address the use of Vs in liquefaction studies in more detail:

> *"Vs of a granular soil generally increases with increasing density, as does the soil's resistance to liquefaction. Empirical correlations have been developed between Vs measured in situ and liquefaction resistance (Andrus and Stokoe, 2000; Andrus et al., 2004; Kayen et al., 2013). The shear-wave velocity is generally measured either between drill holes (cross-hole measurements), or from*

the surface to a downhole receiver, which may be incorporated into a cone penetrometer (Robertson et al., 1992). Cross-hole measurements are preferred for their greater accuracy but they are more expensive and time-consuming because of the need for multiple cased holes at each location. There have been advances in surface methods that have increased acceptance of surface geophysics for detecting liquefiable materials, notably Multichannel Analysis of Surface Waves or MASW (Park et al., 1999), but cross-hole measurement is still the primary method for Reclamation dams.

IV. Overview of Common Survey & Analysis Methods for Estimating Vs30

Since Vs30 is a time-weighted average of s-wave velocities within the upper-most 30 meters of the subsurface, those s-wave velocities generally need to be known in order to facilitate the Vs30 calculation. Therefore, we face the inherent challenge of either implementing some seismic survey technique for acquiring those required velocity data, or otherwise implementing a technique for estimating a Vs30 value. A very basic overview of seismic surveying techniques for measuring Vs is provided in Appendix E2 of Chapter 13 of Reclamation's 2015 *Design Standards No. 13: Embankment Dams* document (Reclamation 2015). This section aims to provide a more detailed overview of these and additional techniques for measuring or otherwise estimating Vs for sake of providing a Vs30 value.

At Reclamation, Vs30 has most commonly been calculated using *in-situ* cross-hole shear-wave profiling survey results, which is a specific seismic surveying technique that typically requires three boreholes (a bare minimum of two holes required) be installed to a minimum of 100ft (30m) depth. If the foundation material consists of hard-rock (or bedrock is shallow across a project site), a single borehole is typically drilled and left open in order to accommodate seismic/acoustic wireline instruments (e.g., full-wave sonic logging) to obtain a Vs30 value. Installation of these boreholes is very expensive, and while cross-hole shear-wave testing is the "tried and true" approach, it may not be necessary in order to obtain an adequately accurate Vs30 value at every dam site.

There are several other candidate techniques/approaches to obtaining a Vs30 value for a given site that don't require the installation of three boreholes, and they are all significantly less expensive (due to less or no required drilling). Some of these include the following:

1) Single-hole techniques such as surface-to-borehole vertical seismic profiling or suspension logging (e.g., full-wave sonic logging)
2) Surface-based and non-invasive approaches such as shear-wave refraction tomography, spectral analysis of surface waves (SASW), multi-channel analysis of surface waves (MASW), and Refraction micro-tremor (ReMi) analysis of surface waves
3) Correlation analysis/extrapolation techniques using pre-existing data, such as geologic logs, standard penetration testing (SPT) data, Becker penetration testing (BPT), cone penetration testing (CPT) data, and lab tested shear-strength of soil samples. Additionally, the US Geological Survey (USGS) has recently developed a ground-surface

topographic slope proxy for Vs30 (e.g. higher terrain slope angle indicates the presence of more stable material/harder rock and thus higher Vs30 value).

In the following sections, these various seismic surveying techniques for informing Vs30 calculations are presented, and non-seismic approaches are additionally discussed.

A.   1D Crosshole Seismic Profiling

Crosshole seismic surveys are typically performed using a "crosshole triplet," which consists of three boreholes placed in a straight line and with equal spacing (nominally 15 to 20ft between holes). The seismic source is placed in one of the outer boreholes of the triplet, and receivers are placed in the other two boreholes (see Figure 4). For measuring s-wave velocities in soils, the borehole spacings are typically 10 to 15 feet. Larger spacing is typically used for deeper boreholes or in instances where materials exhibiting faster seismic velocities are expected to be present between the boreholes, adversely affecting the precision of shear wave velocity calculations (due to errors in arrival time picks). Greater inter-borehole spacing is also advantageous if excessive grout loss into the formation is expected, as this will usually increase the annulus material's s-wave velocity within intervals of excessive grout intrusion and results in a corresponding bias in calculated velocities for those intervals. Greater borehole spacing is also advantageous in the presence of fast material (e.g., hard rock), because the seismic propagation time between the source and receiver becomes very small (e.g., only a few milliseconds), and any errors in first arrival time picks can lead to significant errors in the calculated velocity.

The seismic source and receivers are maintained at approximately equal elevations during a crosshole shear-wave survey. If the ground surface at the crosshole site is fairly flat, the desired geometry is achieved by lowering the source and both receivers the same amount for each measurement. Data are acquired at numerous depths, usually at an equal depth increment.

Seismic s-wave crosshole profiling data are typically acquired at 2.5 or 5-foot depth increments, with data coverage starting at or slightly below ground surface and extending to the bottom of the shallowest borehole. A down-hole shear-wave hammer or vibratory seismic source can be used to generate seismic s-wave energy. An impactive shear-wave hammer source consists of a central cylinder that is locked inside the borehole casing with a pneumatically-powered spring centralizer, and a sliding arm with reversible impact directions that is manually controlled using the suspension cables. The down-hole hammer is designed to preferentially generate shear-wave energy in the vertical plane (SV-waves).

The hammer triggers a seismograph that then records data from borehole receivers that are placed in other boreholes at the same depth. The transmission time for induced s-waves (or p-waves) is measured for each test depth. These transmission times (e.g., first arrivals of energy) and corresponding inter-borehole distances are used to calculate the seismic wave velocity of material between the boreholes at each test depth (e.g., using arrival times of each source and receiver pair).
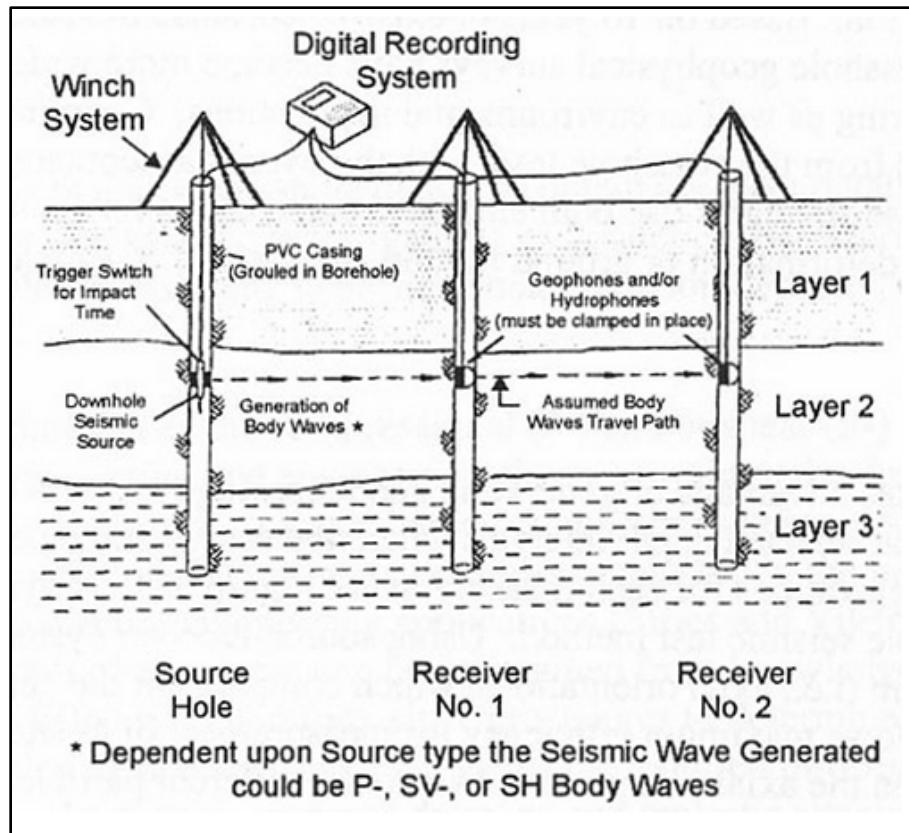
Figure 4 - Schematic of a cross-hole seismic survey for measuring *in-situ* Vs.

In the case of any seismic survey that utilizes a borehole for placing either a downhole receiver or transmitter device (or combination), a precise mapping of the 3D borehole path must be performed for each borehole utilized. Borehole deviation surveys are typically conducted at the time of a downhole or crosshole seismic survey, in order to account for borehole deviation and to calculate absolute depth and source-receiver offsets of each geophysical measurement. Accurate source-receiver offsets are critical in calculation of accurate corresponding velocities (i.e., source-receiver offset divided by wave travel time). Deviation surveys are especially important for crosshole seismic profiling surveys, due to the relatively close proximity of the boreholes, where a small error in source-receiver offset can result in a relatively significant error in the calculated velocity. Furthermore, boreholes that deviate towards each other cause a problematic increase in sensitivity to minute errors in arrival time picks. Therefore, deviation surveys are also important for evaluating data integrity and confidence levels in measured velocities versus depth. Examples of the results of deviation surveys are presented in Figure 5 and Figure 6, where Figure 5 shows the deviation path of a single borehole, and Figure 6 shows the deviations of three boreholes comprising a borehole triplet (Liechty 2018).
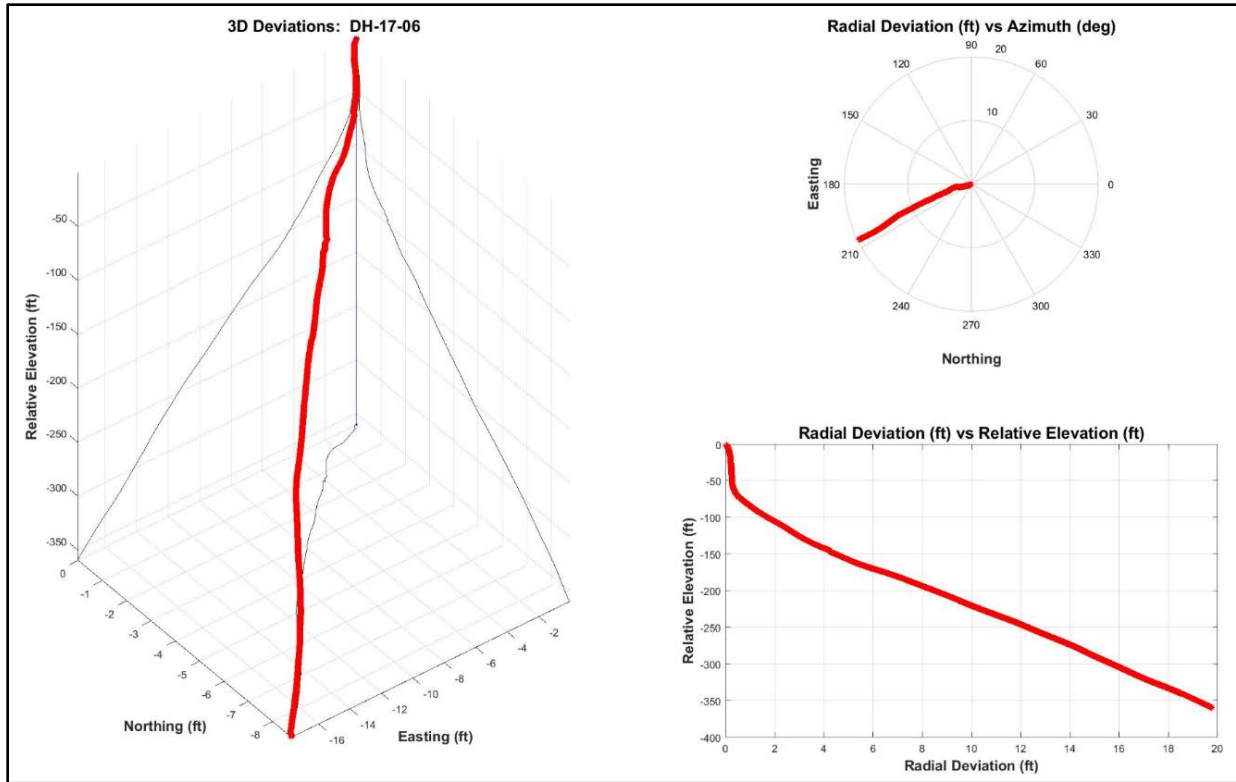
Figure 5 – Results of deviation survey showing 3D relative deviation versus depth along a borehole path drilled at Cougar Dam, Oregon.
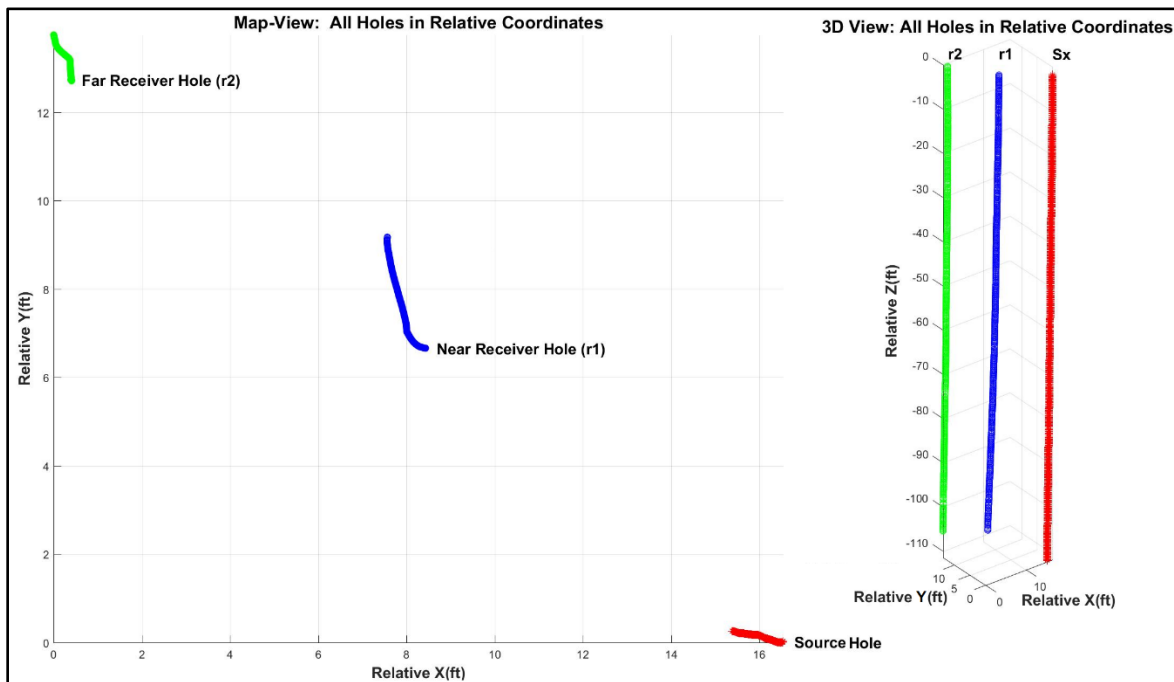
Figure 6 - Results of deviation surveys showing 3D relative deviations along three borehole paths drilled through the crest of Granby Dike #3, Granby Colorado.

B.   2D Crosshole Seismic Tomography

Beyond 1D crosshole seismic profiling, 2D crosshole tomography analysis approaches offer a more robust approach to measuring the distribution of seismic velocities between a given borehole pair. While this approach to data collection and analysis provides a 2D velocity model, as opposed to a 1D vertical velocity profile, results can be depth-averaged to provide the necessary information for calculation of an accurate Vs30 value.

When using the standard assumption of direct-transmission (straight raypaths) in crosshole data analysis, concerns arise with regards to the validity of calculated velocities for data collected within particularly slow depth intervals in the presence of immediately adjacent fast intervals or layers above or below the slow layer. Here, crosshole arrival times are quite possibly affected by refraction of energy along the interface of the adjacent fast layer/material, resulting in an earlier arrival time and a corresponding faster velocity that is not representative of the slow layer's true seismic properties. This error is due to the assumption of direct transmission of crosshole wavefronts between boreholes which is violated in the case of refracted arrivals. As a result, a potentially problematic layer that may be susceptible to non-plastic deformation or liquefaction could be under-characterized or even missed entirely, and an inappropriately high factor of safety could result. This geologic scenario is fairly common directly on top of bedrock, where low velocity alluvial deposits are often encountered at Reclamation sites.
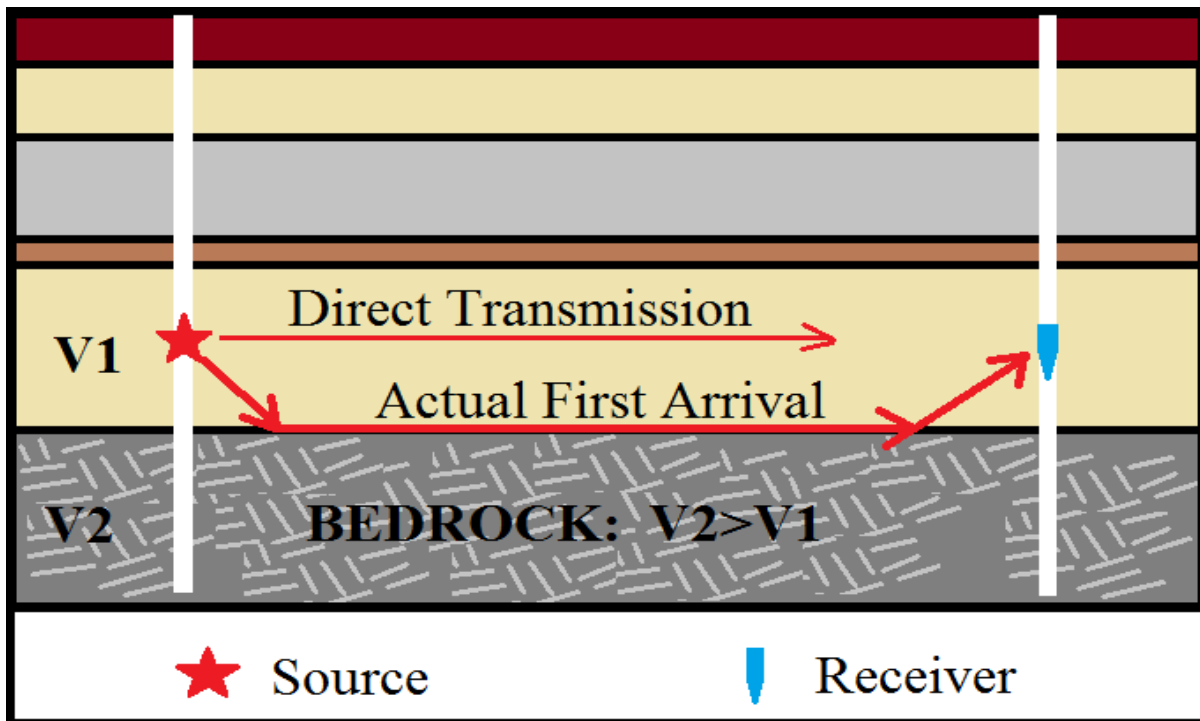
Figure 7 – Schematic of energy refraction along the interface between a relatively slow and fast layer, resulting in earlier first arrivals than energy that propagates directly through a relatively slow layer (direct transmission), as is assumed in standard 1D crosshole seismic profiling data analysis.

Forward Modeling: 4-Layer Refraction Analysis

One approach to addressing this issue involves the use of a simple forward modeled four-layered refraction analysis to estimate the true velocity of a relatively slow layer. An issue of using this four-layer forward modeling approach is that there is an inherent tradeoff between layer thickness and layer velocity that results in non-uniqueness of calculated arrival times. This non-uniqueness can be somewhat overcome by estimating and fixing the layer thicknesses based on other downhole measurements to constrain lithologic interfaces and layer thicknesses (e.g., Natural Gamma and Neutron Density log data). Even with layer thicknesses fixed, there is still an issue with non-uniqueness in that the analyst can vary the layer velocities and still obtain the same forward-calculated first arrival times. This source of non-uniqueness can be reduced by assuming that the fastest calculated velocity using the standard crosshole analysis approach is in fact the true velocity for that one layer. Then the velocities of overlying slower layers can be back-calculated sequentially moving across in stratigraphy until the slow layer's velocity is obtained. This approach should yield a reasonable correction to the calculated velocity of the slow layer, but is relatively arduous and not always feasible.

Inverse Modeling: 2D Layered Velocity Crosshole Analysis

A second option for addressing the issue of refraction in crosshole profiling data analysis involves the use of 2D crosshole layered velocity inversion approach that aims to model all picked arrival times simultaneously, as opposed to building a simple 4-layer refraction model as described above. In support of the second phase of data analysis for Ridgeway Dam, extensive Matlab code was developed to perform this layered velocity inversion approach to crosshole data analysis. This finite element inversion software was developed specifically for this project, and utilizes a ray tracing method called the Multi-Stencil Forward Marching Method (MSFMM, or FMM) in conjunction with smooth model weighting with a large x/y smoothness ratio applied (x-direction smoothness enforced, y-direction roughness allowed to produce layered velocity structure in recovered 2D model). This approach allows for the imaging of complex horizontally layered velocity structures while accounting for the refraction of rays through faster velocity regions of the 2D model space.

Specifically, this code was developed to allow for 2D inversion of standard crosshole data that is not collected in an ideal tomographic sense (there is no overlap of raypaths due to the standard cross-well transmission acquisition geometry typically implemented in crosshole seismic surveys). Here, the bending of rays permitted by FMM approach to ray tracing allows for rays from adjacent tests to interact and help constrain an accurate vertical distribution of layer velocities. A comparison of results obtained using the two approaches (four-layer refraction forward modeling and 2D ray-tracing inversion) for the deeper of the two slow layers of concern are presented in Table 4.

Inverse Modeling: 2D Crosshole Velocity Tomography

In addition to standard 1D crosshole seismic profiling and the 2D horizontally layered inversion approach developed for Ridgway Dam crosshole data analysis, a standard 2D crosshole seismic s-wave tomography survey can be performed at depth between two or more boreholes, in order to better image complex non-continuous or tilted geologic layers, or amorphous targets located

between the boreholes. Here, crosshole seismic data are collected between two boreholes using survey geometries that result in overlapping raypaths, as depicted in Figure 8. Similar to surface-based seismic refraction tomography, this overlapping of wave propagation paths (raypaths) between each unique source-receiver pair allows for high resolution tomographic reconstruction of complex non-layered velocity structures. Example results of these various crosshole seismic techniques are presented and discussed in more detail below.
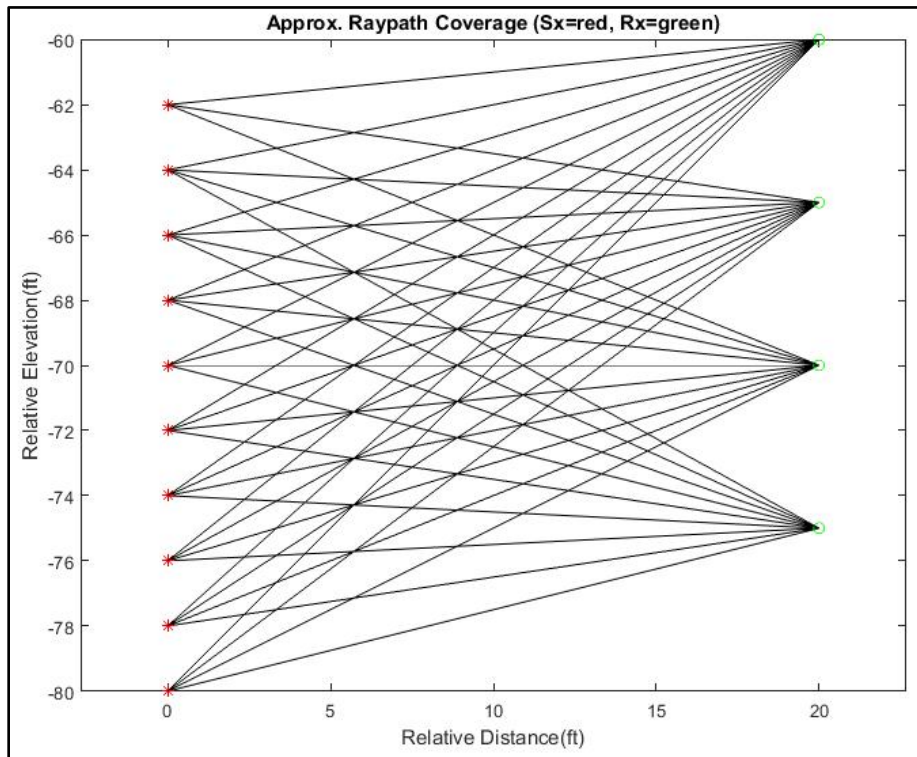
Figure 8 – Plot of approximated raypath coverage for crosshole tomography data collected at Prosser Creek (Rittgers 2017c). Here, data were collected between DH-17-6 (source hole) and DH-17-8 (far receiver hole).

C.   1D Surface-to-Downhole Vertical Seismic Profiling (VSP)

VSP is a relatively simple approach to measuring the vertical distribution of p-wave and s-wave velocities along a single borehole path. S-wave downhole surveys are typically conducted with a sledge hammer impacting either end of a weight-coupled shear-plank. The shear-plank is typically weighted with a field vehicle to maximize mechanical coupling with the ground surface, and the plank is typically placed with an offset of nominally 30ft or less from the borehole (this borehole-to-source offset helps to prevent propagation of seismic energy down the borehole casing). These s-wave signals are recorded at various depths within the borehole with one or more horizontally-polarized borehole geophone sensors (see Figure 9). Each s-wave downhole survey typically utilizes a two to five-foot borehole receiver depth interval, resulting in correspondingly thick pseudo-layers (velocity intervals) defined by the depths of each adjacent geophone placement within the borehole.
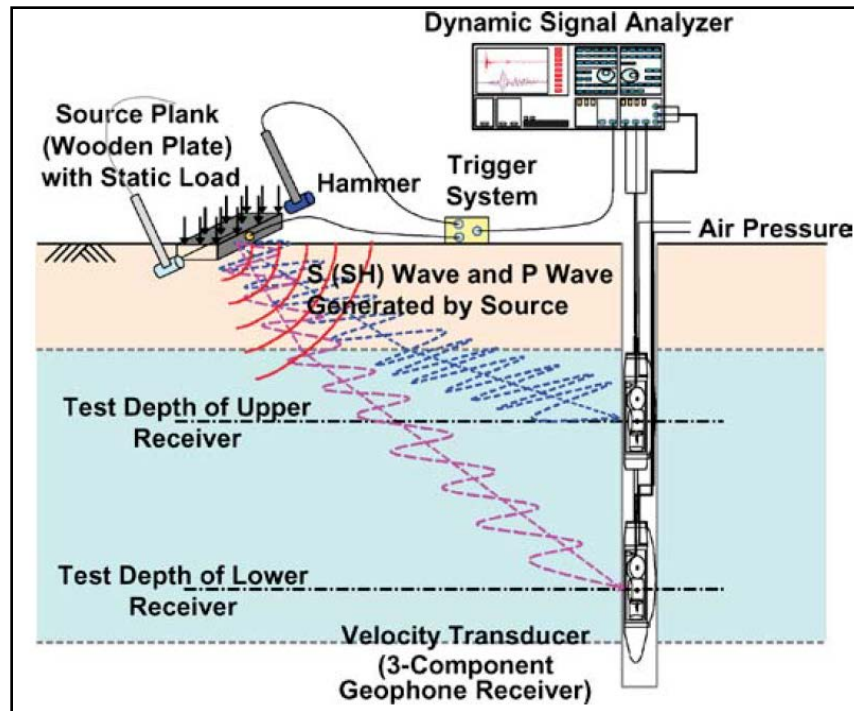
Figure 9 – Schematic of a typical downhole seismic s-wave survey conducted using two borehole receivers simultaneously (Kim et al., 2017). The same data can be collected with a single borehole receiver but requires twice the number of source shots.

The left-hand plot of Figure 10 shows VSP s-wave data plotted as variable area "wiggle traces," and the right-hand plot shows the same (stacked) data plotted using a color scale to represent trace amplitudes and polarities (+ is yellow, - is blue). Each plot presents seismic data with the vertical axis representing the trace/test number, and the horizontal axis representing time (ms). On the left-hand plot, two opposite polarity shots (+ is green/- is red) are recorded at each downhole receiver depth and reverse-stacked (stacked data plotted in black) to help amplify the shear-component of energy (first-arrival picks indicated with red lines) while minimizing (stacking out) contamination of faster [converted] p-waves (indicated with blue lines on left plot) that are generally characterized by having the same polarity regardless of the source impact direction.
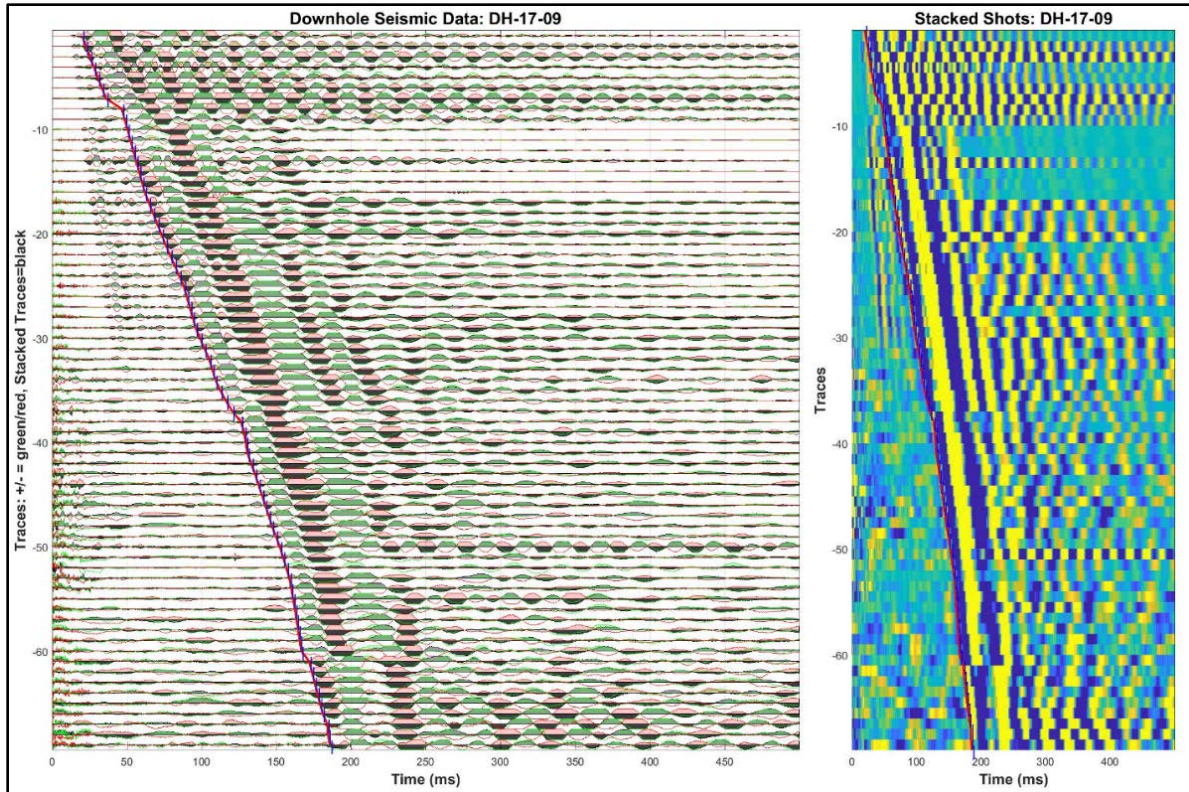
Figure 10 - Figure shows a composite shot record plotted as variable area wiggle traces (left) and as a 2D color contour matrix plot (right) for downhole seismic s-wave profiling data collected in a borehole at Cougar Dam, Oregon (Rittgers 2018).

The red line in each plot of Figure 10 identifies the first arrival times of coherent s-wave energy at each test depth within the borehole. The s-wave velocity of each pseudo-layer can be calculated using these first arrival times versus depth by implementing one of three relatively standard methods; the Direct Method, the Interval Method, and the Modified Interval Method, each of which are described in detail by Kim et al., (2017). These techniques for calculating velocity essentially involve dividing a pseudo-layer's thickness by the difference in arrival time between the top and bottom of the layer (e.g., transmission time).

As described by Kim et al. (2017) and Bailey (2018), these approaches to VSP analysis are reliable within vertically transverse isotropic media (e.g., horizontally layered sediments and rock intervals with little azimuthal anisotropy or lateral variations in seismic velocity in the vicinity of the VSP survey). In this ideal geologic scenario, the seismic s-wave arrival time differences between a given pair of measurements (e.g., adjacent receiver depths defining a pseudo-layer) can be used with minimal issues from refraction in the calculation of seismic velocity for that pseudo-layer. This is the case in most applications of seismic cone penetration testing (SCPT), in conjunction with standard CPT. Here, SCPT systems offer the capability to collect vertical seismic profiling data while performing a CPT survey (Reclamation's SCPT system incorporates a seismic sensor that is imbedded in the tip of the CPT probe, allowing for periodic recording of VSP data). A good example of this SCPT-acquired VSP data is presented in Figure 11, for one CPT test conducted at Kicking Horse Dam, near Whitefish, MT.
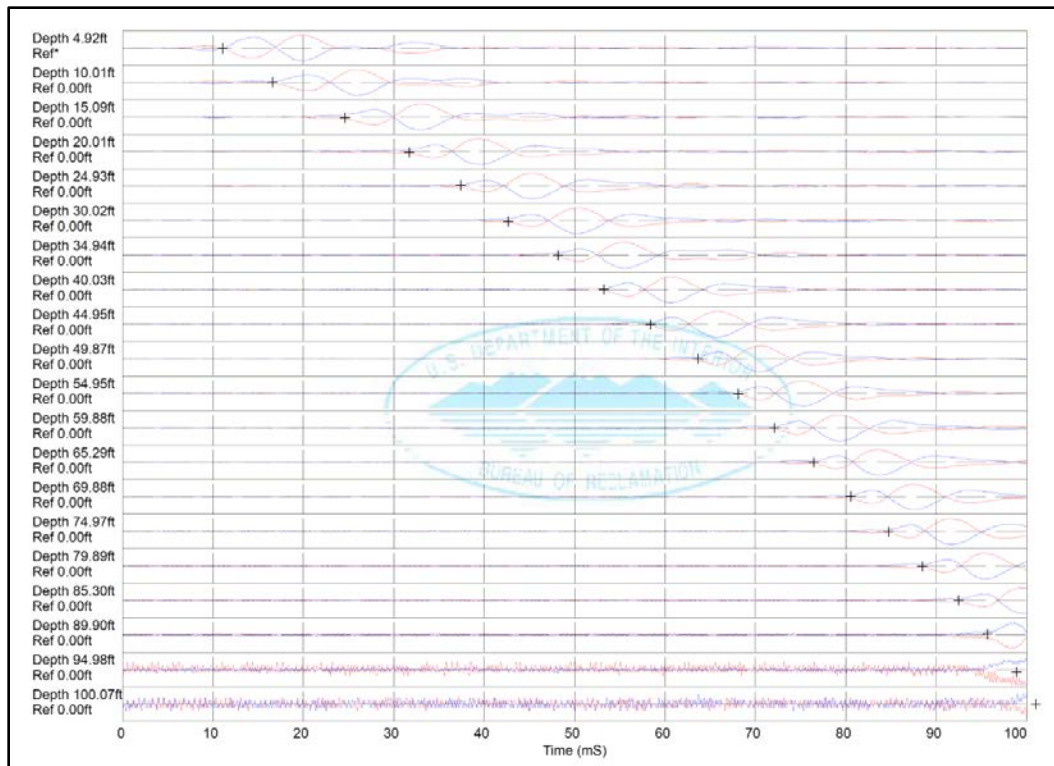
Figure 11 – VSP seismic s-wave data recorded at Kicking Horse Dam (Montana) using Reclamation's CPT rig, showing first arrival picks with black crosshairs.

D.   1D Spectral Analysis of Surface Waves (SASW)

SASW is a non-invasive surface-based seismic technique that produces 1D vertical s-wave velocity models (e.g., vertical Vs profiles). When a seismic source is applied to the ground surface, generated surface waves propagate outward along the free surface with a penetration depth that is wavelength-dependent (i.e., frequency-dependent); higher frequencies/shorter wavelengths are influenced by relatively shallow materials, and longer wavelengths are influenced by deeper portions of the earth (top-center plot in Figure 12). Because of this property, surface waves are usually dispersive (top-right plot in Figure 12), meaning different frequencies have different propagation velocities (Park et al., 1998). Two types of surface waves are generally known: Rayleigh and Love waves. The vibration polarization (particle displacement) of the Rayleigh wave component is mainly perpendicular to the surface (e.g., vertical), whereas Love wave polarization is parallel or torsional relative to the ground surface. Theoretically, the dispersion of surface waves is determined by several physical properties, including depth-variation of mass density and s-wave and p-wave velocities. Among these parameters, the depth-variation of Vs is the most influential factor (Park 2017). Because of this, surface waves are often used to deduce Vs of near-surface earth materials.
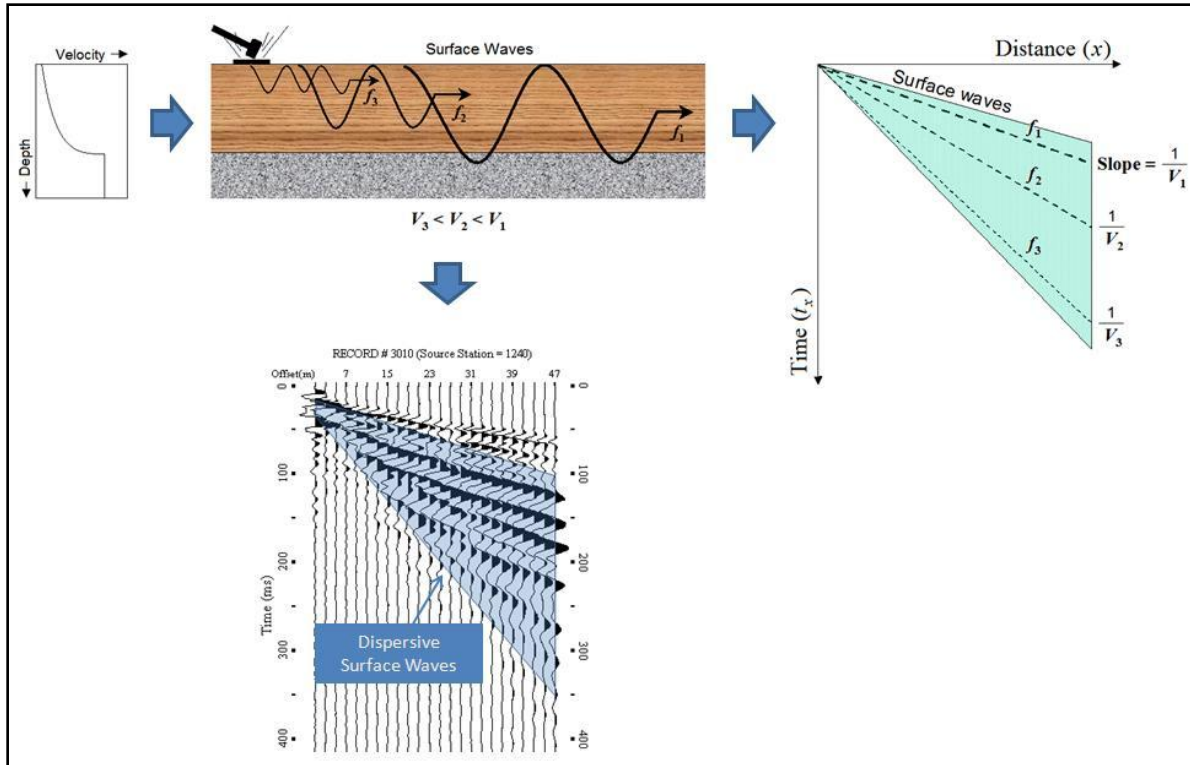
Figure 12 – When seismic velocity increase with depth, longer wavelengths (lower frequencies) of surface waves penetrate to greater depths and travel with a faster velocity than shorter wavelengths (higher frequencies). As a result, different frequencies arrive at different times on a seismic record, characterizing a dispersive seismic event.

The general testing setup for SASW is shown in Figure 13. Here, a vertically polarized active seismic source (e.g., an impactive sledge hammer striking a flat plate) at the surface generates predominantly Rayleigh waves, which are recorded by two receivers placed in a straight line relative to the source location. A seismograph records the ground motions at each receiver, and these waveforms are transformed from the time-domain to the frequency domain via a Fourier transform. Subsequently, the cross power spectrum and coherence are calculated, and the phase angle of the cross power spectrum is unwrapped through an interactive process called masking (Brown et al., 2000a). Finally, the SASW-derived dispersion curve is calculated by the following expression:

$$V\varphi = f * d_2/(\Delta\varphi/360°) \qquad\qquad \text{Equation 3}$$

Here, $V\varphi$ is the phase velocity associated with a given frequency component f, where d_2 is the distance between the receiver pair shown in Figure 13, and $\Delta\varphi$ is the unwrapped phase of the cross power spectrum for the corresponding frequency component f. The last step of an SASW survey is to invert the phase velocities to obtain a vertical velocity profile (e.g., a layered s-wave velocity model), as depicted on the right-hand plot of Figure 16.
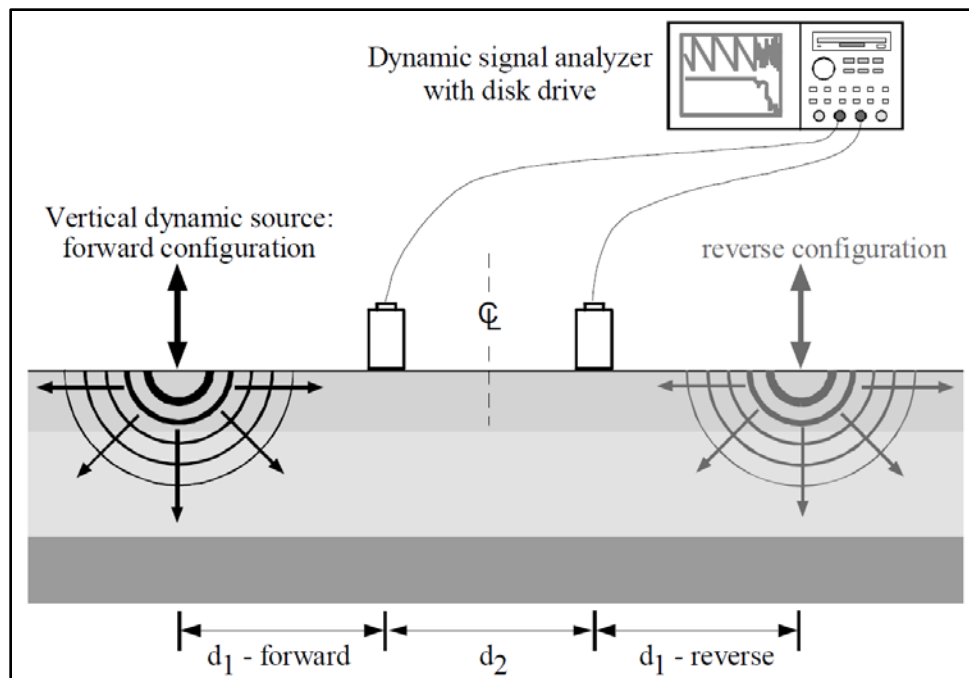
Figure 13 - Basic field setup for Vs30 measurements using the SASW technique (Martin and Diehl, 2004).

One simplified approach to interpretation of the SASW method's data has recently been developed, which utilizes a strong correlation between Vs30 and Rayleigh wave phase-velocities ($V\varphi$) for the frequency component exhibiting an approximate wavelength of 40 meters ($V\varphi40$) at a given site (Brown et al., 2000a, 2000b). This relationship (depicted on the left plot in Figure 14) was identified by the cross-comparison of Vs30 values and corresponding dispersion curves for over 100 test sites throughout California and several other sites outside California. Brown et al. (2000a, 2000b) show that this single phase velocity is adequately representative of Vs30 such that it can be used to provide Vs30 to within 10% of results from more robust survey approaches (e.g., detailed crosshole testing). Figure 15 shows a plot of Vs30 versus $V\varphi40$ values, showing a strong linear correlation between the two values across a relatively low range of s-wave velocities (100-700 m/s). Based on linear regression analysis, the predictive equation for Vs30 is given by the following expression:

$$Vs30 \ = \ 1.045 \ * \ V\varphi40$$
<div align="right">Equation 4</div>

For test sites where the vertical s-wave velocity profile is gradational with generally increasing velocities with depth, the measured dispersion curve using the SASW technique is a good approximation of the fundamental-mode Rayleigh-wave dispersion curve (Brown, 1998; Stokoe et al., 1994). Common exceptions to this assumption include scenarios where strong velocity contrasts or velocity inversions exist (slow layers beneath faster layers), including examples such as asphalt/concrete and compacted base material over softer sediments, and soft soil on shallow high velocity bedrock. At such sites, higher-mode surface waves may dominate the predictive Vs30 equation, which may become invalid as it is based on fundamental-mode Raleigh wave propagation.
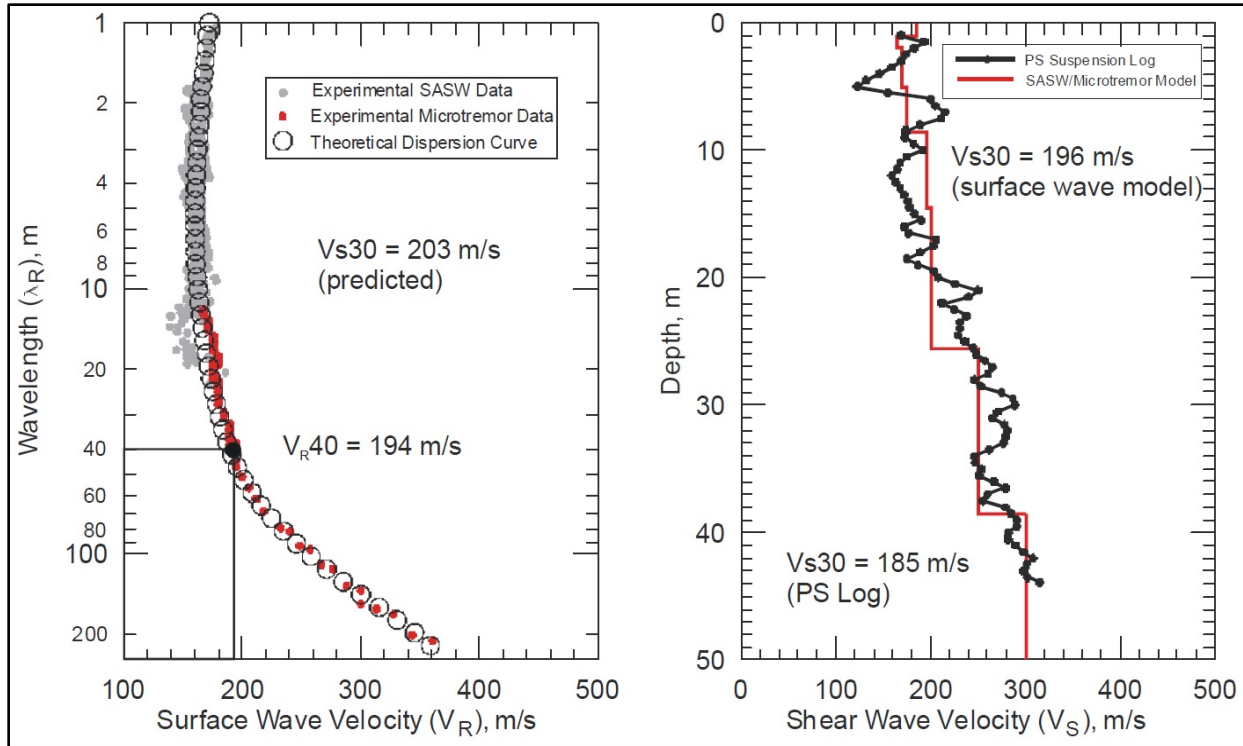
Figure 14 - Example of Vs30 calculation from SASW and refraction micro-tremor data compared with *in-situ* measured sonic logging (suspension log) velocity data. (Martin and Diehl, 2004). Comparison of $V\varphi40$ and Vs30 is shown on the left plot (Figure taken from Brown et al. (2000a).

This same approach to estimating Vs30 can be taken with the use of dispersion curves obtained via other surface wave dispersion techniques, including 1D MASW and ReMi analysis, as described below. The degree of correlation between Vs30 and $V\varphi40$ is high ($r^2 = 0.9864$) and the average error over the range of velocities tested is 14.5 m/s. The error bounds are approximately +/-10% of the estimate for a 95% confidence interval. In essence, this approach to interpreting SASW data allows for a direct estimate of Vs30 without the need for inverse modeling and explicit calculation of Vs30 from a 1D layered s-wave velocity model. However, it should be noted that the relationship appears to deteriorate at increasing Vs30 values.
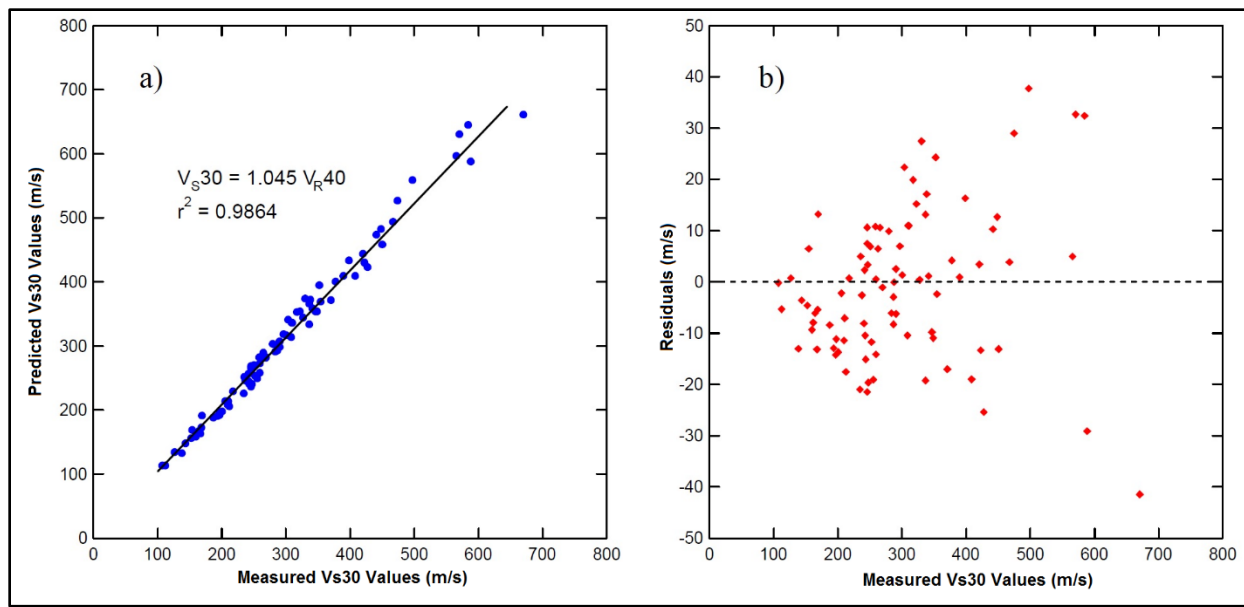
Figure 15 – Figure modified from Geovision (2018a) showing a) VS30 versus $V\varphi40$, with regression line and equations given. b) Residuals.

E. 1D and 2D Multichannel Analysis of Surface Waves (MASW) and Refraction Micro-Tremor (ReMi)

The MASW and ReMi survey techniques are alternative approaches very similar to SASW that can be used to provide vertical s-wave velocities for use in Vs30 calculations. Here, the largest difference between the two methods is that the ReMi technique only utilizes ambient background vibrational energy as a seismic source (e.g., passive seismic sources) and a longer record length is utilized in order to capture sufficient ambient surface-wave energy, while the MASW technique can use either active or passive sources of surface-wave energy. Depending on the software used to perform ReMi analysis, there may be a slight variation in the data transform algorithm used to convert time series data (e.g., multi-trace seismic records) into phase-velocity versus frequency plots (e.g., dispersion curves).

One special advantage of the passive surface-wave dispersion techniques (e.g., passive MASW and ReMi), is that they utilize background vibrational energy emanating from various sources surrounding the test site, such as naturally occurring microseismic activity, nearby trees and buildings swaying in the wind, people walking, vehicular and air traffic, construction and mining activities, waves impinging upon shorelines, wind turbine generators, and water conveyance over dam spillways and through hydroelectric power generators. Most of these background seismic sources are commonly encountered at Reclamation's embankments, especially the latter, where water conveyance through or over embankment structures and power hydroelectric power generators creates strong background vibrational energy. While this background noise can have significant negative impacts on active-source seismic data quality, these noise sources help to produce quality passive seismic data (e.g., broad spectral content and clear dispersion curves). In some cases, background noise levels are so strong that they prevent reliable active-source surface-based seismic data collection (e.g., seismic refraction surveys). In these scenarios, a

passive seismic survey may be the only practical surface-based solution to measuring Vs30, while avoiding the need for a borehole installation; Borehole techniques tend to be less sensitive to background seismic noise, which is predominantly generated by surficial sources and corresponding surface-wave energy that dissipates with increasing depth.

The MASW and ReMi techniques can often be used to isolate the fundamental-mode Rayleigh dispersion curve from higher modes (Park et al., 1999) and should be used in place of the SASW technique in environments where velocity inversions or steep velocity gradients are expected. These multi-channel techniques serve as a second approach to surface-wave dispersion analysis, where more than two sensors are deployed to simultaneously record phase-velocities between various receiver pairs of different spacings. MASW data can be processed in the same way as SASW data to produce 1D layered velocity models, and can be extended to also provide an estimated 2D distribution of s-wave velocity beneath a sensor array. Once data are recorded for a given sensor array layout, they are filtered and transformed into dispersion panels (e.g., phase-velocity images), the primary dispersion curve/energy is picked, and the picked phase-velocities are inverted to create a 1D Vs sounding model (Figure 16). This general analysis workflow is the same for both MASW and ReMi.
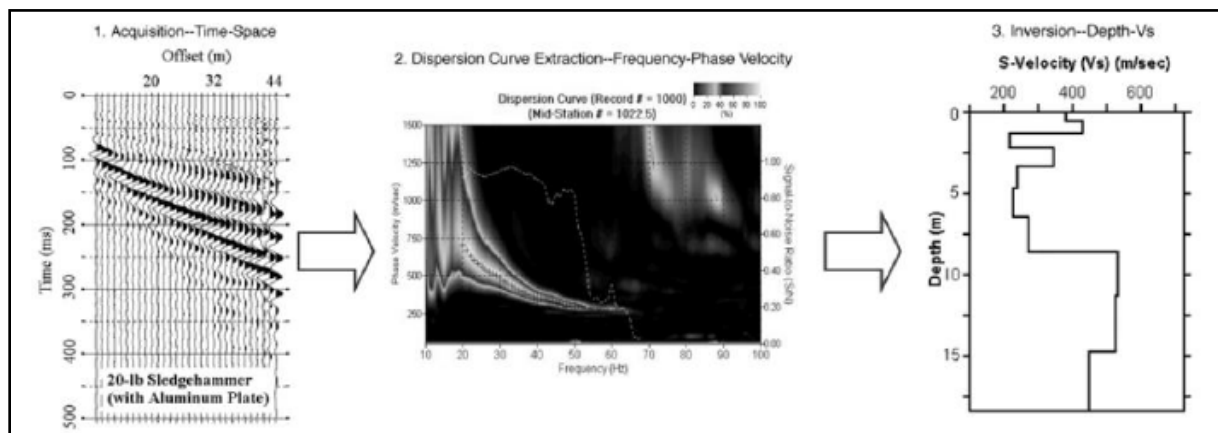
Figure 16 – Generalized MASW data processing-modeling workflow schematic.

Furthermore, both MASW and ReMi data can be collected with a linear array of geophones that are sequentially moved to provide a series of adjacent 1D layered velocity models along a longer survey transect that are subsequently stitched to graphically produce a 2D cross-section of s-wave velocities along the transect (see Figure 43). There are several limitations in implementing either SASW or MASW including the following:

1) The ground surface needs to be relatively flat, especially for a 2D MASW/ReMi survey
2) Geology is assumed to be horizontally layered with constant velocity/density in each layer, and complex or dipping geologic structures can severely violate these assumptions and result in inaccurate velocity models
3) Surface-wave dispersion analysis methods average any lateral variations in seismic properties of earth materials between SASW receiver pairs and beneath the entire length of an MASW or ReMi survey's sensor array (typically 24 or 48 channels

placed with a 10ft geophone spacing or less, resulting in up to 470ft of lateral averaging into a single 1D s-wave velocity model).

4) The process of producing a 2D MASW/ReMi velocity profile typically involves independent inverse modeling of a series of adjacent 1D models with no lateral constraints imposed (e.g., smoothness) between adjacent 1D layered models, oftentimes resulting in "roughness" in the stitched 2D velocity cross-section.

F.   1D Full-waveform Sonic Logging (FWS)

The Full-wave Sonic (FWS) logging technique (analogous and sometimes also referred to as "suspension P-S velocity logging," or simply "suspension logging") is an optional means to record seismic velocity as a function of depth (as needed for Vs30 calculations) using a single instrument within a single borehole. The technique is most typically performed within hard rock, but has been shown to be successful in PVC cased boreholes within unconsolidated materials (Burke 2011; GeoVision 2018b). Specifically, the FWS instrument consists of a stacked piezoelectric crystal transmitter (acoustic source) and four piezoelectric receivers with offsets of 60, 80, 100, and 120cm enclosed in a single wireline tool. Different tools contain different numbers of receivers, where each receiver records the arriving signals of an acoustic pulse emitted from the transmitter.

There are three types of waves that are commonly excited during FWS logging, including the p-wave, the s-wave, and the Stoneley wave. The first two wave types are analogs of the compressional and shear head-waves refracted along the borehole wall. In a "soft" formation where the shear wave velocity is lower than the acoustic velocity of the borehole fluid, there is no refracted S wave arrival, which is one limiting factor in the application of the technique within unconsolidated materials. Conversely, the Stoneley wave is a pressure pulse created by the waveguide effect of the borehole and is commonly referred to as the "tube wave" in downhole VSP profiling surveys. It should be noted that "the refracted P and S wave arrivals along the borehole or formation boundary are not pure p- and s-waves. However, the first arrivals from these packets still travel with the formation p- and s-wave velocities, respectively," (AAPG 2018).

The instrument is lowered to the bottom of the drill hole and raised at a constant rate of nominally 5 feet per minute by an electric winch while providing a nearly-continuous P- and S-wave record versus depth. Data collection is commonly configured such that a FWS measurement/trace is recorded with a high-resolution depth interval of 0.05m. FWS logging requires a borehole to be fluid-filled, where the fluid carries transmission of acoustic energy from the suspended instrument into the surrounding *in-situ* materials, and then back into the borehole to the receiver sensors. The FWS approach depends on seismic mode conversions to record s-wave arrivals (P>S>P converted energy). Here, the source generates a pressure wave in the borehole fluid. The pressure wave is converted to seismic waves at the borehole wall. Along the wall at each receiver location, the P and S wave components are converted back to pressure waves in the fluid and subsequently received by the receiver sensors.
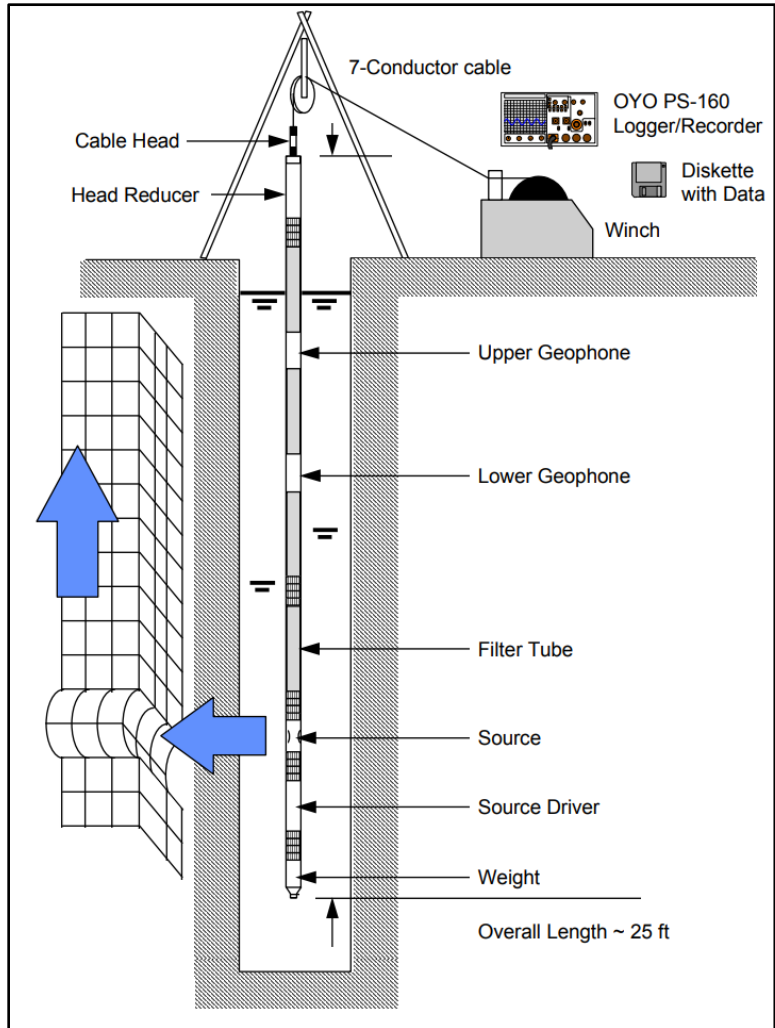
Figure 17 – Schematic of the Oyo suspension logger tool (taken from GeoVision 2018b).

Semblance analysis is commonly performed on sonic logging data (a technique for identifying coherent seismic energy arrivals at each or the four receivers that exhibit a given seismic velocity or slowness). The semblance, S, is calculated as the ratio of the coherent energy of the stacked waveforms to the total energy of the individual waveforms, as represented by the following equation:

$$S = \frac{\sum_{r=1}^{2}[\sum_i X_{ri}]^2}{\sum_{r=1}^{2}\sum_i(X_{ri}^2)}$$ Equation 5

Here, X_{ri} represents the full waveform time signal recorded at receiver r for sequential depths i of the wireline logging measurements (ALT 2009; Burke 2010). Semblance peaks are manually picked and used to calculate Vp and Vs versus depth based on the source-receiver offsets and wave arrival times picked for each measurement (e.g., every few centimeters).

G.   2D Seismic S-wave Refraction Tomography

Seismic refraction velocity tomography is a robust imaging technique, analogous to X-ray tomography imaging used in the medical industry. The seismic refraction tomography technique does not require or otherwise assume a flat ground surface or horizontal geologic layering (e.g., is able to image complex geologic structures and accounts for ground surface topography). Here, refraction tomography surveys can be implemented in a 2D, 3D, or even 4D (3D time-lapse) fashion, where the seismic wave propagation velocity distribution is most typically imaged (velocity tomograms).

Velocity tomograms can be used to calculate Vs30 values for most sites. However, the greatest challenges faced by calculating Vs30 from a s-wave velocity tomogram include:

1) velocity inversions (slow layers at depth are typically not imaged accurately)
2) shallow and extremely fast bedrock (can severely limit the depth of investigation)

In some cases, refraction tomography is implemented with the use of boreholes (e.g., crosshole tomography, surface-to-borehole tomography, etc.), in order to overcome the above limitations of surface-based refraction surveys. Furthermore seismic attenuation tomography can be implemented, in order to image the relative Q-value of materials (a measure of how seismically lossy a material is), as opposed to imaging the velocity distribution within the subsurface.

Refraction Concept

The seismic refraction method is based on contrasts in seismic velocity between two layers (Snell's Law of Refraction). When a compressional or shear wave (i.e., a body wave) meets a contact between materials exhibiting different seismic impedances (e.g., a velocity contrast), a portion of the wave's energy is reflected, and a portion continues through the interface, refracting according to Snell's Law (See Equation 6 below). If the incident angle of the wavefront reaches or exceeds the "critical angle" relative to the boundary, the wave is "critically refracted" and propagates along the contact boundary (minimal energy is transmitted to underlying layers). In general, the denser or more structurally rigid a material is, the faster a body wave will travel through it.

The s-wave refraction method is essentially identical to its compressional wave counterpart, but offers higher sensitivity to air/water filled voids and/or fractured/jointed zones within the subsurface. Surveys typically use a 20 pound sledge hammer impact on a metal shear-wave plate (weight-coupled "shoe" with a 45-degree plate mounted on either side). S-waves are generated at the ground surface, travel down to a contact between the overlying lower velocity rock (or combination of sediment and alluvial materials) and the underlying higher velocity rock. These s-waves are then refracted at this interface, travel along the contact at the faster underlying material's velocity (head waves), and simultaneously travel back to the surface where they are recorded by geophones. Figure 18 below illustrates the seismic refraction in terms of raypaths and the corresponding first arrival.
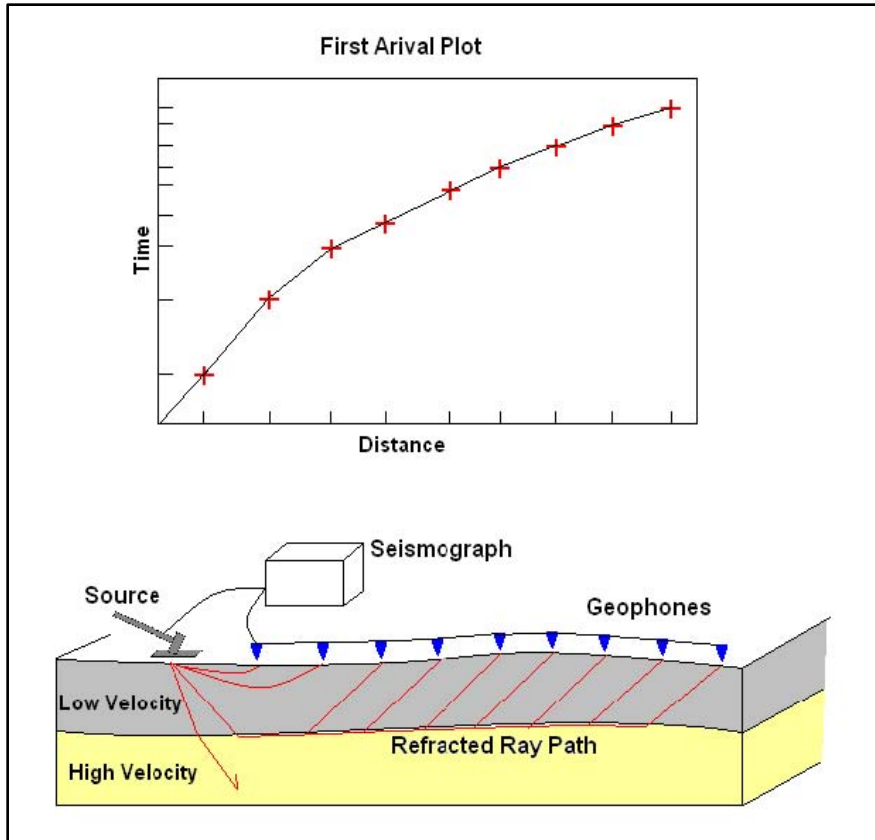
Figure 18 - Raypath seismic refraction concept & travel time plot (Redpath 1973).

Figure 19 illustrates the seismic refraction method in terms of wavefronts at different points in time. As time progresses, the wavefront propagates spherically in all directions away from the source. When the wavefront contacts the boundary between different velocities of rock, some of the energy is reflected back to the surface, and some of the energy continues downward into to the higher velocity rock. The wavefront accelerates in the higher velocity rock passing ahead of the initial and reflected wave in the slower velocity rock above it.

As the wave continues through the high velocity rock it creates a "wake" at the boundary between the upper and lower rock layers. This "wake", seen in dark crimson in Figure 19 below is the refracted wavefront. It propagates upward through the low velocity rock to the surface where geophones sense its arrival ahead of the surface waves and reflected waves.
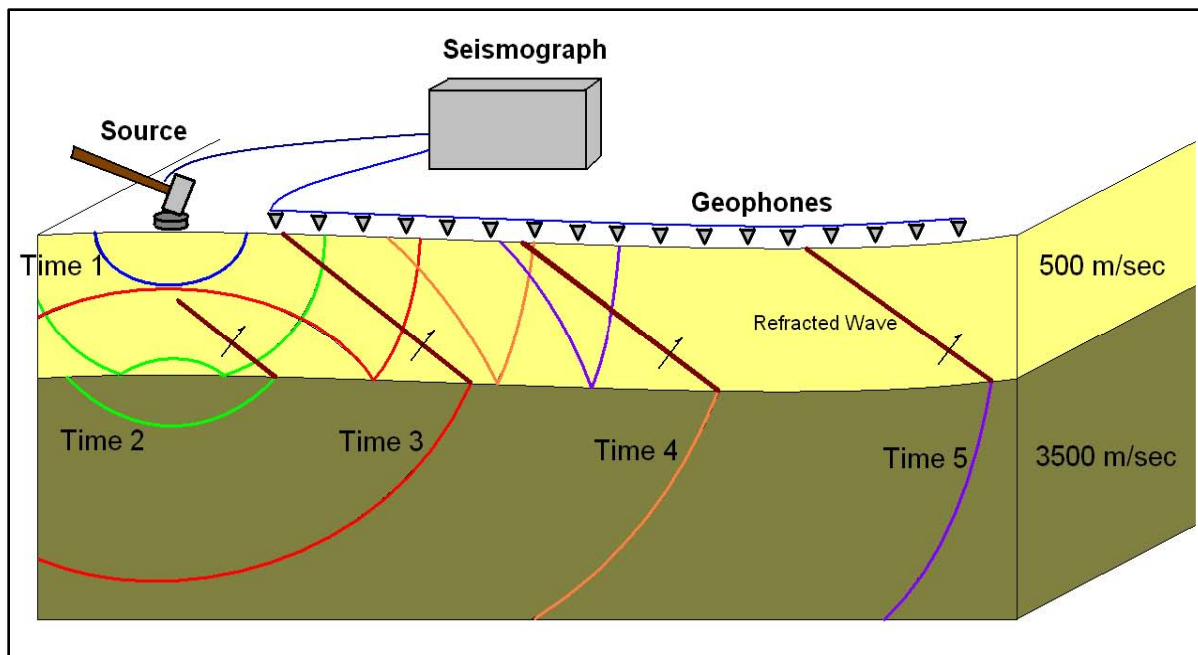
Figure 19 – Wavefront Seismic Refraction Concept.

Raypath Geometry

The rays shown above demonstrate wave direction more clearly than a wavefront itself. A ray is perpendicular to a wavefront and points in the direction of propagation of a given compression or shear wave. Refracted rays are bent at the contact between two rock layers and travel along the top of the underlying layer, moving at the higher velocity of the underlying layer. The angle at which a ray is refracted along the contact is given by Snell's Law:

$$\sin i V_1 = \sin r V_2 \hspace{3cm} \text{Equation 6}$$

where *i* and *r* are incident and refracted ray angles, and V_1 and V_2 are their layer velocities respectively. When angle r is equal to 90 degrees, the bent, or refracted ray, will travel along the interface at the velocity of the denser underlying layer and is called the critically refracted ray.

As it travels along the contact, secondary waves are continually created in the overlying rock layer at the critical angle:

$$i_c = \sin^{-1}(V_1 / V_2) \hspace{3cm} \text{Equation 7}$$

At a certain distance away from the source, known as the critical distance, this secondary wavefront, created by the critically refracted energy, reaches the surface geophones faster than direct arrivals along the ground surface. This can be seen as a change in slope of the "travel-time curve" (i.e., time versus distance) seen in the top plot in Figure 18 above.

Rays transmitted into the underlying basalt layer will continue downward until they intersect with another acoustic impedance contrast and will again be refracted. For this reason there are

limits to the optimal depth of investigation of a refraction survey. In general, the depth of exploration is one fourth to one half of the length of the seismic line, depending on the seismic velocity structure within the subsurface, (Hopkins 1998)

Alternative Refraction Analyses

Besides refraction tomography analysis, other data analysis approaches are available for processing and interpreting seismic refraction data, including the slope-intercept method and generalized reciprocal method (GRM). However, these techniques are slightly less robust and accurate in complex geologic conditions (e.g., non-flat layered geology and complex topography), and so the assumptions used in estimating velocity models can suffer from significant errors. Generally, tomographic analysis of refraction data is the preferred approach to data analysis, and doesn't cost significant additional amounts of time or money to perform. Finally, one factor to consider is anisotropy. Because the seismic reflection/refraction wavefronts tend to propagate in a non-vertical direction through the media, and the suspension log procedure derives its result from vertically propagating waves, seismic velocity measured horizontally along the bedding can be 10-15 percent higher than velocity measured vertically as in a well (Sheriff 1984).

H.   Alternative *In-Situ* Vs measurements and Vs30 Analysis Approaches

In this section, we present less common alternative approaches to estimating Vs30 values based on geophysical and non-geophysical survey and analysis techniques. While these alternative techniques are available options for obtaining Vs30 values, they are generally considered to be sub-optimal, are unlikely to be practical options, offer limited value of information (generally only provide a Vs30 estimate and no additional information related to Dam Safety Analysis), and should only be used in limited scenarios and only for establishing initial estimates of Vs30 or in cases where existing data can allow for the quick and inexpensive estimation of Vs30 when time and budget are of upmost concern (e.g., accuracy is of limited concern).

Seismic Reflections and Interval Stacking Velocities

Seismic reflection data are usually collected and processed to provide an image of geologic structure to depths far greater than of typical interest to Dam Safety studies, where these survey types oftentimes provide reflection images down to depths of several thousands of feet below ground surface (or below the ocean seabed in the case of off-shore surveys). However, useful velocity information can be extracted from shallow depths within a reflection dataset in order to inform Vs30 estimates. Here, shallow hyperbolic "reflection events" (energy reflected back to the ground surface from the geologic interfaces between layers exhibiting a sufficient contrast in seismic impedance) can be used to evaluate the average velocity of materials at various depth intervals.

Here, reflections from geologic interfaces take on a hyperbolic shape when data is plotted as a function of source-receiver offset in the form of a "common mid-point gather" or as a "common shot gather" (see red lines identifying hyperbolic reflection events in Figure 20). The shape of these hyperbolic data patterns is dictated by several factors, including the survey geometry, the angle of the interface (e.g., horizontal or dipping), and the velocity of the overlying material (faster overlying material generally results in flatter hyperbolas, and slower velocities result in

steeper hyperbolas). In the case of a single horizontal interface, the normal move-out (NMO) equation can be used to fit the hyperbola, or by using the dipping move-out (DMO) equation if the interface is non-horizontal.

In each case, the time of the "zero offset" reflection arrival provides a near-vertical two-way travel time that it takes the seismic energy to propagate downward from the source, reflect off of a given interface, and then propagate back up to the zero-offset receiver (a receiver located at the source location). The shape of the hyperbola provides the average "stacking velocity" for a given refection event, and the associated zero-offset arrival time then provides a means to evaluate the associated depth to the geologic interface. This can approach can be sequentially extended to multiple reflections that correspond to multiple geologic interfaces.
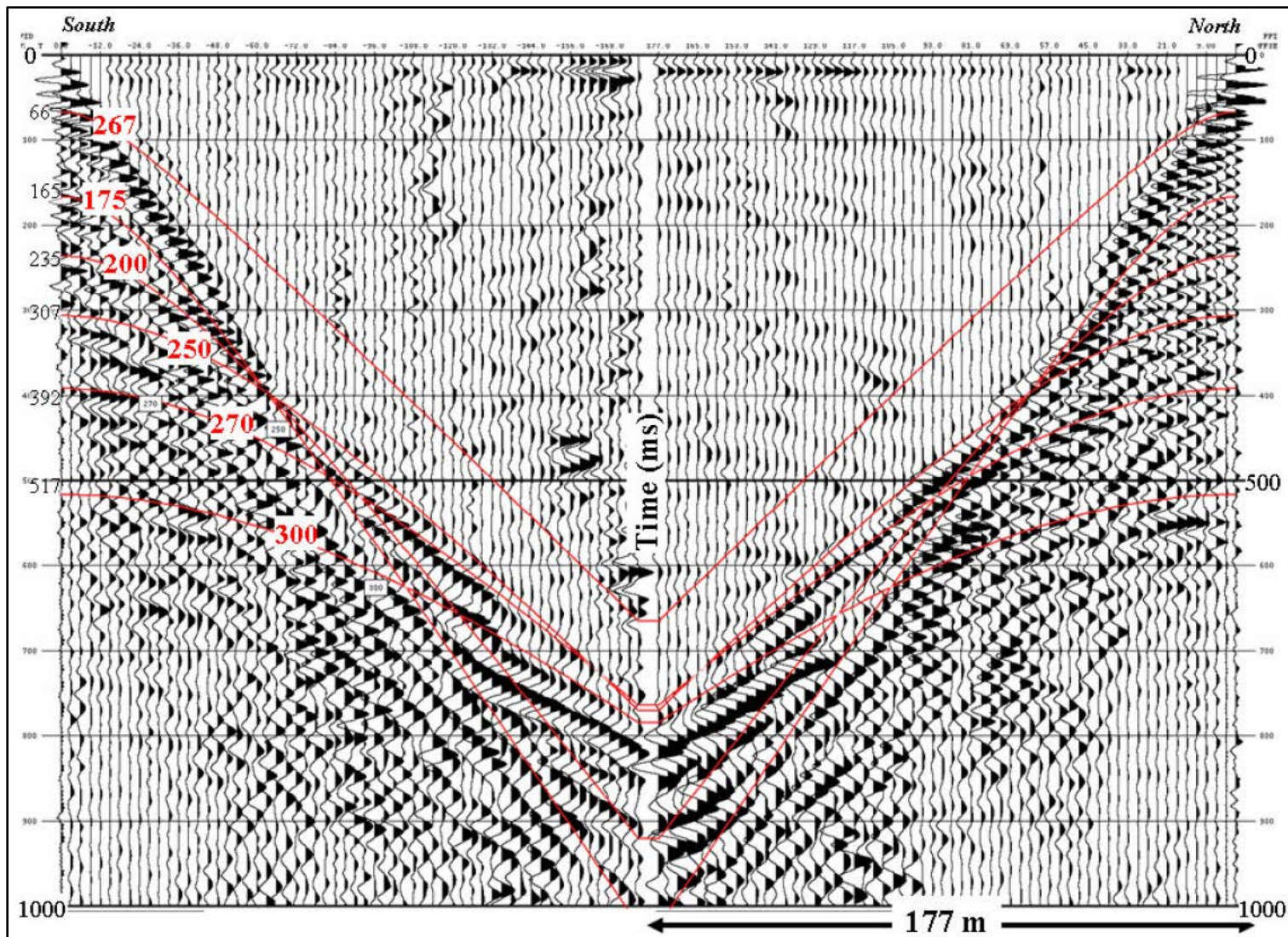
Figure 20 – Example reversed s-wave reflection shot record, where seismic data have been bandpass filtered and scaled by 100ms automatic gain control (AGC), and showing the reflection interpretation (red lines), move-out velocities, and zero-offset times labeled with black numbers on the left next to the zero-offset point of the fitted reflection hyperbola (taken from Asten and Boore 2005).

Horizontal-to-Vertical (H/V) Spectral Ratio Seismic Method

The horizontal-to-vertical (H/V) ambient-noise seismic method is a passive 1D seismic sounding technique that utilizes a single three-component broadband seismometer to record the three components (X-Y-Z) of ambient seismic noise (background vibrational energy emanating from remote sources such as microtremors, wind impinging upon trees, ocean waves impinging upon shorelines, wind turbine generators, anthropogenic activity such as vehicle traffic and construction activities, etc.) that can be used to estimate the depth to bedrock at a single testing location. The H/V method, commonly referred to as the horizontal-vertical spectral ratio (HVSR), records these components over a sufficient length of time at a given test site (e.g. several minutes), in order to provide data that captures numerous seismic events that together provide a seismic dataset with a wide range of frequency content with minimal gaps. Subsequently, the ratio of the averaged horizontal and vertical frequency spectra has been demonstrated to be capable of providing the fundamental site resonance frequency (characterized as a strong spectral peak at the fundamental mode and higher modes/resonant frequencies), which can be then be modeled to estimate sediment thickness and depth to bedrock via nonlinear regression analysis (Lane et al., 2007, 2008; Lui et al., 2007).

Here, Nakamura (1989) showed that the fundamental resonance frequency (f_0) of a site can be determined from the ratio of the horizontal and vertical amplitude spectra of the ambient seismic noise ($A_{NS}(\omega)$ and $A_{EW}(\omega)$, and $A_V(\omega)$, respectively), where ω is the angular frequency. Delgado et al. (2000) developed the following expression for calculating the H/V spectral ratio:

$$\text{H/V}\,(\omega) \;=\; \sqrt{\frac{[A_{NS}^2(\omega) + A_{EW}^2(\omega)]}{2A_V^2(\omega)}} \qquad\qquad \text{Equation 8}$$

Test sites that exhibit a strong seismic impedance contrast between bedrock and overlying sediments (e.g., a non-gradational geologic contact between rock and overburden materials with associated large changes in seismic velocity and mass density across this interface) can be approximated as a two-layer model. In these specific geologic scenarios, a seismic resonant frequency f_n can be related to the overburden layer's thickness with the following equation:

$$f_n \;=\; (2n + 1)(\text{Vs} \,/\, 4Z). \qquad\qquad \text{Equation 9}$$

Here, n is the resonant mode number, f_n is the resonant frequency (in units of Hz) of the nth resonant mode, Vs is the average shear wave velocity of the overburden layer, and Z is the depth to the bedrock-overburden interface at the test location. Researchers have shown that depth to bedrock Z can be related to the fundamental site resonance response frequency f_0 by the following expression:

$$Z = \alpha f_0^{\beta} \qquad\qquad \text{Equation 10}$$

Where α and β are site-specific fitting parameters, and found by solving the regression problem at a nearby location where Z is known (e.g., beside a nearby borehole). Once these fitting terms have been established, other tests can be performed in nearby representative geologic conditions, and Z can be determined in other locations relatively quickly. Similarly, the above equations can

be used to estimate an average Vs value for the overburden material and used for estimation of Vs30 values accordingly.

While this technique is an option for estimating Vs30, it has several limitations including:

1) There is no guarantee that geologic conditions will be conducive to the success of the method
2) Testing must be performed at a location of known Z, in order to solve for the missing parameter of interest (Vs).
3) The resulting average Vs may not represent an entire 30m depth interval, as required by the Vs30 parameter (e.g., bedrock may be shallower than 30m and the associated Vs would be an underestimation of Vs30, or alternatively, bedrock may be deeper than 30m and the associated Vs would be an over estimation of Vs30)
4) There could be significant error in the picking resonance frequency peaks that result in error of calculated Z and corresponding Vs values.
5) There are few occasions where broadband triaxial seismic data are available at the required locations and with sufficient frequency content to support a meaningful analysis result.
6) The technique only provides a single average Vs number, and offers little structural information about the foundation materials other than a rough estimate of depth to bedrock.

I.   Alternative Indirect Approaches for Estimating Vs profiles

In addition to the various direct approaches to measuring s-wave velocity for informing Vs30 calculations, there are several indirect estimation approaches that can be implemented if needed. These indirect approaches involve correlations between s-wave velocity and predictor variables, such as, near-surface geology, average topographic slope angles, standard penetration test N-values, cone penetration test resistances, and undrained shear strength measurements of soil samples. In each case, a relationship is derived that best explains an empirical relationship between s-wave velocity and the predictor data type.

Correlations between Vs and Penetration Testing and Shear-Strength Data

There have been extensive studies performed for the sake of developing correlation equations between s-wave velocity and the three primary penetration testing data types: SPT N-values, BPT N-values, and CPT testing corrected tip resistance data. In each case, the two data types are organized together, and regression analysis is used to develop a correlation equation that best captures the relationship between the two data types (see Figure 21). This equation is then utilized to predict s-wave velocity values where the predictor data type is available (e.g., to convert a 1D CPT log into a 1D Vs profile). Similar to penetration-based correlations, relationships between Vs and undrained shear strength for cohesive soils can be made since both properties depend on common physical parameters.

The figure shows a cross-plot with equation $V_s \, (m/s) = 1.75 \, (q_c)^{0.627}$, Note: q_c in kPa, $r^2 = 0.736$, $n = 481$, axis labels "Measured Shear Wave Velocity, V_s (m/s)" and "Cone Tip Resistance, q_c (kPa)", legend "Clay Structure — Intact, Fissured", "31 Different Clay Sites".
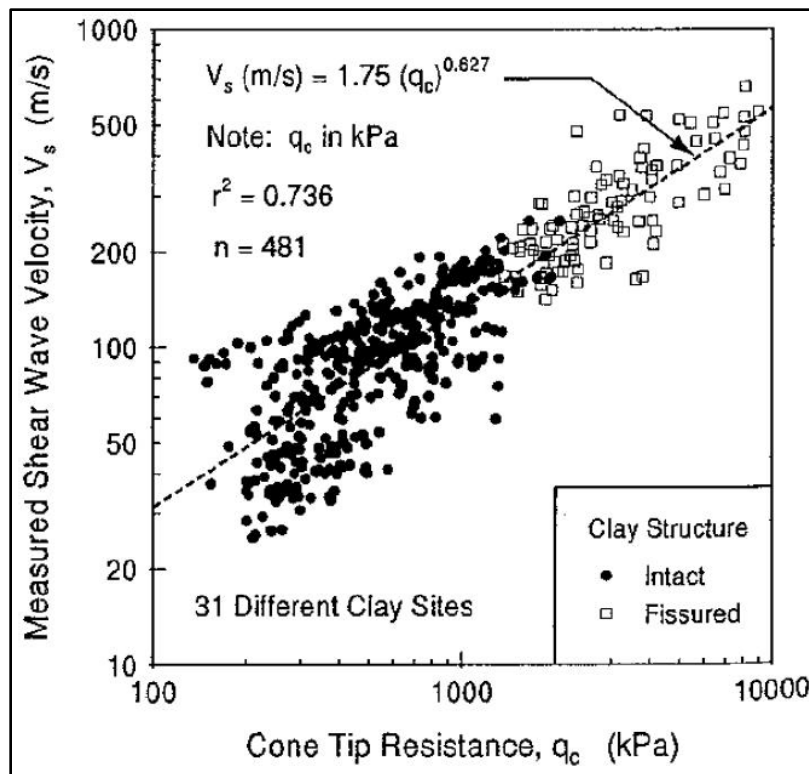
Figure 21 – Example cross-plot of CPT cone tip resistance data versus measured s-wave velocity with a regression-fitted line (correlation equation).

Wair et al. (2012) presents an extensive assimilation of decades of prior work on this topic, and presents various details of these correlation approaches for various material types (e.g., sand or clay-specific correlation functions), and provide extensive discussions on each technique. There are several subtleties involved in these correlation approaches. For example, they were developed for Quaternary aged soils only, and thus the use of age-related scaling factors is required for application to older Holocene and Pleistocene soils. Similarly, confining stresses need to be corrected for, among other considerations in the process of estimating Vs from predictor data. A full discussion of these penetration testing and shear strength testing correlation approaches is beyond the scope of this report, and the reader is directed to Wair et al. (2012) for further reading. Suffice to say here that in the appropriate circumstances, these correlational approaches can be quite useful for estimating s-wave velocity profiles, but they each come with limitations in both accuracy and applicability (e.g., techniques are not feasible in hard rock environments, and inaccuracies arise due to unrepresentative N-counts or tip resistances common within cobbly alluvium or in stiff materials that exceed penetration resistances of 100 blow per foot or more).

Geologic Log Correlation

Another indirect approach to Vs30 estimation involves the use of known or otherwise assumed geologic structure within the uppermost 30 meters of the subsurface in order to predict associated s-wave velocities of each material type or geologic layer, and to calculate an associated Vs30

value. This approach requires a-priori information about a site's geologic history, and expected site type (e.g., soft soil, hard rock, or intermediate site). In the ideal scenario, data from a borehole or test-pit is available with detailed descriptions of material type versus depth. Published values for the various earth material types can then be used to help constrain the estimated velocity of each layer. Similarly, statistical correlations between Vs30 and similar geologic units from previous studies can help provide a means for direct inference of Vs30.

In addition to material types, various physical properties of rocks can have significant influence on s-wave velocity, as described in Table 2. Intuitively, softer rock that is either more weathered or has greater amount of fracturing will exhibit lower seismic velocities compared to hard and intact rock of the same type (e.g., massive hard basalt versus highly fractured and weathered basalt). These physical properties are most commonly observed to be related to geologic history of a given study site. An example of these factors taken from Rittgers (2016, 2017a) is discussed further in a subsequent section of this report (see Figure 54).

Table 2 - Table of physical rock properties that affect seismic velocities, and should be considered when using geologic correlation approaches to estimating Vs profiles and associated Vs30 values for a given site (modified from Wair et al., 2012).

Physical Property of Rocks	Influence on Vs
Hardness	Increases with increased hardness
Weathering	Decreases with increased weathering
Fracture Density	Decreases with increased fracture density
Fracture Spacing	Increases with increased fracture spacing

Topographic Slope Correlation (USGS)

A recently developed approach for the indirect estimation of Vs30 is the based on the use of topographic slope correlation with measured Vs30 values (Allen and Wald, 2009; Wald and Allen, 2007; Worden et al., 2015; Yong et al., 2015). This approach was developed by means of assimilating all available Vs30 records, and utilizing high resolution digital elevation models (DEM) to calculate topographic slope angles in the vicinity of each Vs30 value available. With the two data types organized together, regression analysis is used to develop a correlation equation that best captures the relationship between the two data types. This equation is then utilized to predict Vs30 values everywhere sufficient DEM data is available. These estimated Vs30 values have now been made accessible for most of the world through an online interactive map-based data platform, as depicted in Figure 22 (USGS 2018).
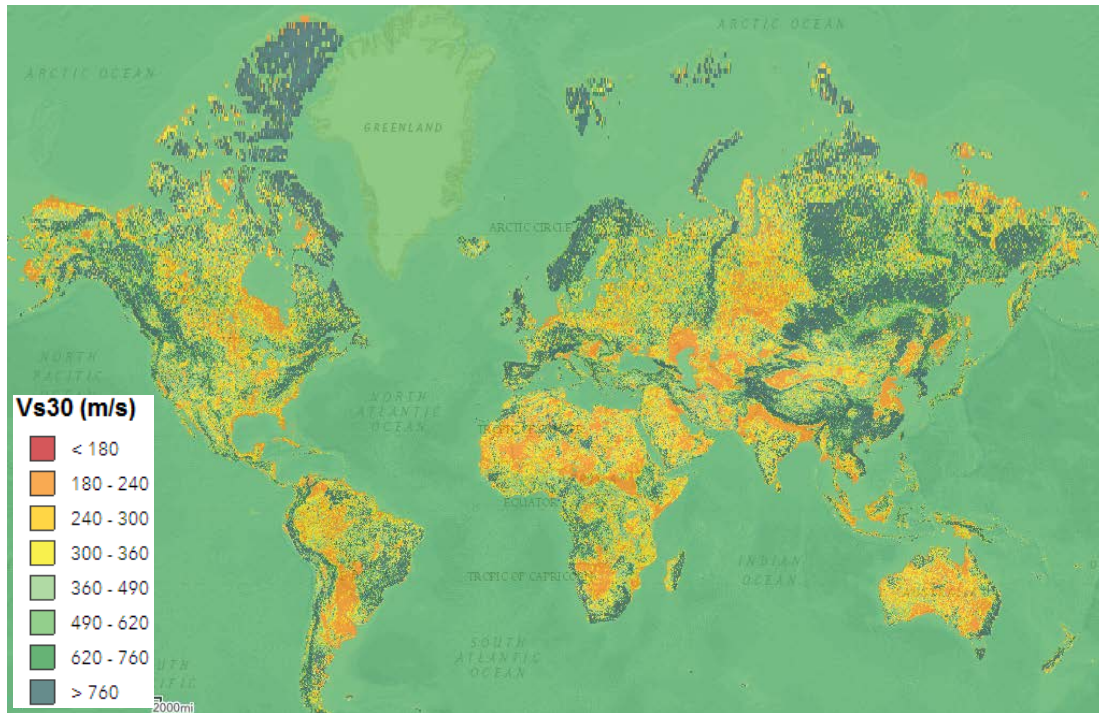
Figure 22 – Map of topographic slope-based Vs30 estimates across the world, where warm colors indicate low Vs30 values associated with elevated seismic amplification and potential risk (USGS 2018).

While this approach can serve as a convenient and free approach to obtaining a Vs30 value, it is deemed as one of the less reliable and least accurate ways to obtain a site-specific Vs30 value out of all presented in this study. In some cases, the approach works well. For example, topographic slope estimates range from approximately 1670 ft/s to 1440 ft/s for the Ochoco Dam area, compared with values derived from crosshole s-wave profiling performed at Ochoco Dam. Here, the Vs30 from the ground surface is calculated as 1275 ft/s, and from the foundation contact (~40 ft below the top of the crosshole triplet) is calculated as 1460 ft/s.

In other cases, topographic slope estimates are quite inaccurate. For example, topographic slope estimates range drastically from about 2350 ft/s to 980 ft/s for the Boca Dam area, compared with a mean of 2100 ft/s from direct measurement techniques (see The Vs profiles and final calculated Vs30 values for each survey technique are presented in Figure 35 and **Error! Not a valid bookmark self-reference.**, respectively. The final FWS Vs30 value of 2402 ft/s is in very close agreement with the Vs30 value of 2865 ft/s calculated using depth-averaged velocities from the s-wave refraction tomography results at the same location. A relatively good match in calculated s-wave velocities from the FWS logging and the other data types offers confidence in the results provided by this method within hard rock environments (see Figure 35 and **Error! Not a valid bookmark self-reference.**). Note that the 1987 crosshole is labeled as "fair" in **Error! Not a valid bookmark self-reference.** due to the limited depth coverage and the need for extensive extrapolation for Vs30 calculations. It should also be noted that, similar to the example study presented below for Ochoco Dam, indications of lithology and fracturing

(interbedded volcanic tuff and basalt layers) can clearly be seen in the FWS data and calculated velocities at Boca Dam.

Table 5 below). Similarly, topographic slope estimates range from approximately 1250 ft/s to 830 ft/s the American Falls Dam area. Using a geologic correlation approach (e.g., using geologic logs and published velocity ranges for typical rock types) the estimated Vs30 for this site fall within a much higher range of 2669 ft/s to 7378 ft/s, with a mean of 5023 ft/s. Again, there is a large discrepancy between the two approaches, where the topographic slope estimates are assumed to be far too low to be realistic for the known geologic conditions at the site. Here, it is assumed that the relatively flat-laying igneous extrusive units (volcanic tuff and basalt flows) do not follow the developed correlational trend between topographic slope angle and Vs30 value, resulting in a severely underestimated Vs30 value.

Statistical Extrapolation of Shallow Velocity Profiles

In some cases, Vs profile data will only be available for some depth interval that is less than the required 30m for sake of calculating a Vs30 value. This situation is typically encountered when survey depth coverage is terminated at some arbitrary depth less than 30m (e.g., depth of investigation of a surface-based survey is insufficient), or at intermediate sites (bedrock within the uppermost 30m) where boreholes or penetration testing terminates at the top of bedrock, only providing Vs values for the soil column depth interval. In order to utilize these shallow velocity profiles, there are generally two options:

1) Perform a vertical extrapolation of Vs values down to the required depth of 30m within unconsolidated materials
2) If top of rock is encountered, assume or assign a published value for the rock-type (if known), and apply that velocity for the remaining depth interval required for calculating Vs30.

Several approaches for vertical extrapolation can be taken, such as extending the lowermost measured velocity value as a constant value down to 30m, or by using a minimum curvature extrapolation function, or by fitting the available velocity trend "by eye." An alternative statistical approach was developed by Boore et al., (2004), where regression analysis was performed using 135 boreholes in California to develop a logarithmic expression that relates Vs30 values to various VsN values for depth-limited Vs profiles from $10m \leq N \leq 29m$:

$$\log (Vs30) = a + b \cdot \log(VsN) \qquad \text{Equation 11}$$

Here, a series of regression coefficient values are established for *a* and *b* that change as a function of the available Vs profile's depth coverage (e.g., *N*), as provided in Table 3. As stated by Wair et al. (2012), "extrapolating shallow velocity data to calculate Vs30 may be appropriate for most sites with relatively uniform soil conditions. This method could lead to errors for sites with a velocity contrast within the top 30 m, such as soft soil over stiff soil or soil over bedrock."

As an example of the use of this extrapolation equation is taken from a depth-limited Kicking Horse Dam CPT survey that was used to estimate a Vs profile from the CPT predictor data. Here, the average Vs for the top 12 m of the profile (VsN or Vs12) is 185 m/sec. Vs30 could be calculated using Boore's equation and the regression coefficients in Table 3 as:

$$\log Vs30 = 0.012571 + 1.0352 \log (185)$$

$$Vs30 = 305 \text{ m/sec}$$

Table 3 – Regression coefficients for extrapolating Vs30 values (Boore et al., 2004).

Input Vs Profile Depth Coverage (N)	Regression coefficient *a*	Regression coefficient *b*
10	0.042062	1.0292
11	0.02214	1.0341
12	0.012571	1.0352
13	0.014186	1.0318
14	0.0123	1.029
15	0.013795	1.0263
16	0.013893	1.0237
17	0.019565	1.019
18	0.024879	1.0144
19	0.025614	1.0117
20	0.025439	1.0095
21	0.025311	1.0072
22	0.0269	1.0044
23	0.022207	1.0042
24	0.016891	1.0043
25	0.011483	1.0045
26	0.006565	1.0045
27	0.002519	1.0043
28	0.000773	1.0031
29	0.000431	1.0015

V. Example Surveys: Comparison and Evaluation of Various Seismic Survey and Analysis Techniques

In this section, we present a series of example surveys performed by Reclamation in recent years, in order to provide quantitative and qualitative comparisons of the various techniques introduced in the previous sections, and to exemplify Reclamation's current abilities and available options for seismic surveying, seismic site characterization, and Vs30 estimations. This section starts by first comparing three different approaches to performing crosshole seismic profiling analysis in the challenging scenario of a relatively slow velocity layer and refracted arrivals. Crosshole profiling serves as the benchmark technique for evaluating the accuracies of other techniques, as it is generally considered the most accurate velocity profiling technique regardless of depth.

Subsequent sections each present examples of various combinations of other Vs30 techniques. In each case, co-located data types are compared both in terms of their ability to produce an accurate Vs30 value, as well as the various challenges, benefits, and limitations of each technique for providing additional information that may be needed or otherwise beneficial for informing subsequent risk analysis efforts. In general, the examples shown here demonstrate that each direct measurement Vs30 technique can be effective in producing sufficiently accurate Vs30 values if the site conditions and local geology are conducive to good quality seismic data. In the case of indirect Vs30 estimation techniques, CPT and geologic and are shown to be sufficiently accurate in certain circumstances and when sufficient data are available.

A. Ridgeway Dam: Comparing 1D Crosshole Profiling and 2D Inversion of Crosshole Seismic Data

As described in the previous section, crosshole seismic testing has been considered the benchmark technique for measuring Vs *in-situ* between two or more boreholes, for the sake of informing Reclamation's risk analysis efforts. The technique is deemed a benchmark, due to its accuracy in recovering Vs at each depth tested within a borehole set. However, the crosshole technique most usually makes the assumption of direct wave propagation between boreholes, which can be violated in the case of refracted waves. This is a particularly problematic phenomenon for tests conducted within slow velocity layers, as described above and depicted in Figure 7.

A good example of this situation was identified at Ridgway Dam, located near Ridgeway Colorado (see Figure 23), where two slow velocity/weak layers were identified directly above the top of bedrock at that site (Rittgers 2011). Here, a calculated s-wave velocity of approximately 1750ft/s was obtained for each of the two layers using the standard (direct) crosshole analysis approach (assuming straight raypaths), which was suspected of being biased due to the possibility of refracted energy (see crosshole velocities identified as "areas of concern" in Figure 23). If these suspicious layers' true s-wave velocities are actually 1200ft/s or less, they would be considered problematically low strength and likely susceptible to liquefaction during a seismic loading event of adequate magnitude. Here, the 1989 version of chapter 13 of Reclamation's *Design Standards No. 13 – Embankment Dams,* recommended that soils with measured Vs (not normalized for overburden stress) exceeding 1,200 feet per second (ft/s) (366 m/s)

can tentatively be considered non-liquefiable. This motivated a second phase of more detailed analysis of seismic velocity of these two suspect layers.

The second phase of data analysis at Ridgeway Dam led to the development of new code for implementing the 2D layered velocity inversion approach to crosshole profiling data analysis described above. This new code was developed in order to overcome the uncertainties involved in implemented the 4-layered refraction forward modeling approach also described above. The results from both approaches were quite similar and resulted in slower estimated velocities compared to the standard direct crosshole analysis approach (as expected). Of the two crosshole analysis approaches that account for refraction, the inversion approach resulted in slightly lower velocity estimates within all layers while maintaining an exceptional match between observed and calculated arrival times (very low data misfit) as seen in Figure 24. The s-wave velocity tomogram can be thought of as a 2D vertical view of the subsurface between the two boreholes utilized for the survey, where cool colors (e.g., blues and greens) represent relatively slow-velocity materials, while warm colors (e.g. yellows and reds) represent relatively fast-velocity materials.

Of all three approaches, the new 2D inverse modeling approach is considered to be the most accurate in recovering true layer velocities, especially in the presence of slow-velocity layers. The new inverse modeling approach also results in the most conservative (slowest) set of velocities, resulting in the most conservative corresponding estimate of Vs30. It is interesting to note that the inversion approach applied for Ridgway Dam resulted in an even slower s-wave velocity of for the upper slow layer of concern (see Figure 23). The shear wave velocity of this layer was calculated to be approximately 1450ft/s which is still above the lower limit of reasonable velocities (1200ft/s) from a liquefaction potential standpoint. Despite the fact that this layer is not directly adjacent to the fast bedrock interface, this more extensive velocity correction from the standard approach is not a surprise, as this overlying slow velocity layer is thinner, and therefore more susceptible to bias from refracted arrivals from adjacent layers.

Table 4 – Comparison of calculated layer velocities obtained within the deeper slow-velocity layer of concern using the four-layered refraction analysis forward modeling approach, and by using the crosshole curved-ray inversion approach.

Layer #	Crosshole (Direct) Velocity (ft/s)	4-Layer Velocity (ft/s)	Layered Inversion Velocity (ft/s)	Elevation to top (ft)	Thickness (ft)	Description
1	1750	1745	1651	6558.2	1.2	Sandy/Clayey
2	1900	1895	1861	6557	3.5	Wx Bedrock
3	2750	2225	2152	6553.5	1.0	Bedrock
4	4050	4044	4005	6552.5	Infinite	Hard Bedrock
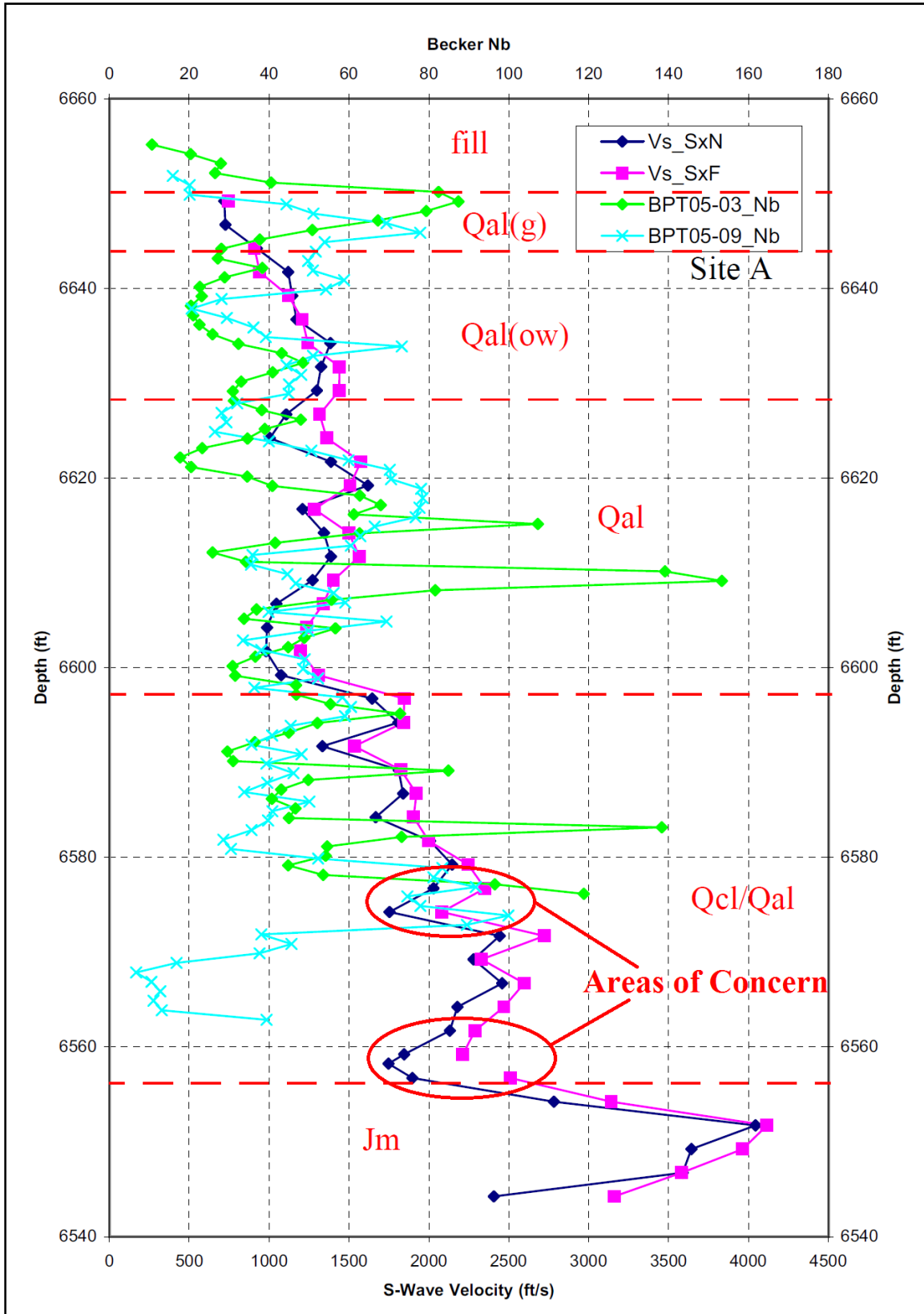
Figure 23 – Comparison of calculated standard crosshole S-wave velocities and Becker testing data collected at Ridgway Dam, Colorado.
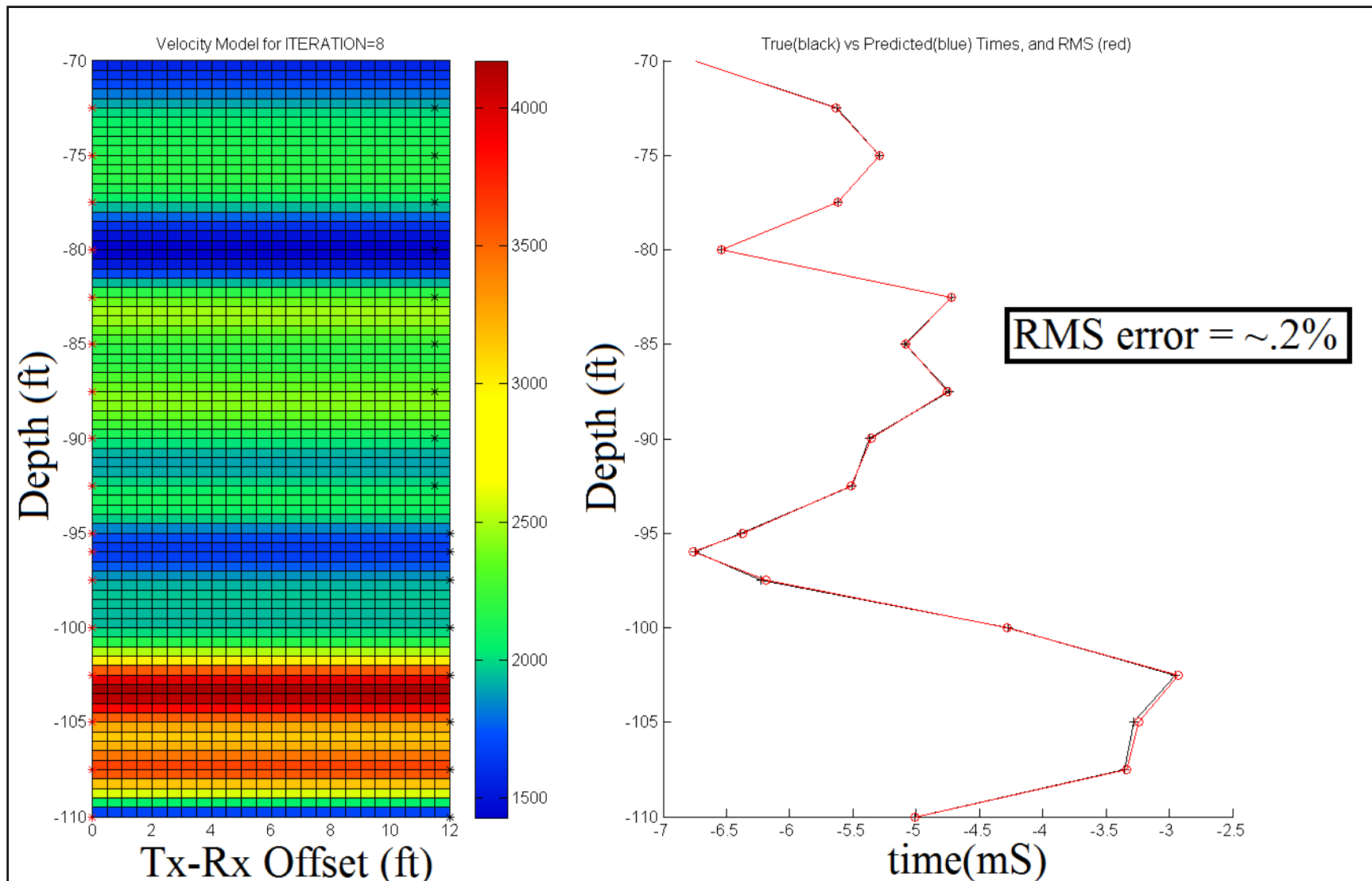
Figure 24 – Result of a 2D nonlinear ray-tracing inversion of a subset of the crosshole shear wave data from Ridgeway Dam. Velocity tomogram model is plotted on the left, and the observed (black) and predicted data (red) are plotted on the right.

B.   Prosser Creek Dam: Comparing 1D Crosshole profiling and 2D Crosshole Tomography

Similar to the Ridgeway Dam case study presented above, an example crosshole seismic study conducted at Prosser Creek Dam located near Truckee California is presented here. Like the Ridgeway Dam survey, the Prosser Creek Dam crosshole study was conducted to better assess the material properties of a Quaternary alluvium (Qal) layer identified nominally 70 to 74 feet below ground surface at the borehole location (Rittgers 2017c). This soft Qal layer was previously identified during borehole logging as being potentially problematic from a liquefaction standpoint. Therefore, an accurate measure of Vs was needed for this thin layer in order to assess liquefaction potential, and a borehole triplet was installed to support seismic crosshole testing.

After collecting and processing the crosshole data using the standard direct transmission approach (assumption of straight raypaths between the source and near and far receivers), there was concern that the soft layer's Vs was being over-estimated due to refracted arrivals from overlying/underlying layers (see Figure 25). Furthermore, embankment zone interfaces and this Qal layer were discovered to be a non-flat pinching layer that was likely not obeying the assumptions made in the standard crosshole velocity analysis approach, or the assumptions used in the 2D layered velocity inversion approach discussed above. Therefore, extensive Matlab code was developed to perform 2D crosshole seismic velocity tomography modeling, in order to capture the complex layer geometry and verify the Vs values estimated for the Qal material. Similar to the 4-layered forward modeling and 2D layered velocity inversion approaches described above, a 2D tomographic technique can be used to confirm the velocity of relatively slow zones while accounting for refraction of waves off of nearby relatively faster layers (see Figure 7), but has the added benefit of accounting for complex non-layered velocity structures.

At Prosser Creek Dam, crosshole tomography data were collected between DH-17-6 (source hole) and DH-17-8 (far receiver hole) from 60 feet to 80 feet below ground surface. A plot of the approximate raypath coverage of the crosshole tomography survey is shown in Figure 8, where source locations are plotted along the left-hand side, receiver locations are plotted along the right-hand side, and a black line (e.g., raypath) is shown connecting each unique shot-receiver pair. Similar to 1D crosshole seismic s-wave profiling data collection, two records are acquired at each source depth, where one shot record is recorded for each source polarization direction (one downward shot and one upward shot). This approach allows for a more clear identification of the first arrival of s-wave energy, where the two waveforms plotted together can more readily show the opposite polarity arrival for each shot depth.

Figure 26 presents the results of 2D crosshole seismic s-wave refraction tomography surveys conducted at Prosser Creek Dam. Specifically, this figure presents a 2D s-wave velocity tomogram, viewed looking downstream. Velocities are in units of feet per second. Figure 26 also includes dashed lines corresponding to the interpreted interfaces between the various layers also labeled on the figure (as identified in geologic logs). The possible location of the Gardner Fault, as indicated in the draft geologic report, is also indicated with a vertical dashed-line in Figure 26 (Sturm 2017). Here, an excellent correlation is observed between the modeled seismic

s-wave velocities and the known depths/trends of the geologic interfaces (based on geologic logs recorded during installation of the crosshole triplet).

This structural match was achieved without incorporating this prior information into the data analysis or modeling, providing added confidence in the crosshole refraction tomography method and results presented here.
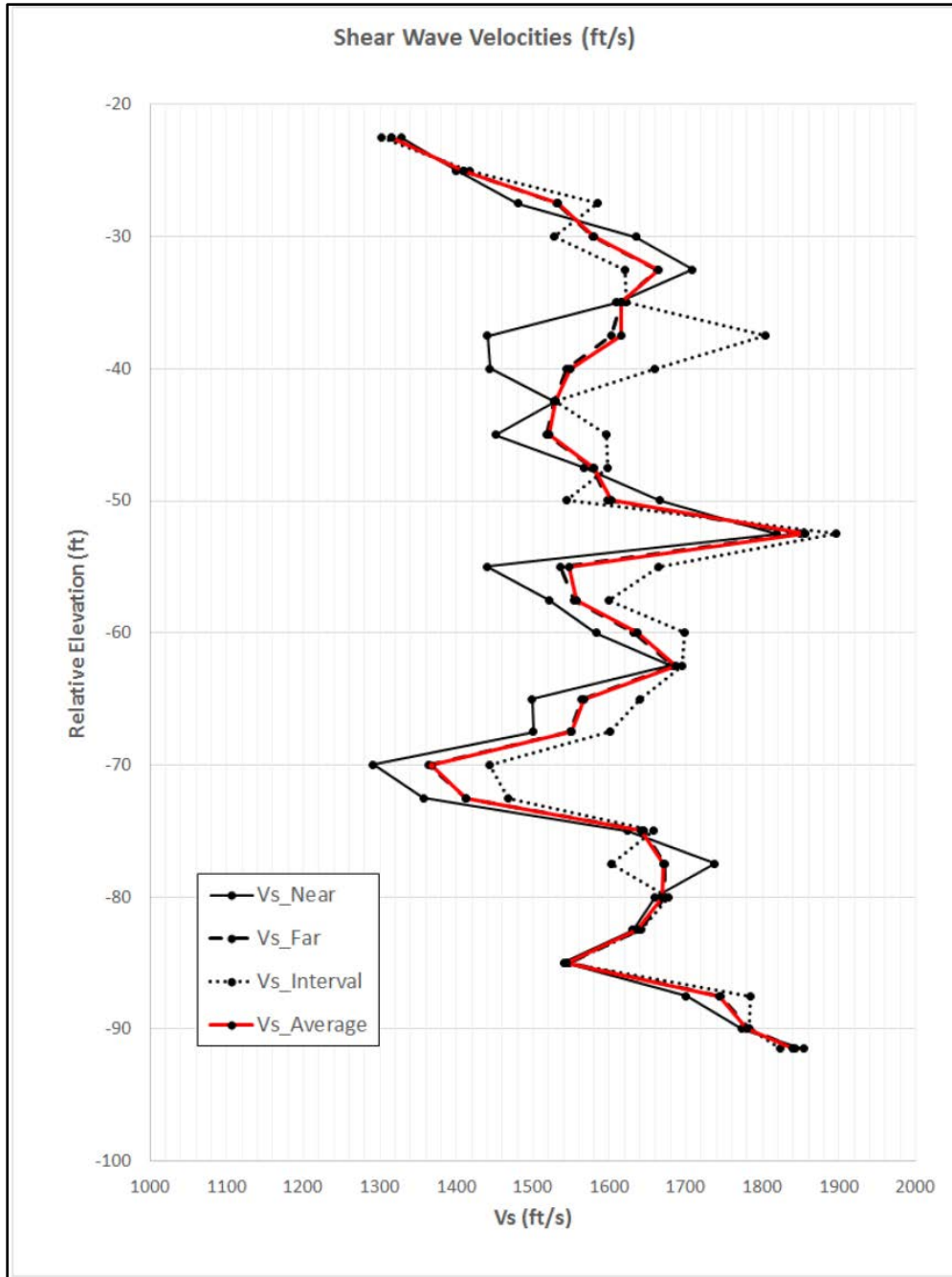
Figure 25 – Prosser Creek Dam: 1D crosshole seismic s-wave velocity profiles calculated using the standard direct transmission approach for the near receiver, far receiver and for the interval between receivers. The average of all three velocities is plotted in red.

The Qal layer of concern appears as a zone of decreased shear wave velocity relative to overlying and underlying zones, where the lowest s-wave velocity imaged within the Qal material using the 2D tomography approach is approximately 1,700ft/s. Furthermore, similar s-wave velocities can be seen in the 1D crosshole profiling results for these depth intervals (approximately 1,400ft/s).

Based on the 2D crosshole s-wave tomography results, lower s-wave velocities appear to manifest within the thickest sections of the variable-thickness Qal layer, but these lowest velocities (i.e., the dark blue region on the left-side of Figure 26) are still slightly higher than the 1D crosshole profiling velocities at the same depths (see Figure 25). This observation could be due to errors in first arrival picks, or it could be an artifact of the smooth-model constraints applied during the inversion process: These smooth model constraints may have resulted in the smearing of higher velocities across the relatively thin Qal layer from above and below, especially where this layer is seen to pinch out towards DH-17-8 on the right-hand half of Figure 26. Furthermore, the 2D crosshole tomography dataset has relatively low-aperture (maximum angle of intersecting rays), and also has relatively limited raypath coverage density (less-constrained velocities), and so it is reasonable to deduce that the Qal material most likely has a seismic s-wave velocity of 1,400ft/s to 1,500ft/s at this location. Regardless of this minor discrepancy identified between the results from the two processing techniques implemented at Prosser Creek Dam, this example demonstrates crosshole seismic tomography's additional capability for detailed velocity imaging in complex geologic environments not otherwise achieved or accounted for by the other crosshole analysis techniques.
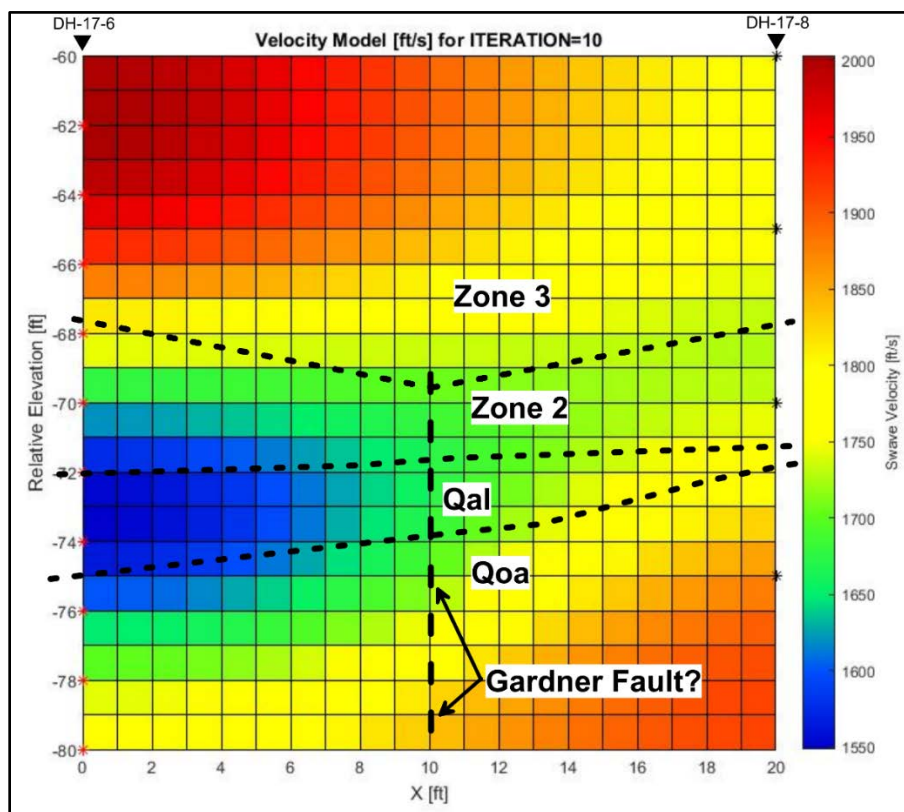
Figure 26 - 2D crosshole seismic s-wave tomography velocities for the depth interval of 60 feet to 80 feet below ground surface.

C. Granby Dam and Dike 3: Comparing 1D Crosshole Profiling with 2D Refraction Tomography and Seismic Reflection

A recent seismic loading study for Granby Dam and Dike 3 near Granby Colorado provided the opportunity to utilize a series of crosshole seismic survey datasets for this study, by means of collecting co-located s-wave refraction tomography data for evaluating repeatability and various trade-offs and values of the two techniques (Liechty, 2018). In general, this example comparison of the two survey techniques demonstrates the ability to capture the same overall velocity structure using refraction tomography, albeit an averaged and more or less monotonically increasing velocity versus depth that may under-characterize or miss velocity inversions seen in the crosshole data.

Crosshole s-wave data were collected at three different locations, using 1) a crest borehole triplet that extended through the unconsolidated embankment and foundation materials to top of bedrock, 2) a borehole triplet at the downstream toe right abutment extending to bedrock, and 3) a borehole doublet at the downstream toe left abutment that extended through the foundation materials and approximately 20 feet into metamorphic schist bedrock. Results from the crosshole doublet are plotted in Figure 27, showing the sudden increase in measured s-wave velocity within the lowermost portion of the doublet that extended into bedrock.
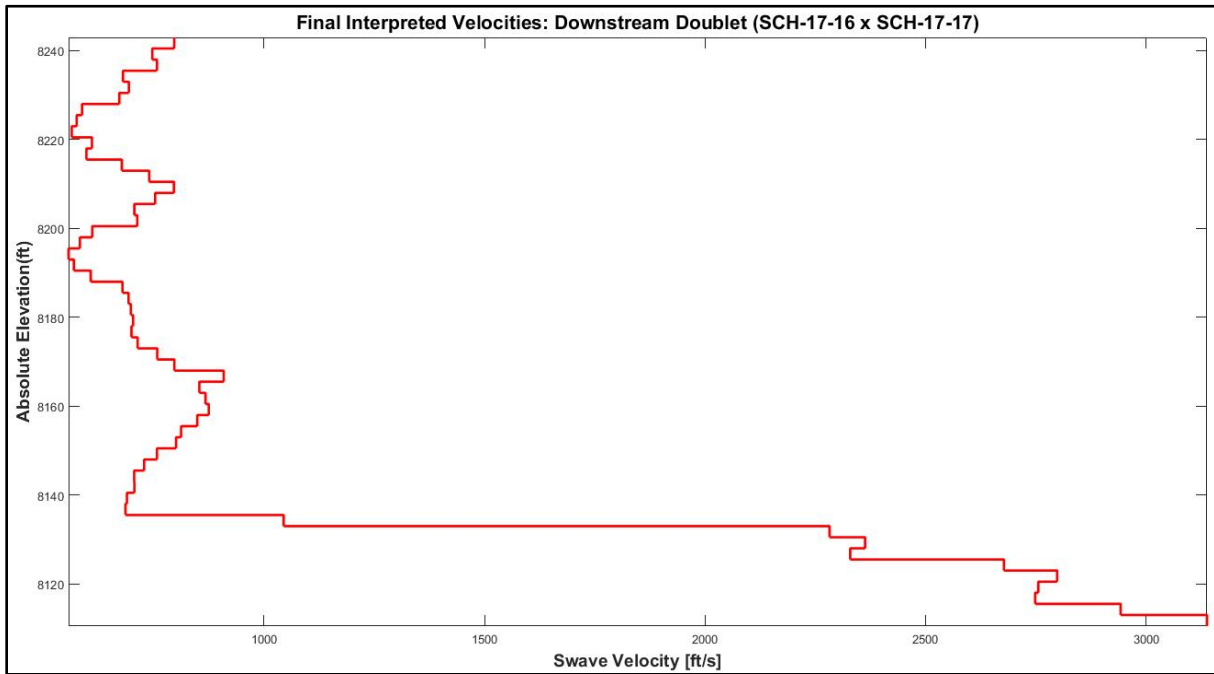
Figure 27 – Crosshole s-wave velocity profile for the downstream toe left abutment doublet at Granby Dike 3, Colorado.

In support of this study, a 2D s-wave refraction tomography survey was conducted along the downstream toe immediately between the two adjacent crosshole surveys (see Figure 28). The same crosshole velocity profile shown in Figure 27 is overlain in Figure 28, in order to depict the close match between the two survey techniques. Here, we see both a close match in depth to bedrock and also the absolute velocities versus depth within each material type.
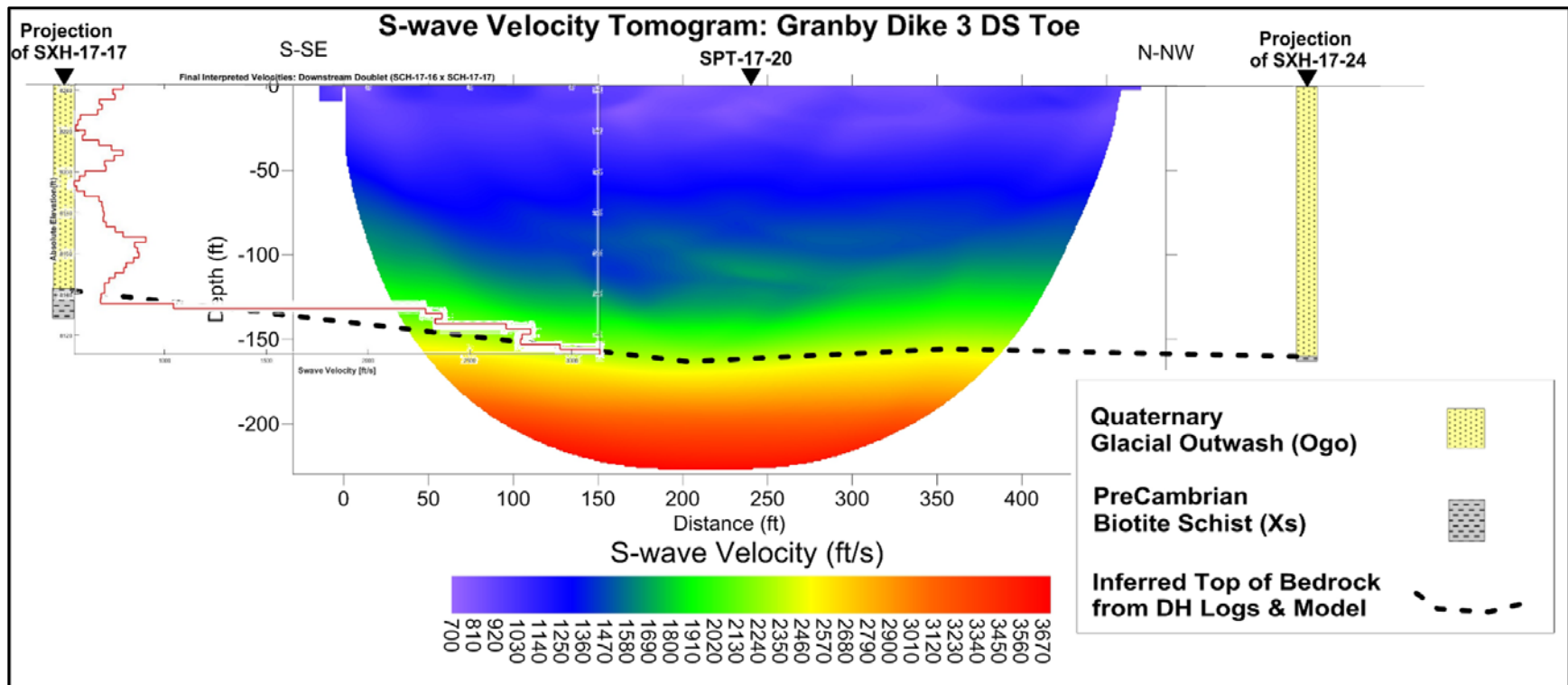
Figure 28 – Seismic refraction s-wave velocity tomogram showing the interpreted top of bedrock dipping towards the right abutment along the downstream toe of Granby Dike 3, as verified by two boreholes drilled near either end of the survey line.
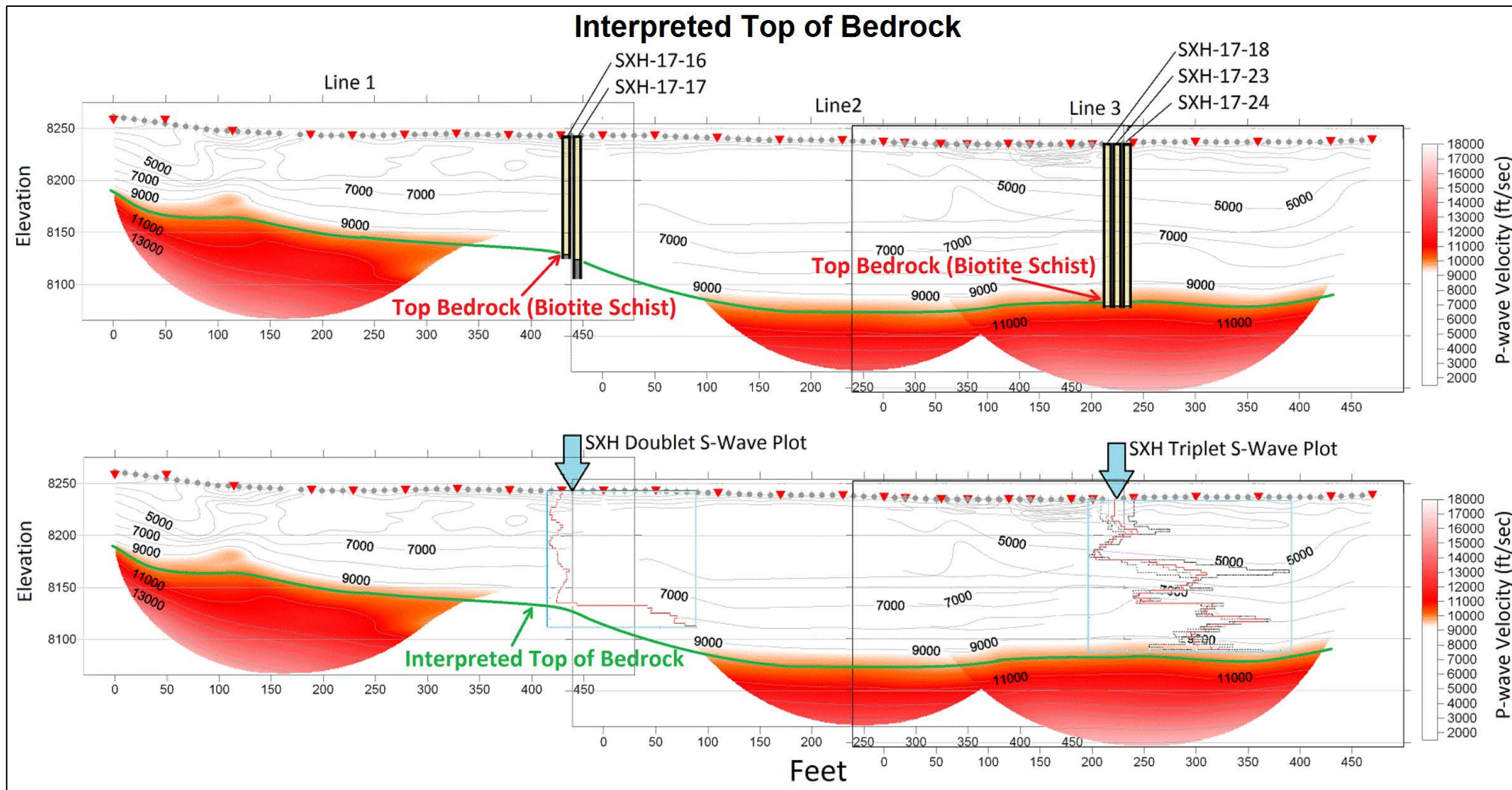
Figure 29 – P-wave velocity tomography with crosshole s-wave velocity profiles and borehole data superimposed to show an overall interpretation of top of bedrock (green line). This example shows the close match between velocity structures at common points using the two seismic surveying techniques, with close agreement to borehole data.

At this particular study site, a very low velocity glacial overburden material is overlaying a very hard and fast biotite schist bedrock with minimal weathering at the interface. The bedrock encountered in the various boreholes was shown to be dipping slightly towards the right abutment, and this was captured almost perfectly by the refraction tomography results (see Figure 28 and Figure 29).

This geologic scenario enables the use of the seismic reflection technique described above for estimating an average interval velocity that corresponds to the overburden material at this site. Here, a one-second recording time was used during s-wave refraction surveying, providing adequate record length to capture a seismic s-wave reflection event from the soil/bedrock interface. A corresponding shot gather from this s-wave refraction survey is presented in Figure 30, showing an asymmetric hyperbola that exhibits a dipping move-out pattern resulting from the dipping bedrock. In this example, bedrock is known to be at a depth of approximately 150 feet below ground surface at the zero-offset location (where the shot is located and indicated with the red star in Figure 30). The associated two-way travel-time of the reflection event at this zero-offset location is approximately 300ms, so the observed average velocity of material above this interface (e.g., Quaternary foundation sediments) is equal to 160ft/(0.5*300ms)=1067ft/s.

This calculated average velocity matches almost perfectly with the recovered velocities from the s-wave refraction tomography, and from crosshole seismic profiling, where a Vs30 for the same location was calculated as 1,156ft/s. These average velocity values agree to within approximately 7% of each other. Had the depth to bedrock not been known, the NMO or DMO equation could be used to estimate the average stacking velocity of this reflection event, and then the two-way travel-time of the zero offset reflection could be used to calculate an approximate depth to the interface.

Note that while Granby Dike 3's geologic setting makes for a convenient comparison of this atypical approach to estimating Vs30, this technique is only applicable in cases where there is a sufficiently strong seismic impedance contrast between geologic layers (as observed at Granby Dike 3), and may not provide adequate information, depending on the geologic nature of a given site, and the corresponding seismic data. Furthermore, seismic reflection data are not typically available, and reflection events such as observed at Granby Dike 3 are not common in refraction data.
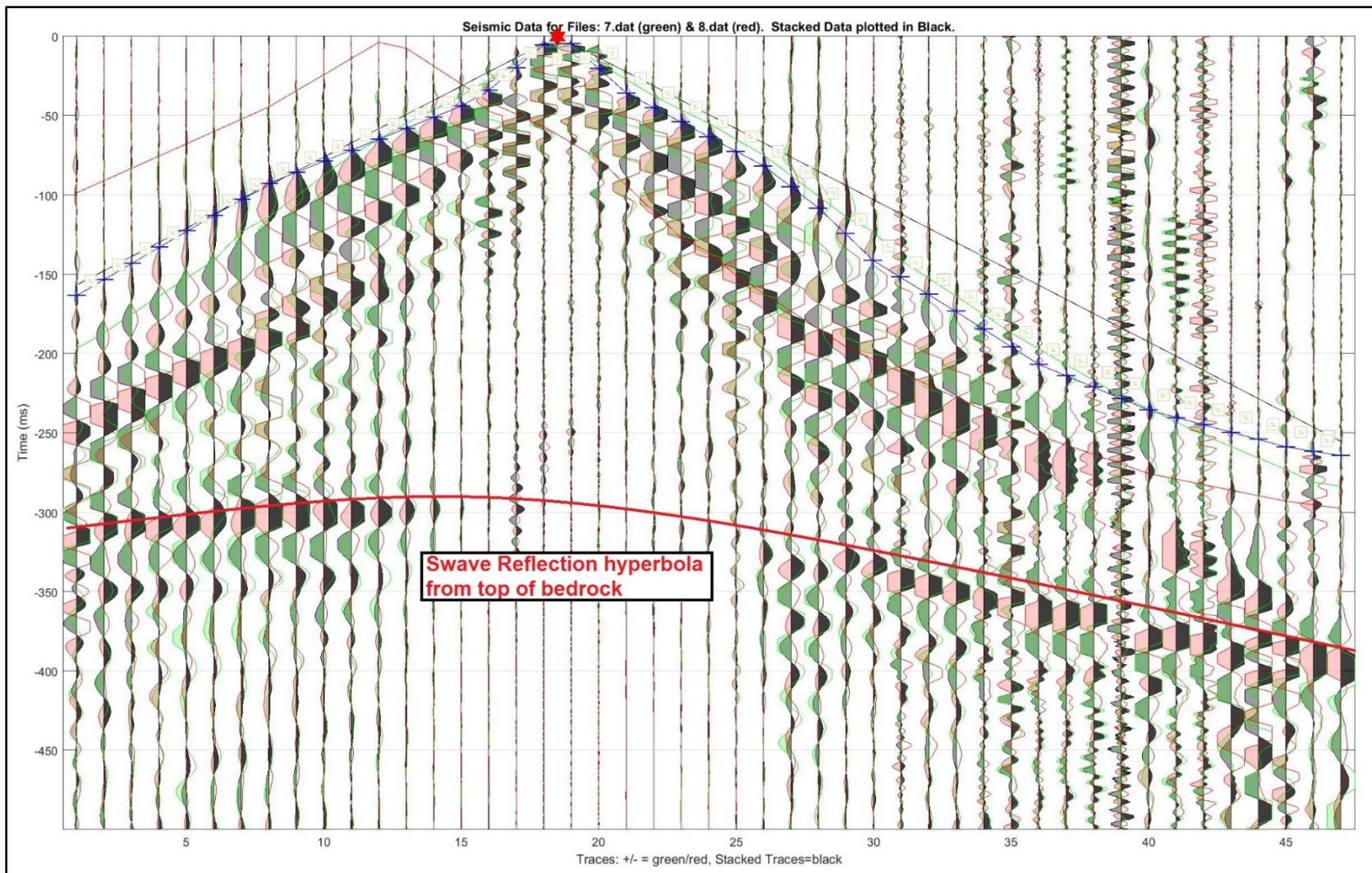
Figure 30 – Example of a strong reflection event observed in seismic refraction data (refracted first arrivals indicated with blue dashes) collected along the downstream toe of Granby Dike #3, near Granby Colorado.

D.   Foster Dam: The Benefit of 2D Imaging in Complex Geology

As an additional brief example of refraction velocity tomography's ability to perform well in relatively challenging (noisy) field conditions and in the presence of complex geologic structures (e.g., complex foundation contact and bedrock geometries), results are presented from a series of surveys performed by Reclamation on behalf of the USACE at Foster Dam (Rittgers 2018). Tomograms from eight separate refraction tomography surveys are presented as aerial imagery overlays in Figure 31. Here, we see the value of 2D tomography velocity models, in that they can be used to reveal complex geologic structures and lateral variations in seismic velocities needed for more comprehensive site characterization and subsequent seismic hazard analysis efforts.

In this particular example taken from Foster Dam, a suspected fault is located directly at the left side of the concrete spillway structure where a known prominent shallowing of seismically fast bedrock can be observed in the tomograms (see tomogram SL2b in Figure 31), with a corresponding deepening and slowing of bedrock velocities on the opposite side of the concrete spillway (tomograms SL1 and SL6 in Figure 31).
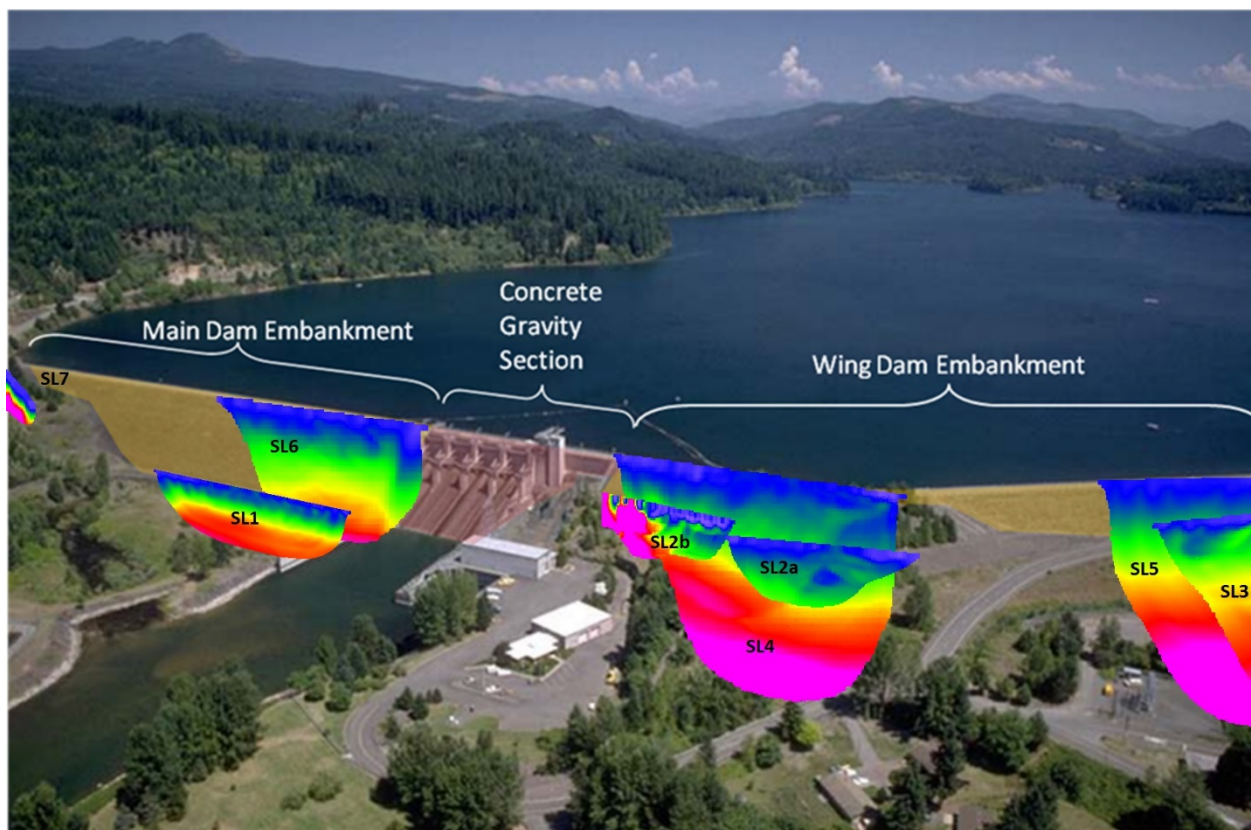
Figure 31 – Example of seismic refraction tomography results for data collected at Foster Dam in Oregon. Here, several 2D velocity tomograms are graphically overlain on an aerial photo of Foster Dam, depicting the approximate 3D distribution of seismic s-wave velocities within and below the earthen embankment structure.

E.   Boca Dam: Comparing 1D Crosshole profiling, 1D FWS Logging, 1D MASW, and 2D Refraction Tomography

Boca Dam serves as an opportunity to compare four different seismic surveying techniques, including 2D refraction tomography, FWS logging, crosshole seismic profiling, and active and passive MASW (Rittgers 2014a). Figure 32 presents the locations of various seismic survey data types collected at Boca Dam, where a 43 channel seismic sensor array was placed along the downstream toe of the embankment near and extending between previously conducted FWS and crosshole survey locations (see projected survey locations along tomogram in Figure 34). This seismic array served to collect both 2D tomography profiles and 1D MASW soundings, which were conducted in 2017 specifically to support this study.

The s-wave refraction tomography survey conducted at Boca Dam offers a good example of the challenges of background seismic noise levels often encountered at embankment dams due to high-energy water conveyance through power tunnels, downstream outlet works, and over spillways. Figure 33 shows three shot-gathers for s-wave refraction data collected with the seismic source placed at channel 1 (top plot), near the center of the sensor array (center plot), and placed at the opposite end (bottom plot). Here, Noise from these sources becomes problematic with increasing source-receiver offsets. Here, strong noise contamination is observed with end-shots (source placed at the left or right end of the array as depicted with the red star in the top and bottom plots), and the best signal-to-noise ratio is observed with a center shot location where the source-receiver offsets are at a minimum (center plot). This background noise can create significant challenges to accurately picking coherent first arrivals of refracted s-wave energy at far offsets, resulting in inaccurate velocity models (incorrect picks) or limited depths of investigation (omission of far offset picks). However, this background noise also serves as a good source of seismic energy for sake of conducting passive MASW soundings (see MASW Vs profiles in Figure 35, where MASW3 was obtained with passive MASW data).
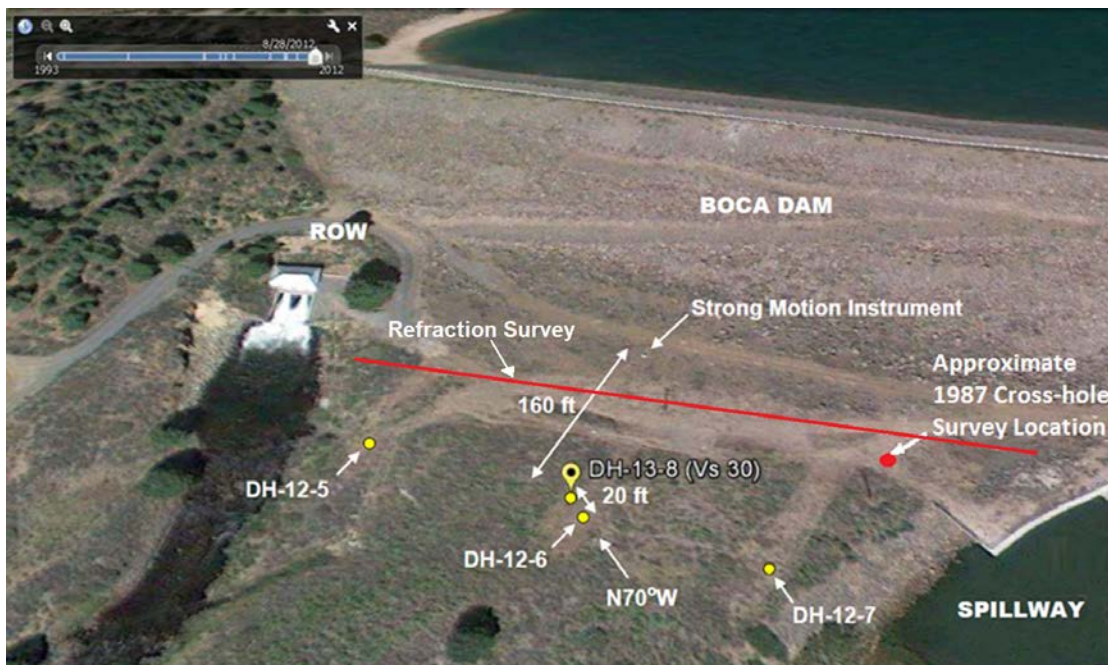
Figure 32 – Locations of various seismic survey data types collected at Boca Dam.
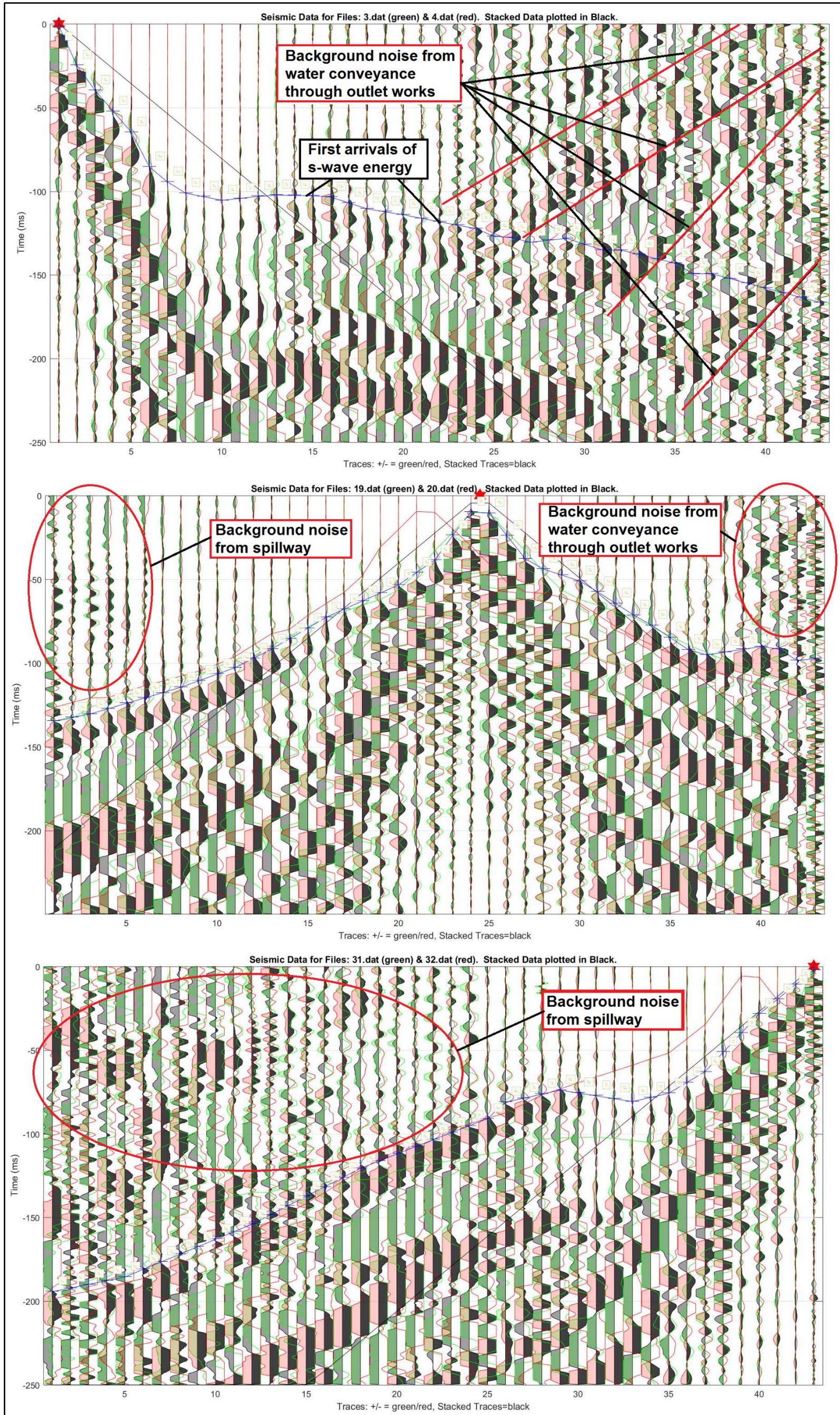
Figure 33 – Three shot –gathers for s-wave refraction data collected at Boca Dam, showing noise contamination from sources located off-end from the sensor array.
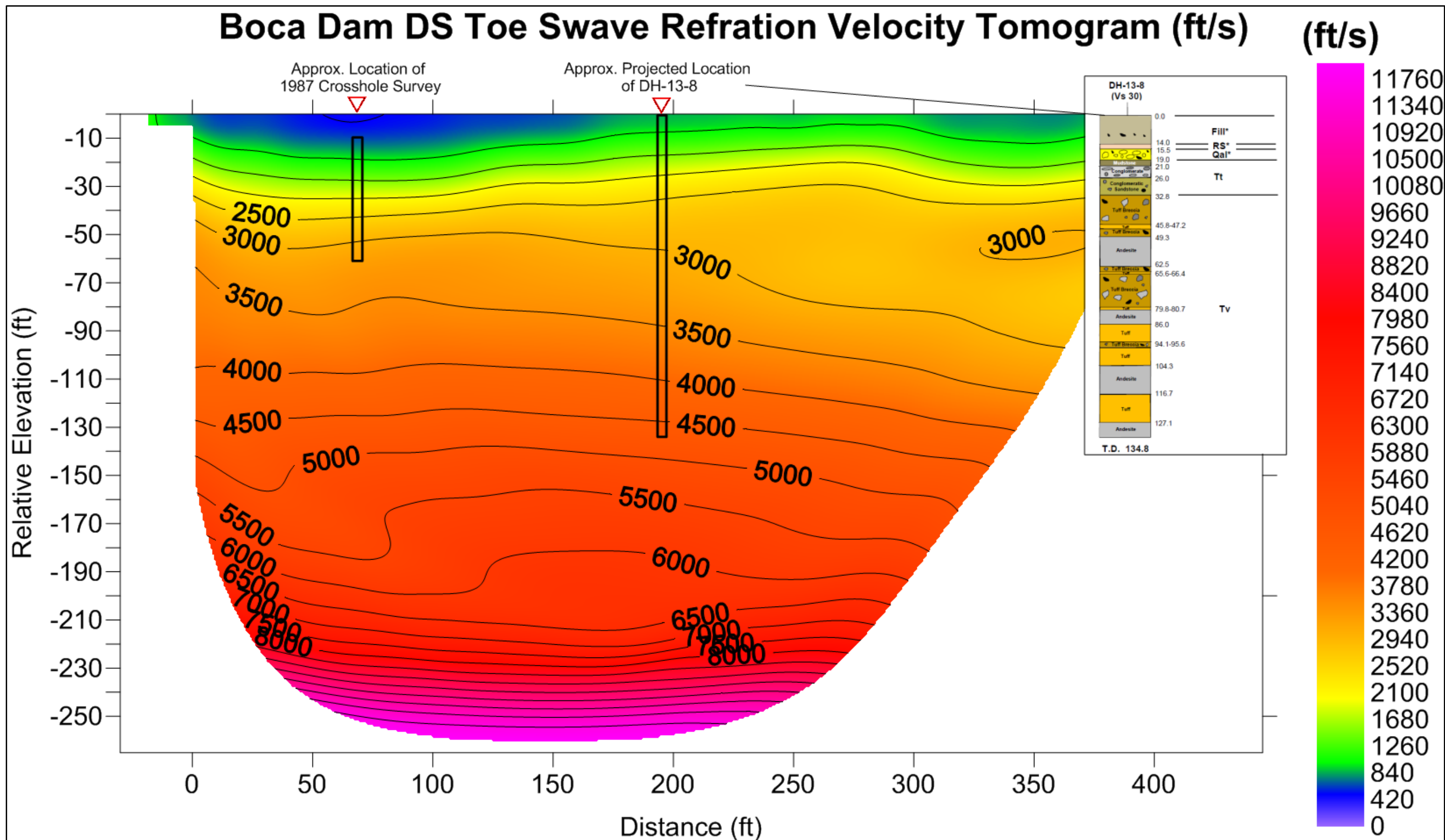
Figure 34 – S-wave tomogram for seismic s-wave refraction tomography survey performed along the downstream toe of Boca dam.
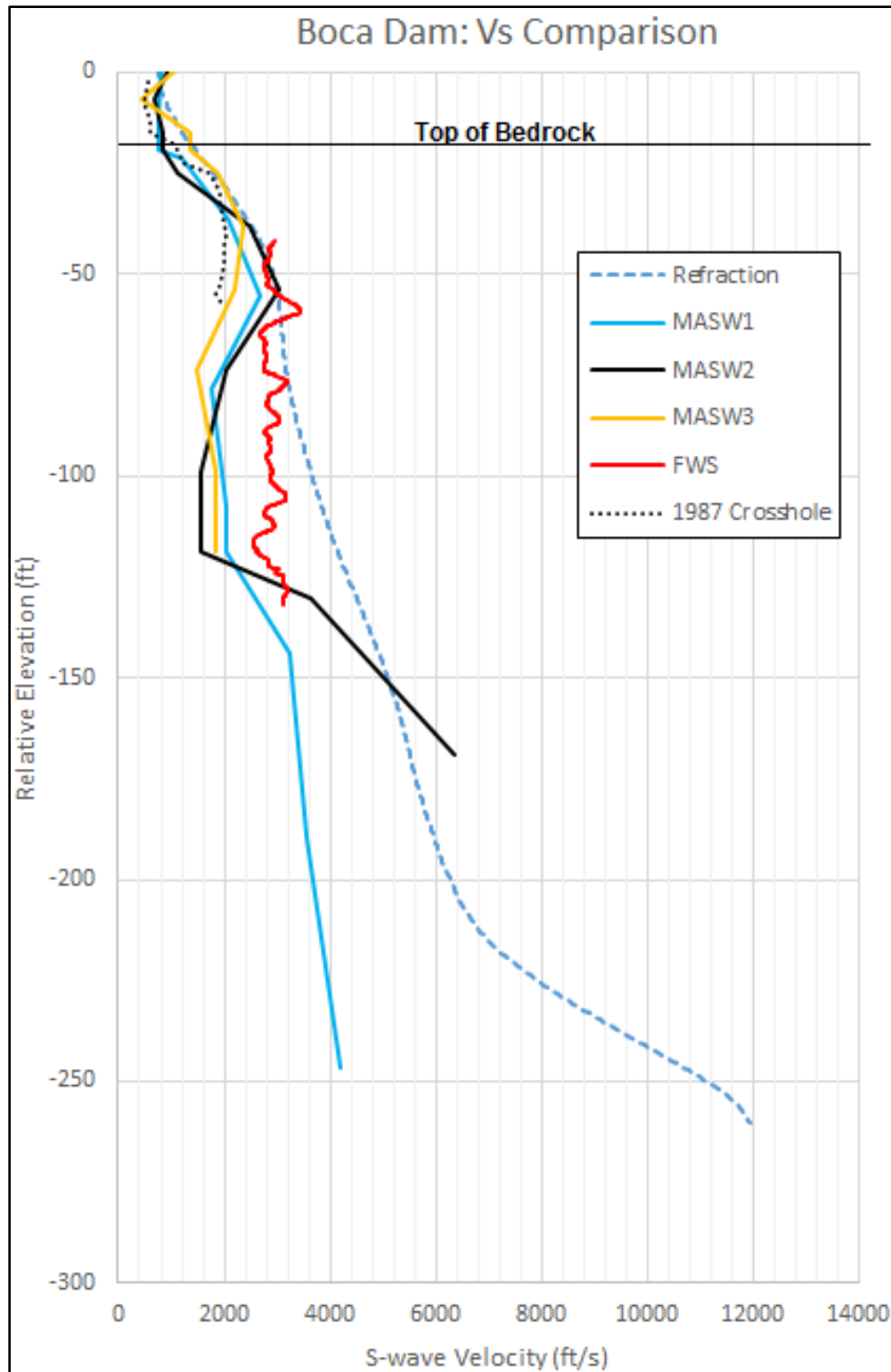
Figure 35 Plots of s-wave velocities obtained at Boca Dam from various seismic testing, including 2017 seismic refraction tomography (blue-dashed line) and three different 2017 MASW soundings, a 2012 FWS profile (red line), and 1987 cross-hole profile (black dotted line) as a function of relative elevation. Top of bedrock is annotated on the figure.

The Vs profiles and final calculated Vs30 values for each survey technique are presented in Figure 35 and **Error! Not a valid bookmark self-reference.**, respectively. The final FWS Vs30 value of 2402 ft/s is in very close agreement with the Vs30 value of 2865 ft/s calculated using depth-averaged velocities from the s-wave refraction tomography results at the same location. A relatively good match in calculated s-wave velocities from the FWS logging and the other data types offers confidence in the results provided by this method within hard rock environments (see Figure 35 and **Error! Not a valid bookmark self-reference.**). Note that the 1987 crosshole is labeled as "fair" in **Error! Not a valid bookmark self-reference.** due to the limited depth coverage and the need for extensive extrapolation for Vs30 calculations. It should also be noted that, similar to the example study presented below for Ochoco Dam, indications of lithology and fracturing (interbedded volcanic tuff and basalt layers) can clearly be seen in the FWS data and calculated velocities at Boca Dam.

Table 5 – Comparison of Vs30 Values obtained using various data types from Boca Dam, California. The FWS and crosshole data are considered "fair quality" for calculating a Vs30 value due to limited depth coverages.

Data Type	Quality	Vs30 (ft/s):
2017 2D Tomography	Good	2909
2012 FWS	Good	2402
1987 Crosshole	Fair	1908
2017 Active MASW1	Good	1817
2017 Active MASW2	Good	1806
2017 Active MASW3	Good	1761
Mean of All Values (ft/s):	2101	
Max Deviation of All Values (ft/s):	1148	
Max % Deviation from Mean:	16	

F.   Ochoco Dam: Comparing 1D Crosshole profiling and 1D FWS Logging

Previous seismic surveys conducted at Ochoco Dam near Prineville, Oregon provide a good opportunity to further compare and evaluate FWS logging relative to crosshole seismic profiling results (Rittgers 2014b). This example also provides a good example of the detail captured in FWS data, where the technique can be implemented as a continuous profile with measurements nominally every 5cm along the borehole. Despite spatial averaging of material properties between the source and receivers, FWS is demonstrated to be a highly sensitive instrument to subtle vertical fluctuations in seismic impedance. Figure 36 presents an example of FWS data recorded at Ochoco Dam, where four channels of recorded waveforms versus depth are plotted on the leftmost four plots, followed by the semblance plot used for picking arrivals. Here, the corresponding lithologic units observed in geologic cores are indicated on the right-side of Figure 36, vertically aligned with the FWS data to demonstrate the expression of lithology/physical properties captured by FWS.

Similarly, Figure 37 presents these FWS data (the four channels of recorded FWS waveforms versus depth plotted on the leftmost four plots), followed by the semblance plot used for picking arrivals, and the calculated p-wave and s-wave velocities and corresponding Vp/Vs ratio values

in the right-hand plots. These same FWS-derived p-wave and s-wave velocities are plotted with crosshole velocity profiling results in Figure 38 and Figure 39. Note the strong match between the two data types collected in both crest and downstream toe boreholes, and also the strong correlation between FWS data and observed volcanic bedrock intervals. Here, we see a good match between FWS logging velocities and bedrock lithology (Figure 36 and Figure 38) and also between velocities derived using FWS and crosshole profiling approaches. While there is no direct overlap in crosshole and FWS depth coverages, the velocities show reasonable continuity across a data gap at the top of bedrock (see Figure 38 and Figure 39). This offers confidence that FWS-derived velocities are adequately accurate for the sake of calculating Vs30 values. In this example, Vs30 values are presented for three depth intervals, and using two different data interpolations across a data gap across the top of bedrock. Here, Vs30 has been calculated from the ground surface, from the foundation contact, and from top of bedrock.

It should be noted that the crosshole surveys performed at Ochoco Dam demonstrate typical lateral variations in both contact elevations and seismic velocities of layers across an embankment site. Here, dipping geologic or engineered material contacts result in corresponding velocity profile patterns that have vertical offsets from one another, and lateral variations in physical properties of these materials result in different velocities within each layer (see crosshole velocity profiles plotted in Figure 38 and Figure 39. While the crosshole Vs profile variations observed at Ochoco Dam are relatively minimal, complex geologic structure can lead to significant variations in profiles and associated Vs30 values. Therefore, care must be used in placement and utilization of crosshole data for Vs30, where the survey should be placed in a location that is considered most representative of the embankment's foundation.

Furthermore, soil profiles can be compacted under the weight of embankment structures, and this compaction and increased confining stresses can increase the seismic velocity of vertical wave propagation within these materials relative to adjacent areas not beneath the structure. Therefore, engineers and seismologists should consider performing seismic profiling within foundation materials below the structure. This is especially the case for soft soil sites, where the foundation materials are seismically slow, and minor variations in measured velocity could have significant effects on subsequent analysis outcomes (e.g., if a layer is close to the limit of liquefaction potential). In these circumstances, the added cost of borehole placement through the embankment structure may be justified, in order to obtain *in-situ* velocities beneath the foundation contact.
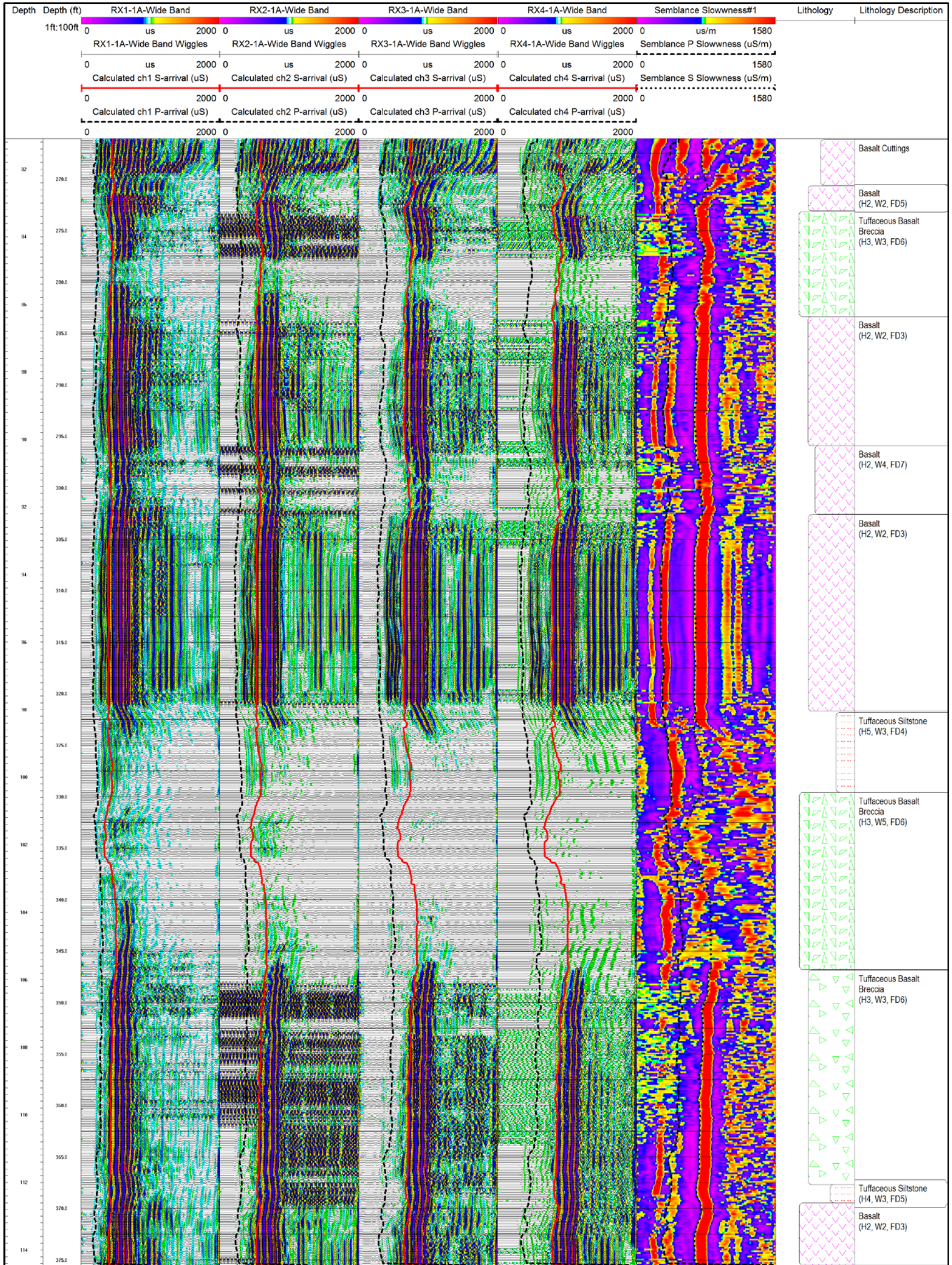
Figure 36: FWS data recorded at Ochoco Dam near Prineville, Oregon. From left to right: Wide-band data plotted in time (uS) versus depth for receivers 1 through 4 (with associated calculated arrival times plotted), Semblance plot of slowness (uS/m) versus depth (with P and S-wave slowness picks plotted), bedrock lithology log, description log with hardness/weathering/fracture density indices.
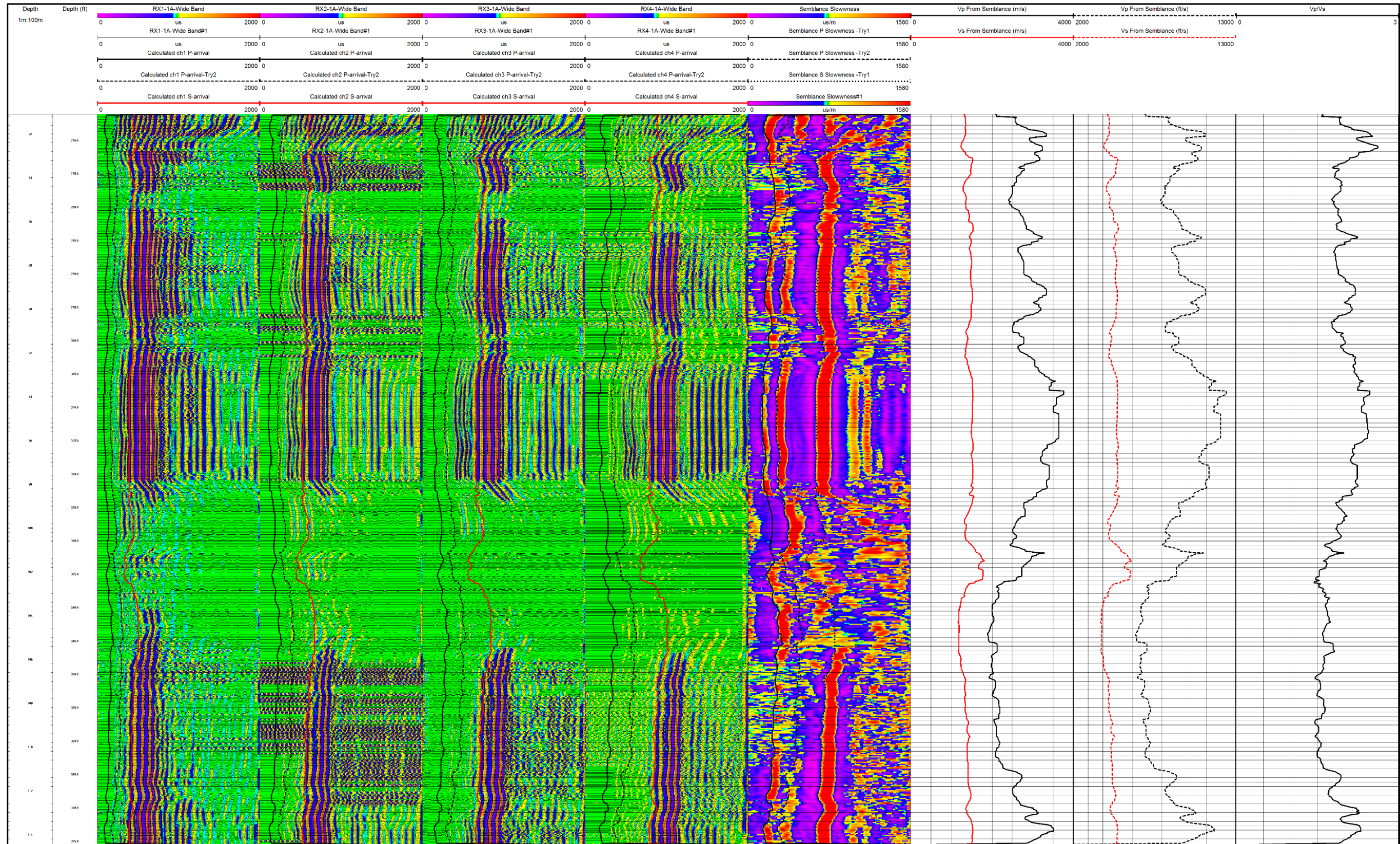
Figure 37 - Full wave sonic logging data recorded at Ochoco Dam near Prineville, Oregon.
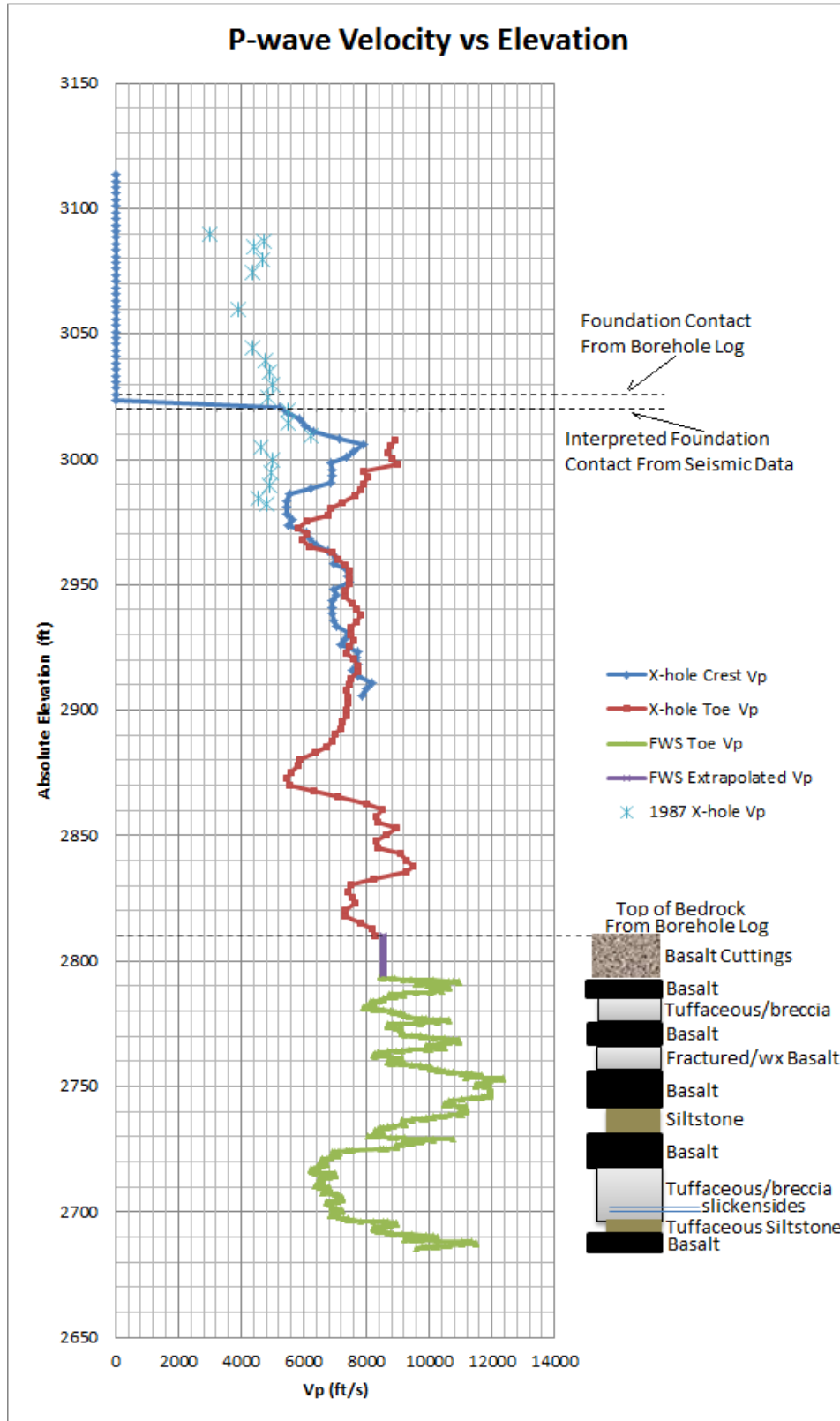
Figure 38 – Seismic p-wave velocities plotted versus absolute elevation for FWS and crosshole data collected at Ochoco Dam near Prineville, Oregon.
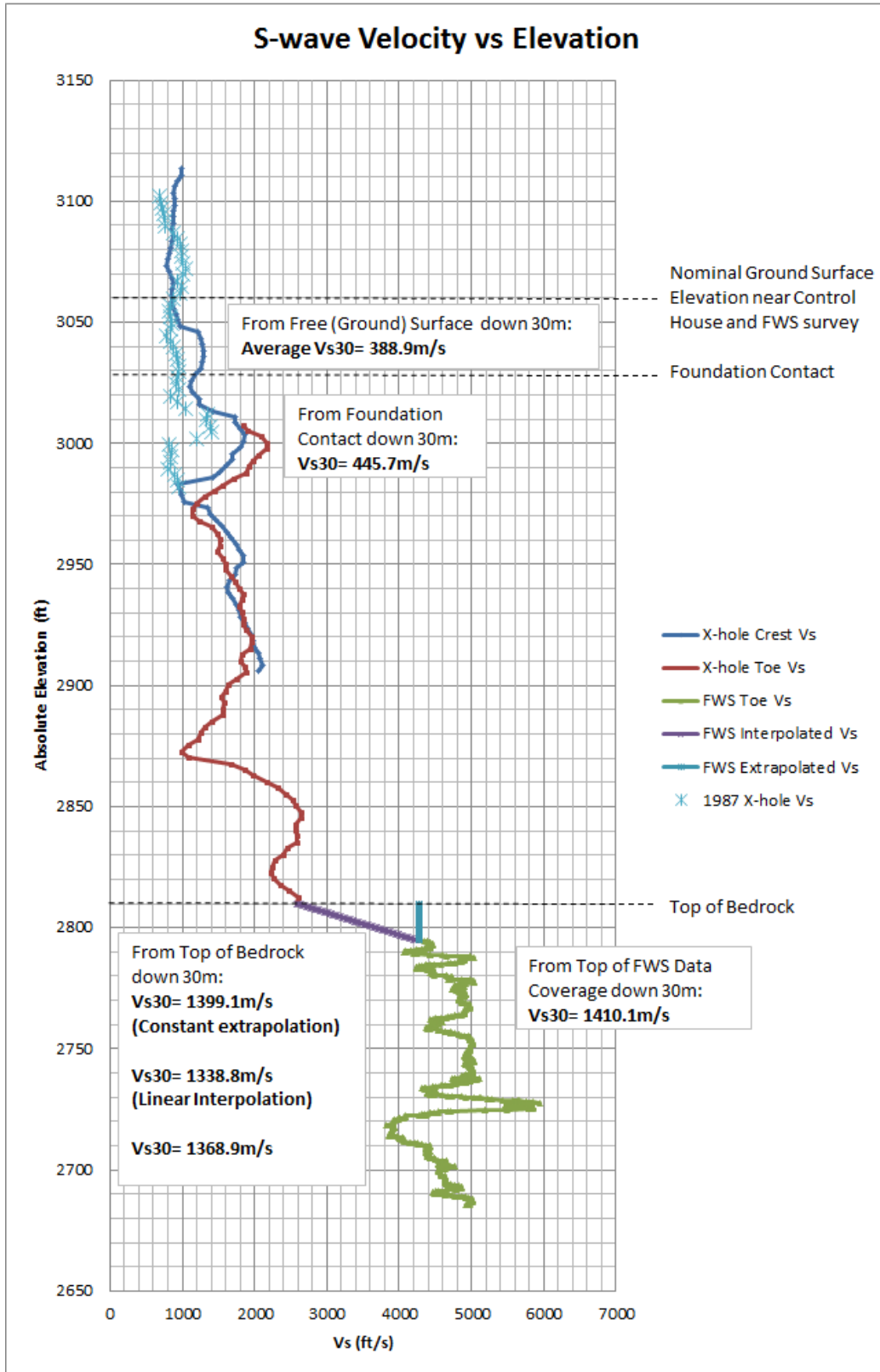
Figure 39 - Seismic s-wave velocities plotted versus absolute elevation for FWS and crosshole data collected at Ochoco Dam near Prineville, Oregon.

G. Huntington North Dam: Comparing 1D Crosshole profiling and 1D FWS Logging

As part of prior field investigations performed at Reclamation's Huntington North Dam, a series of both crosshole seismic surveys and FWS logging surveys were performed at various locations across the facility (Pierce 2012). This serves as a good opportunity to compare the results of 1D FWS and crosshole profiling for this study. In this example, 1D FWS logging data were collected at survey location Vs12-30 at the downstream toe of the West Main Dam, while 1D crosshole seismic profiling data were collected through the East Main Dam embankment at survey location SW12-3 (see Figure 40). Here, the crosshole triplet was placed on the embankment crest, and the data coverage extended through the unconsolidated embankment and foundation materials and approximately 45 feet into the underlying Mancos Shale bedrock. This 45 depth interval of crosshole data coverage allows for a reasonable comparison with the nearby FWS logging data collected at Vs12-30.

Figure 40 – Locations of various 1D crosshole seismic profiling surveys (red labels) and 1D FWS surveys (blue labels) conducted at both the west and east main sections of the Huntington North Dam facility in Utah.

In this Huntington North Dam example, the two data types were collected at different locations, and so data alignment is required to make a comparison of velocities obtained in each survey. Here, the data are aligned based on stratigraphy, as opposed to elevation, because of an approximate 15 foot dip in the Mancos Shale bedrock interface between the two test locations. Figure 41 shows a comparison of the two data types, where the top of bedrock has been used to align the two data types. As seen in Figure 41, there is an excellent match between the two seismic survey techniques (discounting the interval velocity profile, which has a tendency to diverge from the measured velocities in the presence of refracted arrivals), where both the absolute value of s-wave velocity is matched well between the near/far receiver crosshole profiles and the FWS profile. Furthermore, the same patterns of vertical variation of velocity are seen within the shale bedrock interval of both data types (e.g., see step-over in velocities near an elevation of 5730 ft in Figure 41).

Table 7 presents the various Vs30 values (top of Vs30 depth interval is top of bedrock in this case) and associated statistics calculated using the FWS and crosshole data collected at Huntington North Dam. Here, the crosshole interval velocity is labeled "bad" due to a likely bias resulting from refracted arrivals at the far receiver, and has been omitted from the Vs30 statistics at the bottom of Table 7 accordingly. This problematic phenomenon in crosshole data, as discussed earlier, causes non-representative variations in the calculated interval velocity profile.

Relatively minor discrepancies between the two data types could be due to either processing errors in either data type (e.g., first arrival picking or crosshole deviation surveys), or could be the result of anisotropy of the shale bedrock. Here, the crosshole seismic survey technique measures vertically polarized and horizontally propagating s-waves and the FWS logging survey technique predominantly measures horizontally polarized and vertically propagating s-waves. While it is difficult to say if the difference between FWS and crosshole profiles is due to anisotropy or biases introduced by processing errors, the variance is still within a reasonable range for the sake of utilizing either data type for Vs30 calculations. It should be noted that the FWS velocity profile is well within the bounds of error of the crosshole velocity profiles, where a 500 ft/s or more variance is observed in the crosshole data alone.

Table 6 – Comparison of Vs30 Values obtained using crosshole and FWS data from Huntington North Dam, Utah.

Data Type	Quality	Vs30 (ft/s):
FWS Logging	Good	3996
Crosshole (near receiver)	Good	3114
Crosshole (far receiver)	Good	3703
Crosshole (near-far interval)	Bad	4388
Mean of "good" values (ft/s):		3833
Max Deviation of "Good" Values (ft/s):		882
Max % Deviation from Mean:		19
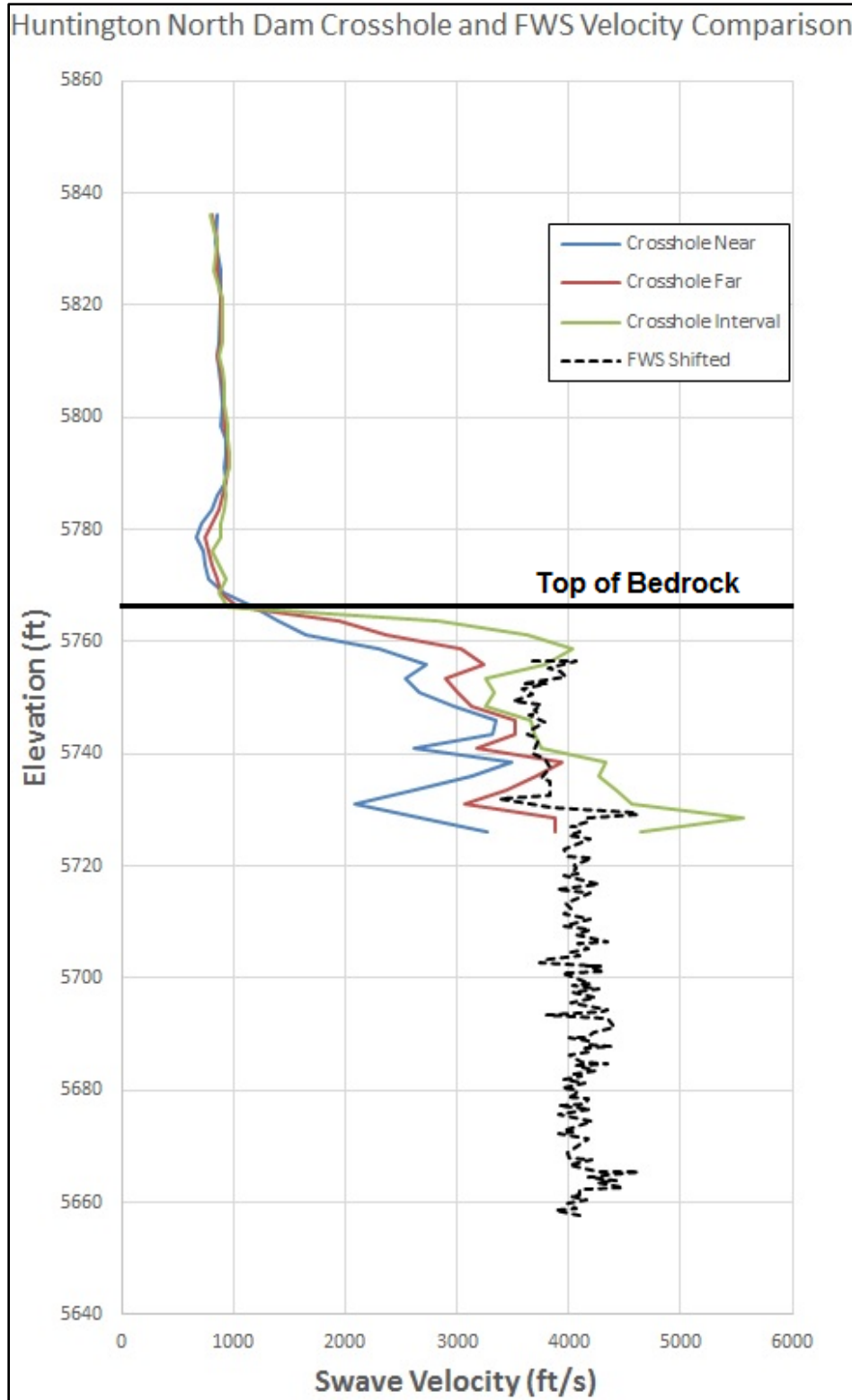
Figure 41 –Comparison of Huntington North Dam crosshole and FWS seismic s-wave velocity profiles for data collected at different locations but with overlapping elevation coverage of the two data types.

H.   Hills Creek Dam: Comparing 1D Crosshole profiling, 1D Downhole VSP, 1D Sonic Logging, 2D Refraction Tomography, and 2D MASW

An interagency agreement between Reclamation and the USACE resulted in a unique opportunity to collect and compare results for multiple seismic survey techniques conducted at several co-located points across Hills Creek Dam, Oregon (USACE 2018; Rittgers 2017b). Specifically, seven borehole locations were utilized to collect both 1D downhole s-wave VSP profiling data and 1D suspension logging data (e.g., sonic logging). One of these seven borehole locations was also installed as a cross-hole triplet, where suspension logging, downhole VSP profiling and crosshole seismic profiling surveys were performed for comparison of results (see DH-16-01, DH-16-02, and DH-16-03 on Figure 42). Furthermore, a series of 2D seismic s-wave refraction tomography surveys and 2D MASW profiles were collected near or at each of the borehole locations (see red and blue lines on Figure 42, respectively). These co-located datasets offer an excellent opportunity to compare the various techniques and their associated benefits and limitations for support of this study.
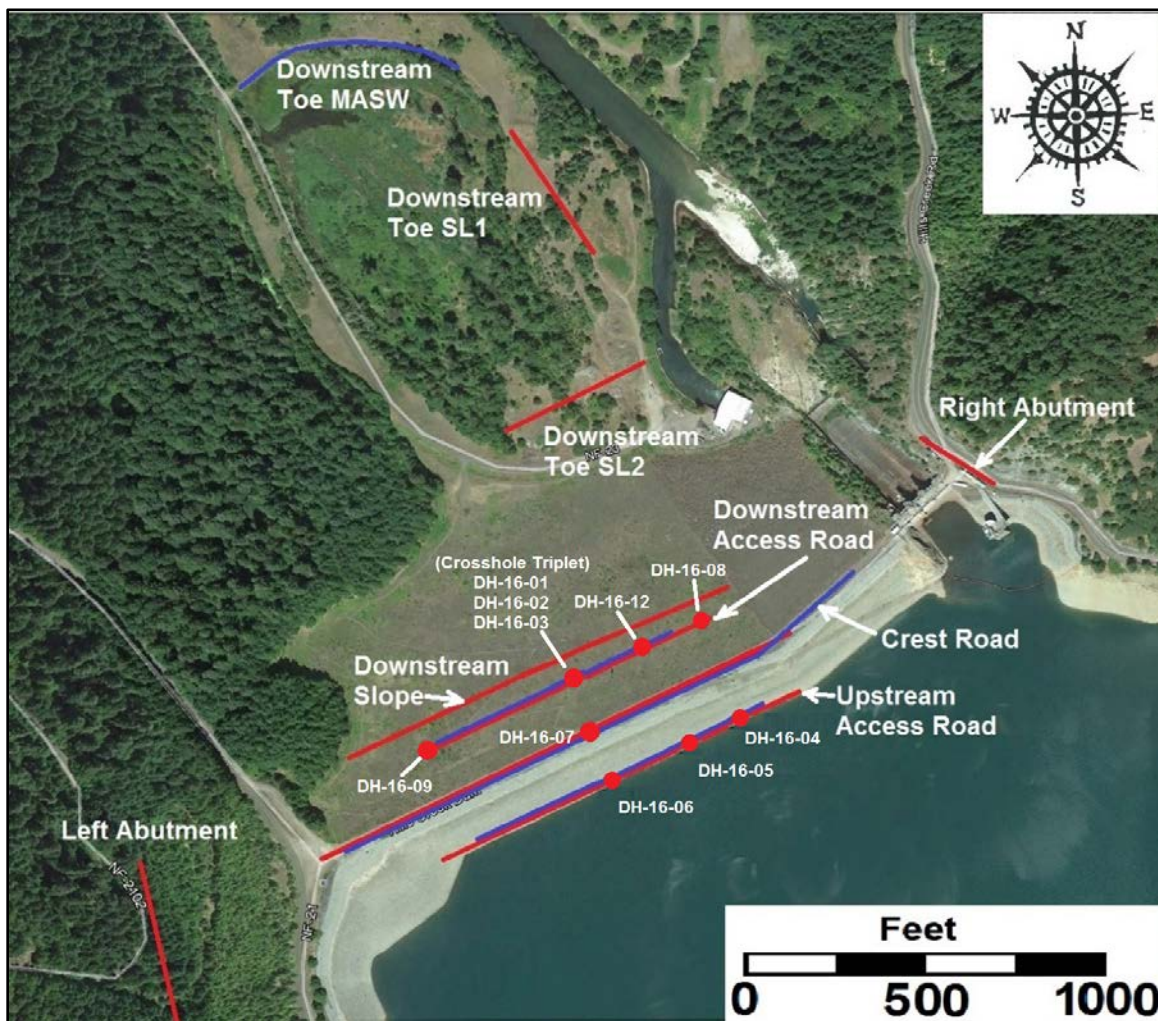
Figure 42 – Map showing eight borehole locations used for seismic surveying, and data coverage of surface-based 2D refraction tomography (red lines) and 2D MASW (blue lines) at Hills Creek Dam, Oregon.

In refraction tomography, raypaths can concentrate and propagate laterally in layers of low impedance. This effect reduces raypath coverage at deeper intervals and may mask lower velocity zones. Conversely, MASW can overcome these masking effects, but is prone to producing false heterogeneity when inconsistent soundings are stitched together develop profiles (each sounding is usually processed and modeled as a 1D velocity profile independently, resulting in modeling artifacts that appear as excessive lateral variations or "chatter" in recovered velocities). These false heterogeneities can be seen by comparison of 2D MASW and 2D refraction tomography results presented in Figure 43 for collinear surveys conducted across the downstream face of Hills Creek Dam (downstream access road depicted in Figure 42).

As described above, refraction tomography modeling can handle and account for both complex surface tomography and complex geologic/velocity structures without violating assumptions made in the processing workflow or compromising the accuracy or validity of the resulting velocity model. Conversely, MASW assumes that the ground surface is flat (minimal topography, or a constant slope) and also assumes that the underlying geologic structure and corresponding velocity structure is flat and layered (each layer is assumed to be flat with a constant thickness and velocity beneath the length of the surface geophone array used to collect each 1D sounding).
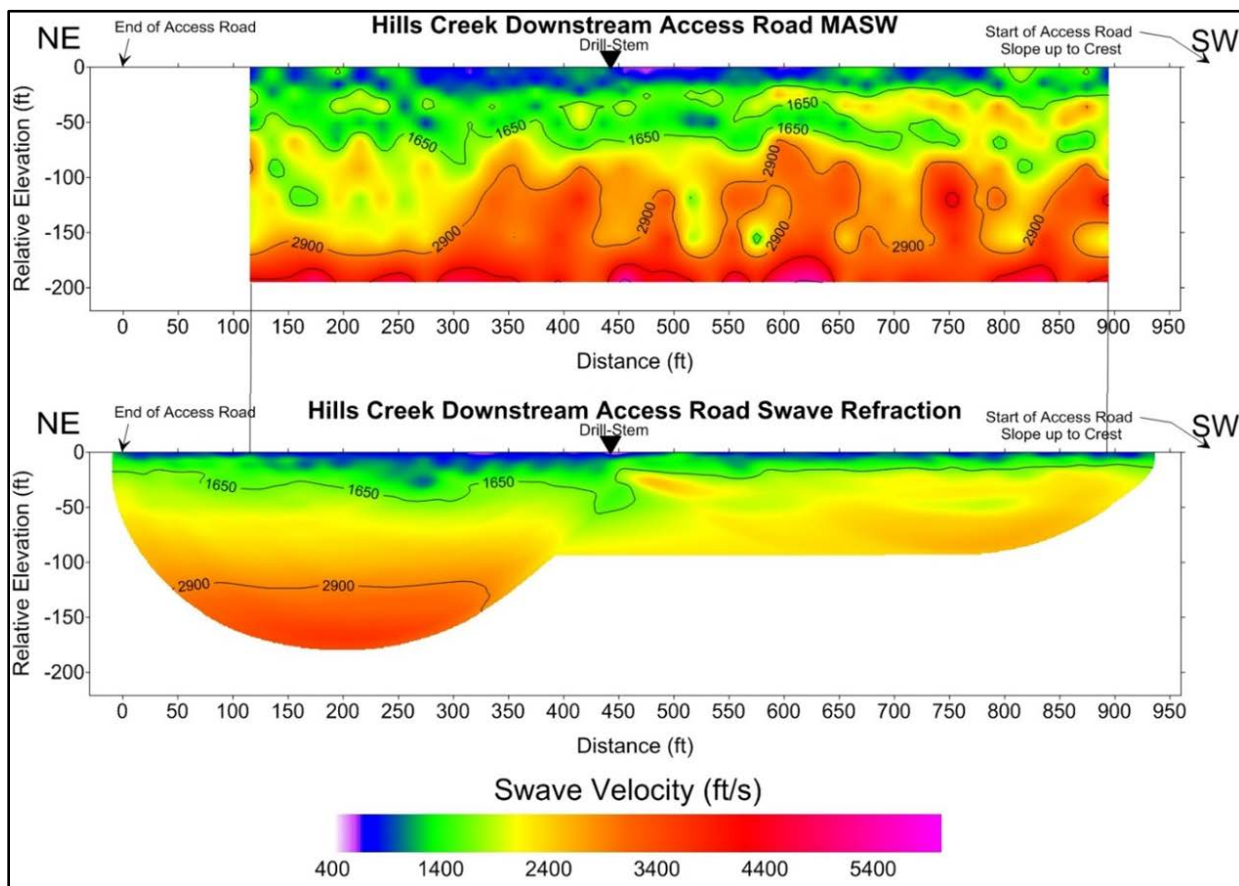
Figure 43 – Laterally-aligned 2D MASW s-wave velocity profile (top) and corresponding s-wave refraction velocity tomogram (bottom) for the downstream access road seismic line at Hills Creek Dam, Oregon. Viewer is looking upstream into each cross-section.

While these assumptions and inherent limits on the resolution and practical implementation of the SASW and MASW/ReMi techniques can be problematic in certain geologic scenarios and field site conditions, the general distribution of s-wave velocity from these surveys is most usually sufficiently similar to other techniques such as 1D crosshole profiling or 2D refraction tomography results for Vs30 calculation (e.g., see comparison of 1D and 2D velocity models presented in the right plot of Figure 15 and in Figure 43, respectively).

Figure 44 presents a detailed comparison of interpreted sonic logging and downhole VSP interval velocities extending through unconsolidated embankment and foundation materials and slightly into bedrock, as obtained within DH-16-07 at Hills Creek Dam. Here, the right-hand plot presents a scatterplot of all measured FWS and downhole VSP velocities as a function of depth, while the left-hand plot presents interpreted (averaged) velocities for interpreted layers (interpreted based on patterns observed in the velocity profiles in the right-hand plot). Recall that in the downhole VSP technique, interval velocities can become skewed due to refracted arrivals, as discussed above. Averaging segments of these velocity profiles, as is done on the left-hand plot of Figure 44, is often done to address this pitfall. However, this approach results in grossly averaged velocity "layers" and poses the risk of not accounting for potentially problematic slow layers. This challenge is addressed in more detail, as described in the following section from Cougar Dam downhole VSP surveying, where a new approach to processing VSP data was developed and presented here.

Figure 45 provides seven plots that each present overlays of Vs profiles obtained by FWS, downhole VSP, MASW and refraction tomography methods for seven boreholes located across Hills creek Dam. A significant caveat to presenting data in this way is that the 1D velocity profiles plotted for surface-based data types (e.g., 2D MASW and 2D tomography velocity profiles) have simply been extracted from the approximate location of a given borehole, but not the exact location. The various methods may be comparing velocities of elastic waves that have propagated along different paths through heterogeneous material. The biases and limitations of the various methods may also impact correlations (e.g., slow-velocity layer masking in refraction tomography).

Here, refraction Vs generally increase more monotonically with depth and exceed borehole methods at the deeper intervals. MASW profiles correlate more consistently with suspension or downhole methods and shows less of a monotonic response. The overall trend in MASW Vs, however, is still for the Vs to generally increase with depth. On the whole, surface Vs techniques appear to correlate better to suspension and downhole methods at shallower intervals, and then tend to diverge to higher Vs with depth. Note that the downhole VSP interval velocities in Figure 45 show the greatest variability, most likely resulting from issues caused by refracted arrivals (as presented above and addressed in detail in the Cougar Dam VSP section below).
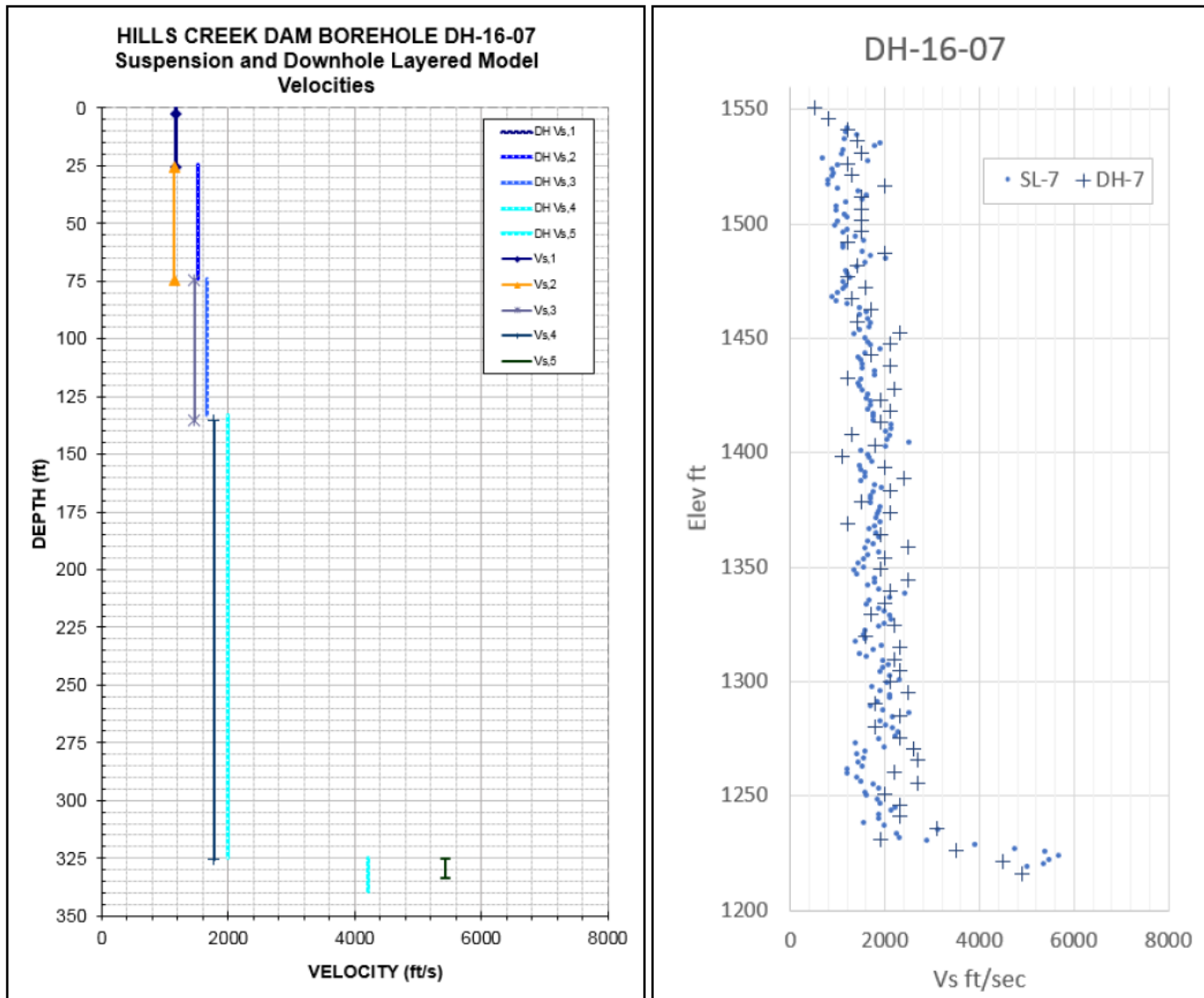
Figure 44 – Comparison of interpreted sonic logging and downhole VSP interval velocities (right plot) and VSP layered velocity model (left plot) for a single borehole at Hills Creek Dam.
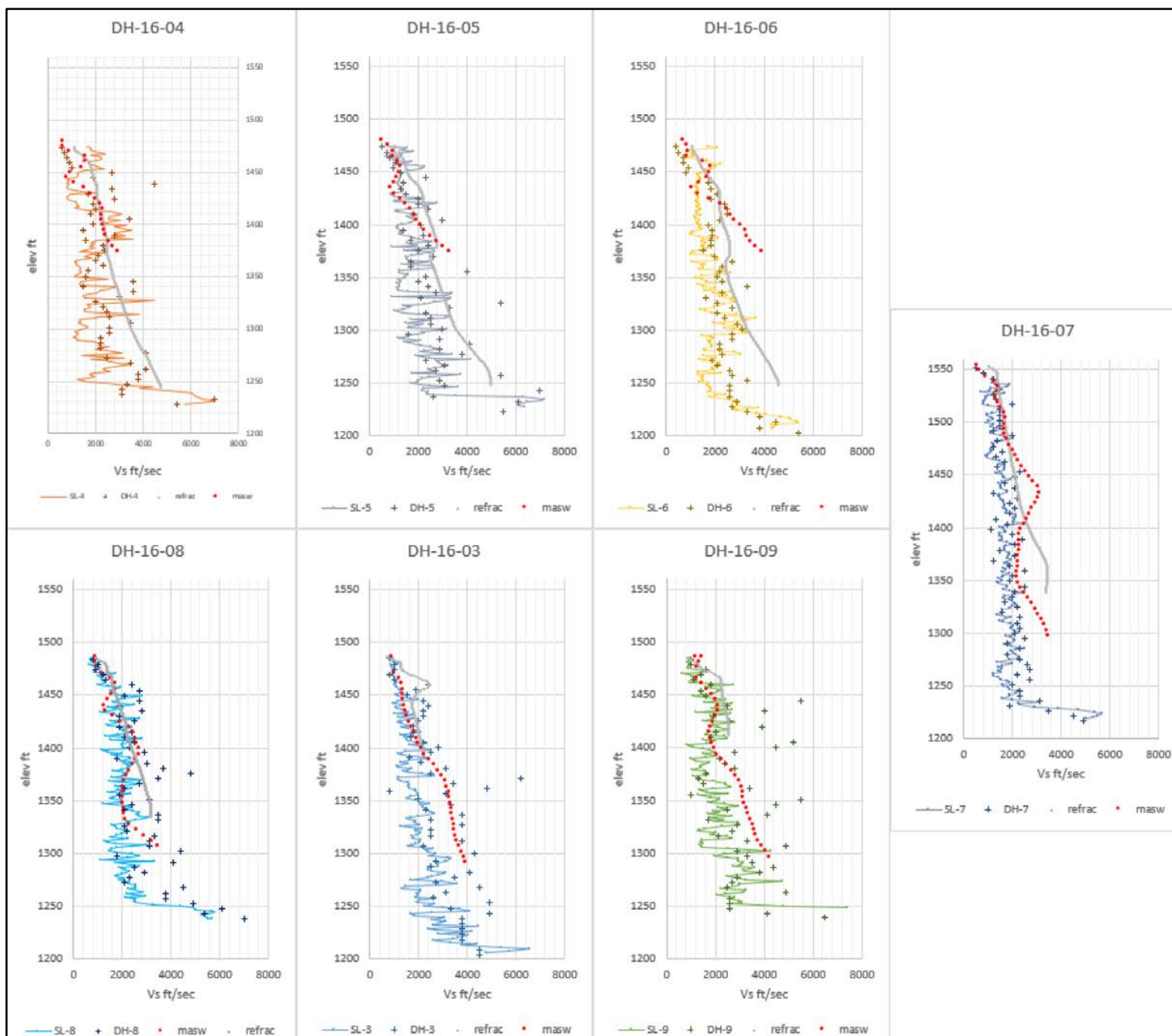
Figure 45 – Overview of comparisons of various co-located seismic data types collected within seven different boreholes at Hills Creek Dam, Oregon. Here, extracted refraction tomography velocities are plotted as grey solid lines, MASW velocities are plotted as red dotted lines, downhole VSP velocities are plotted with crosshair symbols, and sonic logging velocities are plotted as solid lines of various colors.

Lastly, Figure 46 presents a comparison of co-located crosshole seismic profiling, suspension logging and downhole VSP layered model velocity profiles within the crosshole triplet installed in downstream shell materials at Hills Creek Dam, Oregon (see DH-16-01 through DH-16-03 on Figure 42). Here, each measured crosshole and FWS velocity is plotted versus depth, while only the interpreted (e.g., highly averaged) layered velocity model derived from downhole VSP profiling results is plotted (solid green line plotted in Figure 46). Here, we see a very close match between the FWS and crosshole velocity profiles, and a similar match between the VSP layered velocity model and other data types.

Overall, these unique co-located seismic surveying datasets at Hills Creek demonstrate excellent agreement between Vs profiles obtained using the various survey techniques, especially within the uppermost 100 to 200 feet of depth coverage. While these various data are generally not located where one would normally calculate a Vs30 value (e.g., on or within an embankment structure), these data demonstrate the various techniques' abilities to provide sufficiently accurate seismic velocities within the required depth interval (ground-surface and down 30 meters) for providing a Vs30 value that will be within 10% of the assumed actual value (assuming crosshole seismic velocities as a benchmark technique).
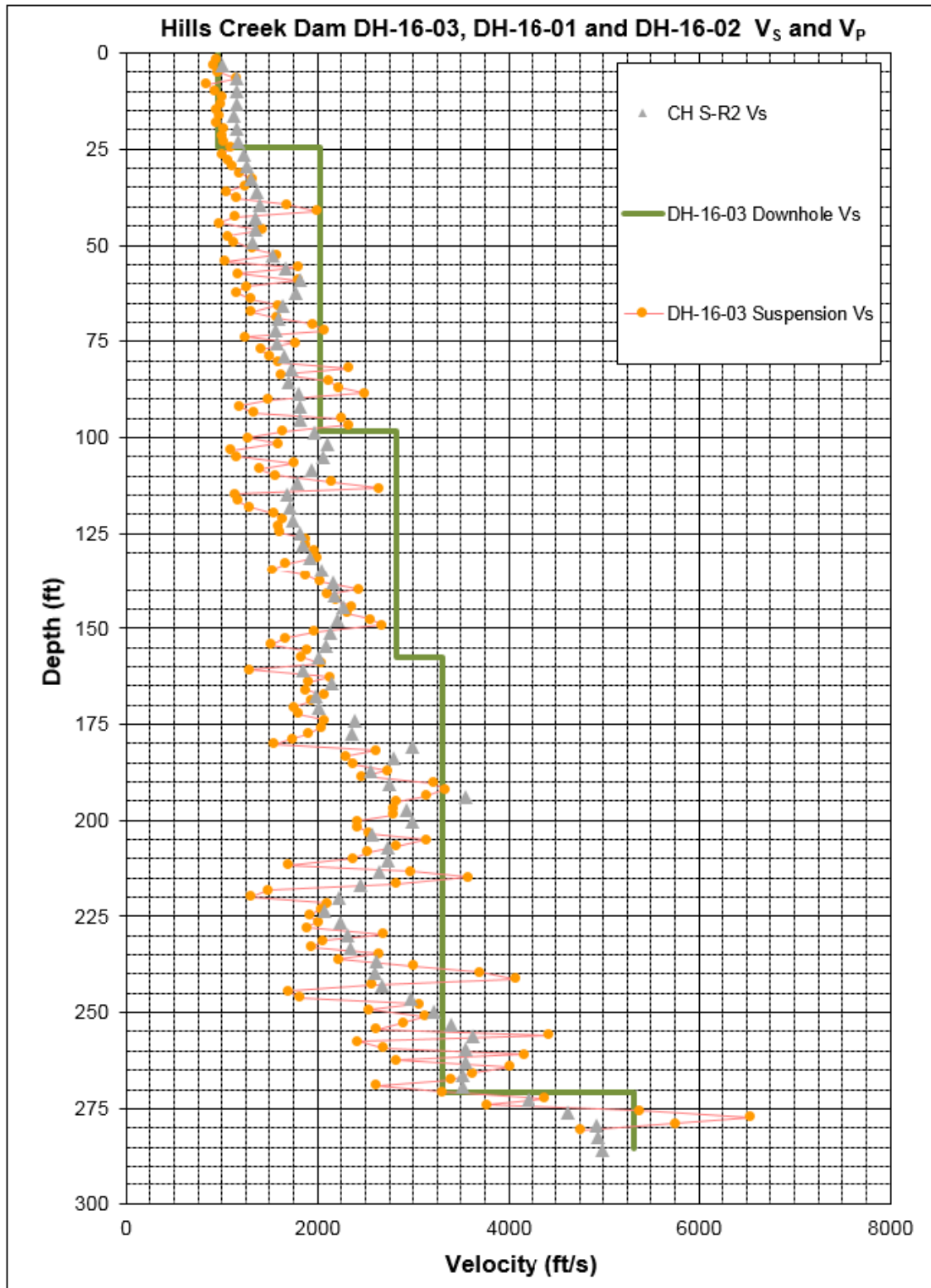
Figure 46 - Comparison of co-located crosshole seismic profiling, suspension logging and downhole VSP layered model velocity profiles within the crosshole triplet installed in downstream shell materials at Hills Creek Dam, Oregon.

I.   Cougar Dam: Downhole VSP Challenges and Development of New Processing Approaches

As part of a study performed at Cougar Dam in Oregon by Reclamation on behalf of the USACE (Rittgers 2017b), and in support of this study, extensive Matlab code was developed to extend the "Direct" and "Modified Interval" methods of downhole VSP data analysis described above (see Kim et al., 2017), in order to help address some of the pitfalls described above. This is achieved by accounting for all possible segmentations of depth intervals, or combination of downhole receiver/depth-pair spacing (pseudo-layers). The standard approach to implementing the Direct Method first requires the interpreter to visually identify "slope-breaks" within the first arrival picks. These slope-breaks theoretically represent interfaces between two different materials exhibiting different seismic velocities. The different velocities are represented by the supposed different slopes of first arrivals for a corresponding depth interval (slope = distance/time = velocity). However, depending on the nature of the seismic data, these slope-breaks are not always readily apparent, and the interpreter risks introduction of bias in the final calculated velocity profile.

Additionally, by fitting a line to a selected large set of first arrival picks representing an interpreted layer, the calculated velocity represents an average for the corresponding depth interval/assumed layer (e.g., see layered velocity model in Figure 46, as interpreted at Hills Creek Dam, Oregon). This averaging presents the risk of missing thin-beds (e.g., smaller depth intervals) that exhibit marked slower or faster velocities that may be of concern or of interest. Conversely, selecting every adjacent receiver/depth-pair for calculating velocities oftentimes introduces sensitivity to subtle errors in the exact arrival picks and corresponding arrival-time differences calculated for very closely spaced receiver depths. These arrival-time errors can introduce large errors in calculated velocities.

Furthermore, a particularly challenging aspect to downhole seismic data reduction is encountered when refraction of the downward-propagating wavefront occurs, resulting in seismic energy arriving at deeper receiver points at earlier times than above shallower receiver points/test-depths. This situation violates the assumptions used in velocity calculations, and the resulting calculated velocities are negative and not representative of the true interval velocities. This refracted arrival phenomenon is frequently observed within random rock-fill embankment materials, such as surveyed at Cougar Dam. This phenomenon is described quite eloquently by Michael C. Bailey in the following excerpt taken from Bailey (2018):

> *Stokoe (2000) and Lane (2014) describe elastic waves (e.g., S and P waves) being subject to perturbation in anisotropic media. Refraction of raypaths induce distorted wavefronts and quasi-propagation velocities. In a medium such as clayey sand, heterogeneity on the scale of individual particles is sufficiently random such that the material imparts no directionality to wave transmission on a macro scale and the material response to elastic wave propagation is essentially isotropic. The [Cougar Dam] embankment [zones and lifts] contain significantly more particle size variation on localized and macro scales and are expected to induce complex wave fields. There are innumerable potential perturbants within [these zones] and the longest and more vertical raypaths are likely to encounter the most. When the direction of propagation of a raypath is not normal to an*

interface with different impedance characteristics, refraction of the raypath occurs according to Snell's Law. The angle of incidence dictates the amount of refraction in the raypath. In the case of the [Cougar Dam zones], raypath refraction may occur at the boundary of an individual large clast or at the interface with a layer exhibiting relatively uniform impedance... The [Cougar Dam] embankment [zones and lifts] decidedly do not meet either fundamental assumption. Any horizontally layered anisotropy is assumed to be superimposed on significant local anisotropy dictated by wide grain size variation and the inclusion of large, rounded clasts. Raypath impedance is assumed to vary widely with azimuth around a given point within the shells.

Wide variation in downhole interval velocity profiles is the product of wave field complexity and not an accurate measure of the velocity calculated for discrete intervals. The direct method for downhole processing attempts to average sets of interval velocities that are likely significantly affected by material anisotropy.

Due to the vertical orientation of the raypaths and long distances between source and receiver, elastic wave velocity determined by the downhole method is expected to be the most affected by anisotropy-induced refraction and wave field distortion. ASTM D7400, Standard Test Method for Downhole Seismic Testing, includes the following caveat:

> *A fundamental assumption inherent in the test methods is that a laterally homogeneous medium is being characterized. In a laterally homogeneous medium the source wave train trajectories adhere to Snell's law of refraction. Another assumption inherent in the test methods is that the stratigraphic medium to be characterized can have transverse isotropy. Transverse isotropy is a particularly simple form of anisotropy because velocities only vary with vertical incidence angle and not with azimuth.*

Wide variation in downhole interval velocity profiles is the product of wave field complexity and not an accurate measure of the velocity calculated for discrete intervals. The direct method for downhole processing attempts to average sets of interval velocities that are likely significantly affected by material anisotropy.

In order to avoid these potential biases and pitfalls to VSP, the code described above was developed by Reclamation to extend the Direct Method to every permutation of pseudo-layer discretization, as exemplified in Figure 47 through Figure 49. Here, the p-wave first arrival picks are plotted as red points and the current segmentation is indicated with the blue line on the left-plots, the current segmentation's corresponding velocity profile is plotted in the center-plot, and the resulting cumulative sets of 1D velocity profiles for a given dataset/survey are plotted together, (along with the Interval and Modified Interval method results and median absolute deviation (MAD) weighted averages plotted as dashed green and dashed blue lines on the center and right-plots). The cumulative velocity profile plots on the right-side of Figure 47 through Figure 49 can be thought of as a statistical distribution of potential velocity values at a given depth where tightly-clustered velocity values for all segmentations at a given depth interval indicate a higher probability of that velocity being correct for a given depth interval.

The difference between the dashed-green and dashed-blue MAD-weighted averages on these figures corresponds to the manner in which a given segment's velocity was calculated (dashed-green for a line directly fit to the first and last pick of a given segment, dashed-blue for least-squares linear regression fit of all picks within a given segmentation). Final Direct Method results presented in the Results section below were obtained with the least-squares linear regression fitting of segmented picks, as this was deemed more accurate for a given segmentation/depth interval.

Lastly, it should be noted that an additional new approach to processing downhole VSP data was developed and tested on the Cougar Dam VSP data. This new approach involves inverse modeling of arrival times in a fashion similar to crosshole tomography which utilizes curved-ray tracing. While this new inverse modeling approach was successful at recovering accurate velocity profiles, it was deemed too unstable to present here as a reliable VSP processing technique. The instabilities observed in the new technique likely stem from a severe lack of aperture/no overlapping raypaths due to the simple seismic data acquisition geometry used in VSP surveys. Further development of inverse modeling approaches could prove useful in systematically accounting for and avoiding the pitfalls of refracted arrivals in downhole VSP survey data.
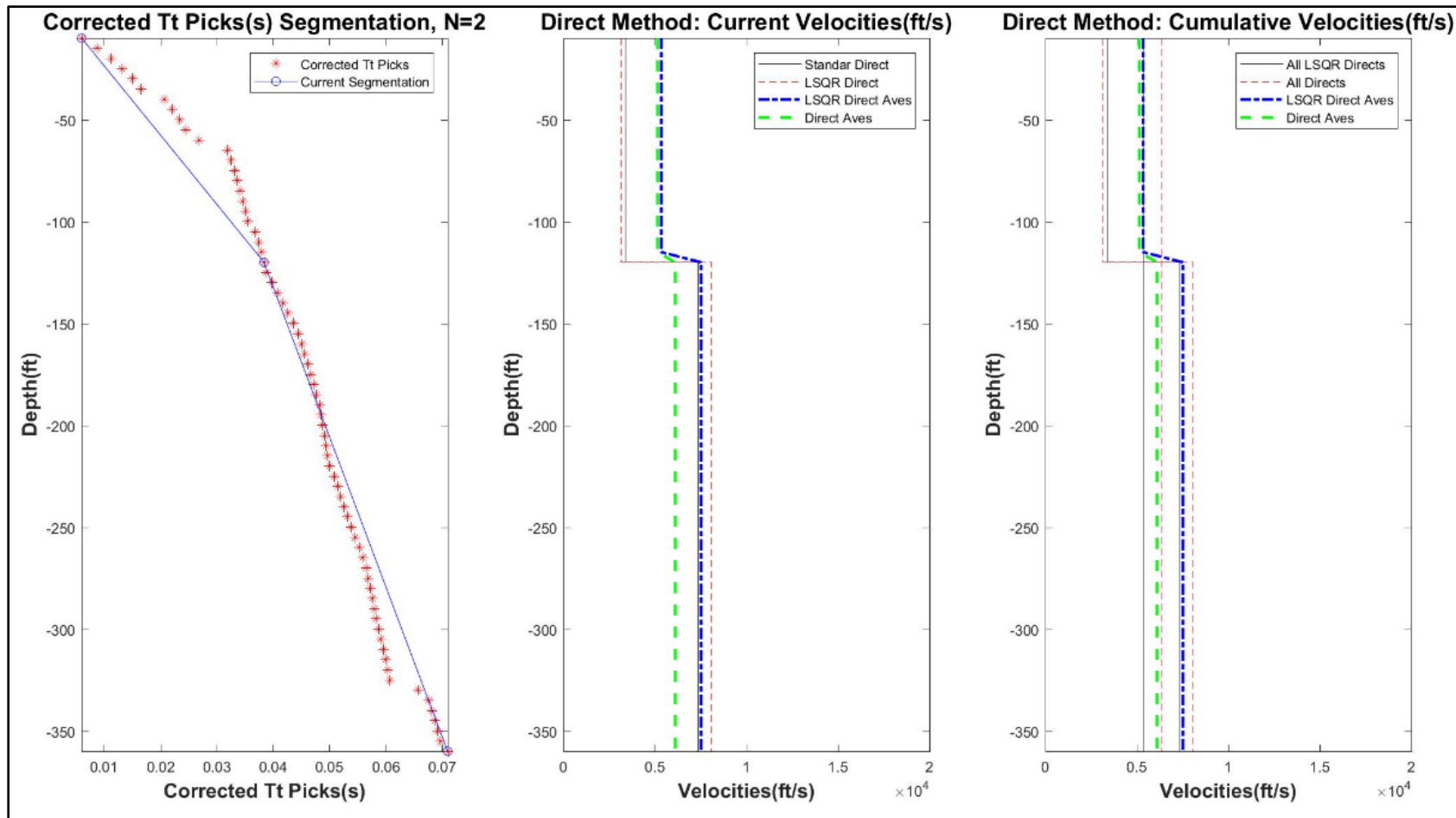
Figure 47 – Example plot of VSP p-wave data, showing a very coarse segmentation of first arrival pairs and the corresponding depth intervals' (pseudo-layers) calculated velocities.
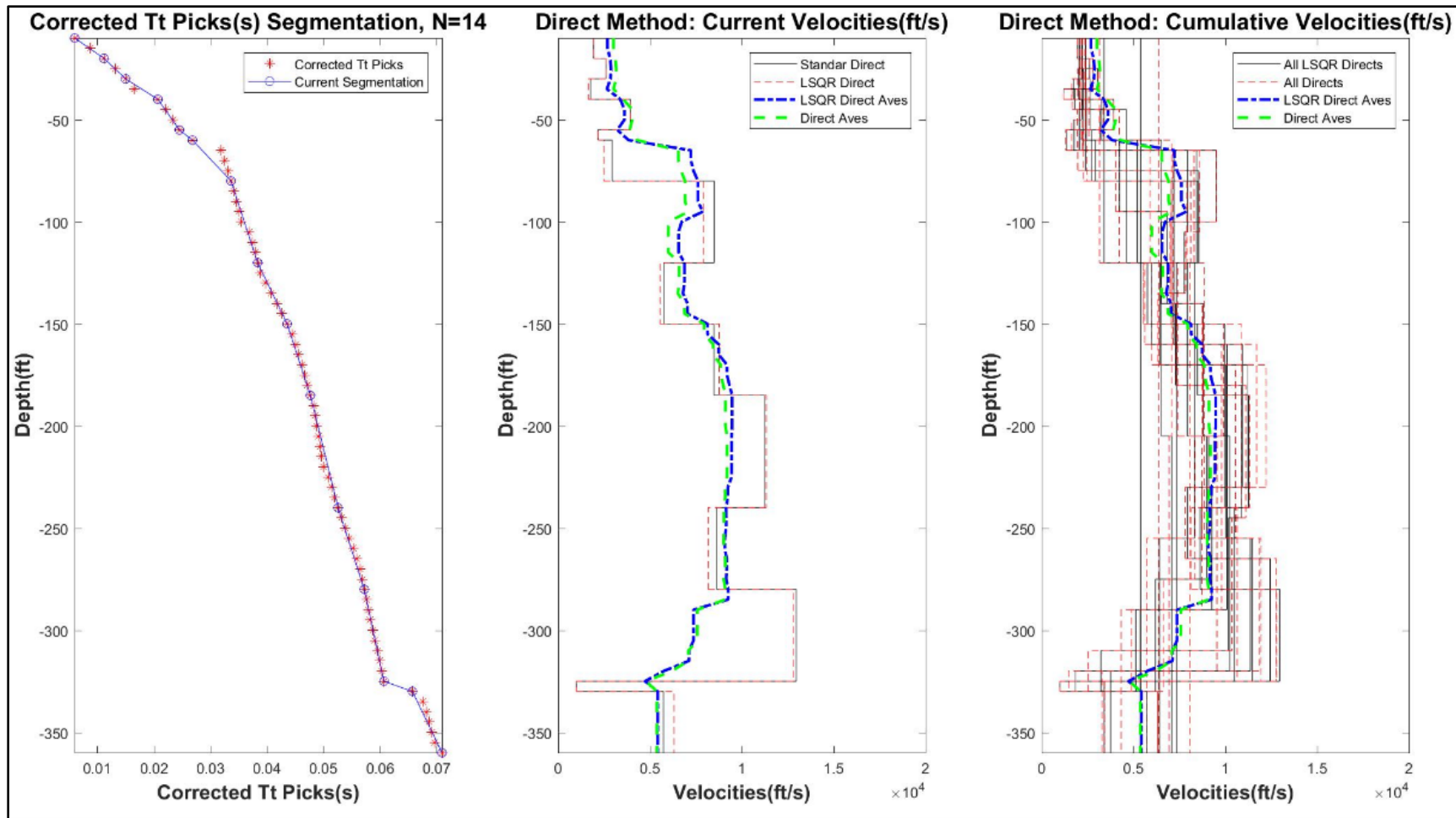
Figure 48 – Example plot of VSP p-wave data, showing an intermediate segmentation of first arrival pairs (left plot) and the corresponding depth intervals' (pseudo-layers) calculated velocities .
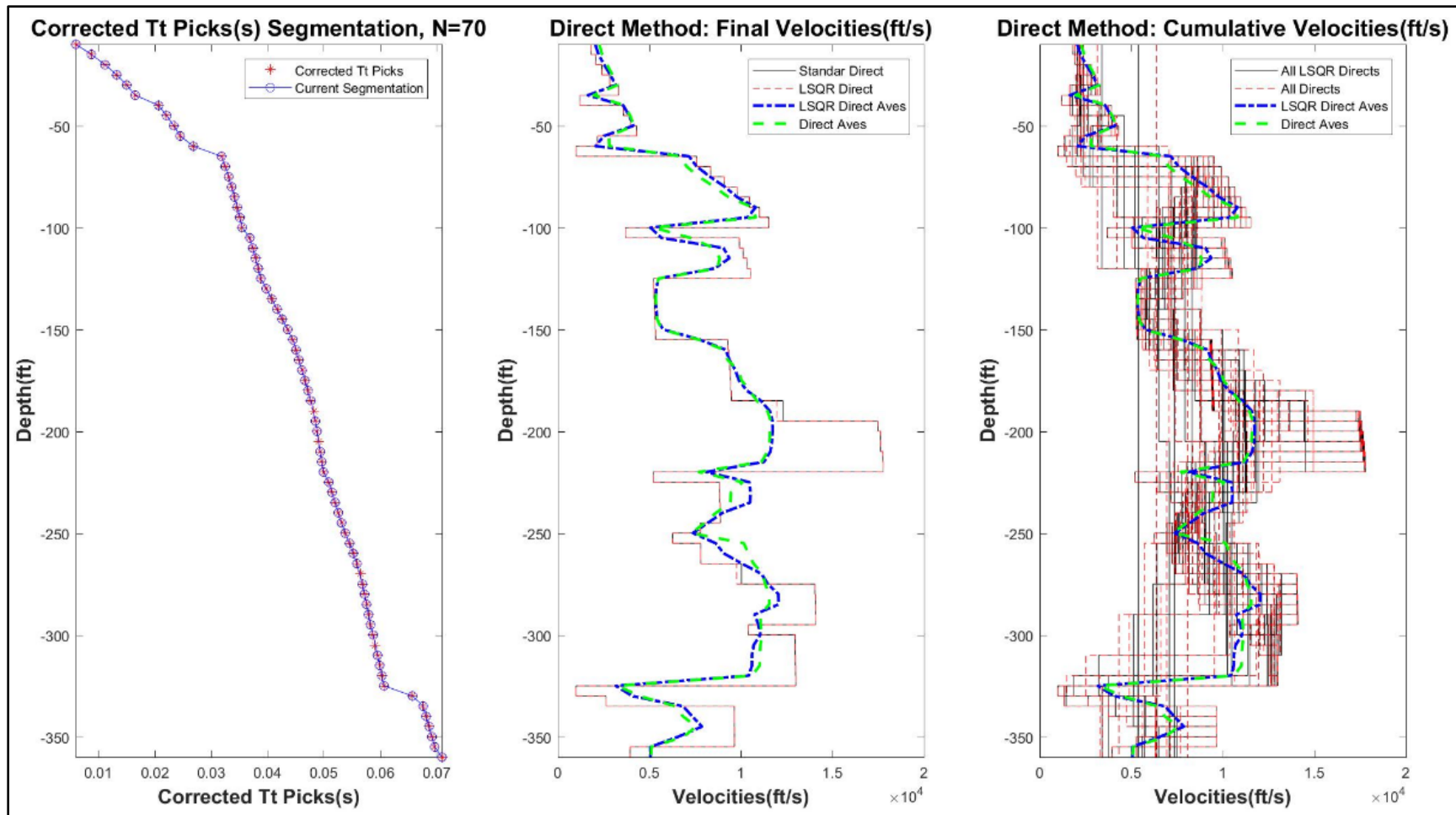
Figure 49 – Example plot of VSP p-wave data, showing the finest possible segmentation of first arrival pairs (left plot) and the corresponding depth intervals' (pseudo-layers) calculated velocities .

J.   Kicking Horse Dam: Comparison of 2D Refraction Tomography, 1D MASW, 1D SCPT downhole VSP, and CPT Correlation Estimations of Vs

Several seismic survey techniques were implemented near the downstream toe of Kicking Horse Dam near Whitefish Montana, in order to compare the various approaches to obtaining 1D Vs profiles for use in calculating a Vs30 value. These techniques include 1D seismic CPT (SCPT) surface-to-downhole VSP profiling (see Figure 11), 2D refraction tomography (see Figure 50), and a series of 1D MASW and passive (ReMi) surface-wave soundings. The surface-based seismic testing was conducted in 2017 specifically in support of this study, so that existing SCPT testing results could be evaluated by comparison of resulting velocity profiles.
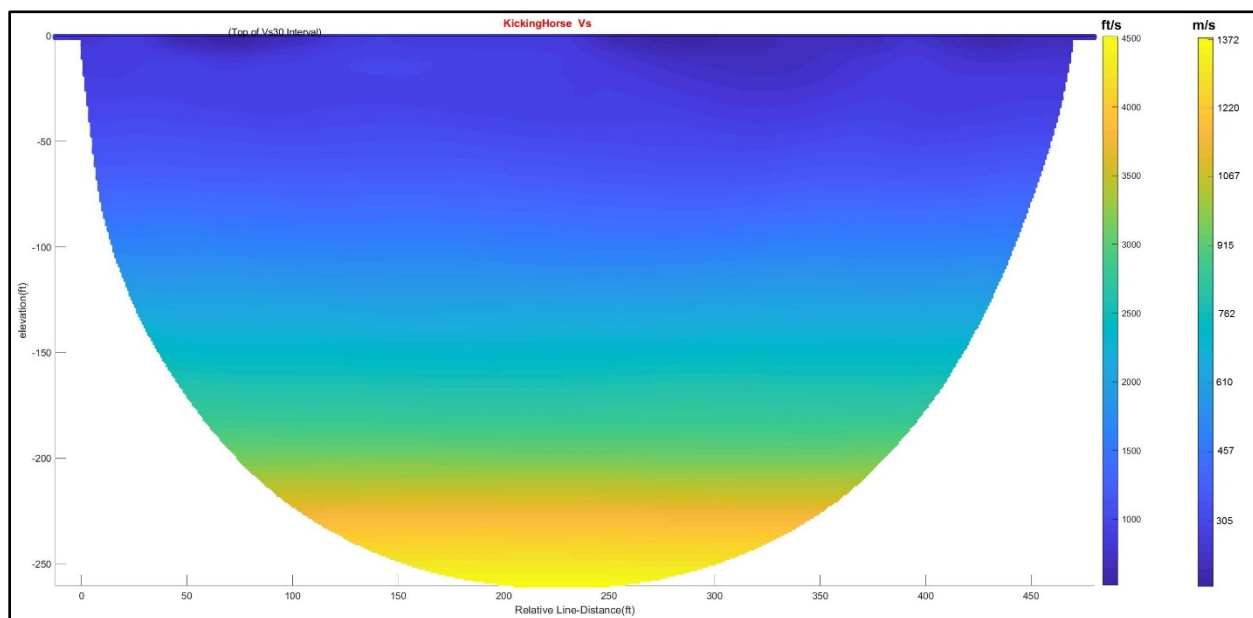
Figure 50 – 2D s-wave refraction tomography velocities for Kicking Horse Dam, Montana. Note some of the shallow velocities are near 700 ft/s or slower within the uppermost 20 ft.

In the case of the 1D MASW soundings, both passive MASW soundings and active-source MASW field testing was performed to record both Rayleigh wave energy and Love wave energy, by means of using both p-wave (vertical component) geophones and s-wave (horizontal component) geophones, respectively. Here, Rayleigh surface-waves have elliptical particle displacement that is predominantly vertical and also horizontal in-line with the direction of wave propagation. Love surface-waves have horizontally torsional particle displacements perpendicular to the direction of wave propagation. These experiments were performed to compare resulting dispersion curves from the different surface-wave types, as each approach has potential benefits and tradeoffs in data quality and fieldwork efficiency (e.g., data collection rates).

Generally speaking, dispersion curve energy was observed to be sufficiently similar using both vertical (p-wave) and horizontal in-line oriented (s-wave) geophones. This potentially offers opportunities for time-savings by avoiding the need to switch geophones between s-wave refraction tomography and MASW data collection (e.g., if p-wave tomography is not needed for

a given project, just collect in-line s-wave geophone component of Rayleigh wave). Additional testing will be required to evaluate the reliability of Love waves for this application.

In addition to seismic surveys, standard CPT data (see Figure 51) were used to estimate Vs versus depth (right-hand plot in Figure 51) using correlation techniques discussed above and described in detail by Wair et al. (2012), Robertson et al. (2009), and Robertson and Cabal (2012). This CPT correlation technique was applied to all nearby CPT data from Kicking Horse Dam. In each case, the CPT profile only extended to approximately 40 feet below ground surface, and so calculation of Vs30 from these estimated Vs values requires significant extrapolation of velocity coverage (60 feet of extrapolation is required in this example).

The various resulting velocity profiles are plotted with refraction tomography and MASW velocity profiles in Figure 52 and Figure 53. Corresponding estimated Vs30 values are presented in Table 7, where the CPT-estimated Vs30 values are labeled "Bad" due to the constant value extrapolations used. These estimates were omitted from the statistics listed at the bottom of Table 7. Again, we see a very close match in the Vs30 values from the various techniques.

There is the added benefit of seeing the lateral variations captured in the 2D tomography results, and the simple 1D MASW soundings are also sufficient for calculation of a reasonable Vs30 value. However, the surface-based techniques result in more averaging of material properties and result in smooth models that can miss subtle velocity structures and velocity inversions that are better captured with the downhole SCPT technique (see Figure 52 and Figure 53). While surface-based techniques are prone to modeling error, the SCPT downhole technique has its own challenges, as described above (refracted arrivals, thin-beds, anisotropy, etc).

Table 7 – Comparison of Vs30 Values obtained using various data types from Kicking Horse Dam, Montana.

Data Type	Quality	Vs30 (ft/s)
SCPT	Good	982
Tomography	Good	1039
CPT est 15-9 (constant extrapolation)	Bad	607
CPT est 15-11 (constant extrapolation)	Bad	672
CPT est 15-12 (constant extrapolation)	Bad	828
Active s-wave MASW (Love)	Good	1062
Passive s-wave MASW (Love)	Good	1150
Active p-wave MASW (Rayleigh)	Good	1002
Mean of "Good" values (ft/s):	1047	
Max Deviation of "Good" Values (ft/s):	104	
Max % Deviation from Mean:	10	

In general, there is an excellent match between the various Vs profiles and corresponding Vs30 values using the various techniques (excluding the significantly extrapolated CPT estimated Vs30 values). As shown in Table 7, there is a very close match of Vs30 values obtained with the various techniques, with the exception of the CPT correlation estimates when using a constant

value extrapolation to a depth of 30 m (e.g., using the lowermost Vs value estimated using CPT data correlation approach).

As a demonstration of the improvement obtained by using the statistical extrapolation technique proposed by Moore et al. (2004), below shows a comparison of the constant-value extrapolated Vs30 values and the extrapolated Vs30 value obtained using the approach developed by Boore et al. (2004). The two approaches are compared to the mean value of all "Good" data types, as presented in Table 7. Here, we see that while the regression-based extrapolation approach proposed by Boore et al. (2004) results in estimated Vs30 values that have an absolute deviation from the mean of all "good" values listed in Table 7 by a max of 185 ft/s, this corresponds to only an 8% deviation. This is a vast improvement when compared with the constant-value extrapolation approach that results in a 42% deviation. It should be noted that the Kicking Horse Dam site is considered a very deep "soft soil" site and in characterized by a fairly consistent soil profile that is conducive to the successful use of this regression extrapolation approach. Other sites with large vertical variations in Vs versus depth will not be as applicable to the use of this approach (e.g., thin stiff layers at depth, or intermediate sites with bedrock less than 30 m deep but below the deepest extent of the input Vs profile)

Table 8 – Comparison of constant value extrapolation and regression extrapolation (Boore et al., 2004) approaches applied to the depth-limited CPT correlation estimated Vs profiles for sake of Vs30 estimation.

CPT Survey Location	Vs30 (ft/s) (Constant Extrapolation)	Vs30 (ft/s) (Regression Extrapolation)
CPT est 15-9	607	1001
CPT est 15-11	672	816
CPT est 15-12	828	858
Mean of "good" values (from Table 7):	1047	
Max Deviation of Extrapolated Values	221	185
Max % Deviation from Mean of "good" values (from Table 7):	42	8
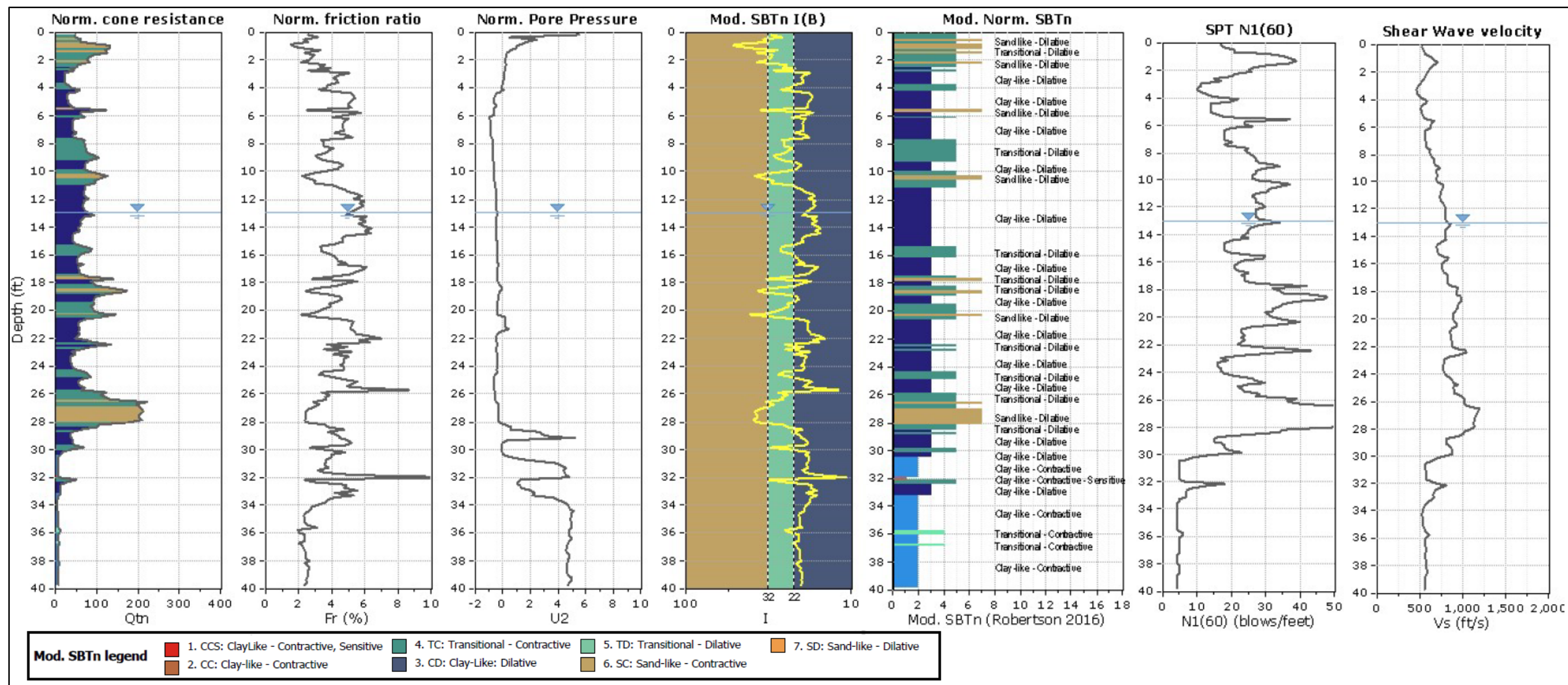
Figure 51 – Example of CPT data collected at Kicking Horse Dam, Montana. The corresponding predicted s-wave velocity profile is presented in the right-hand plot, as estimated using CPT correlation techniques as outlined by Robertson 2009 and Robertson and Cabal 2012.
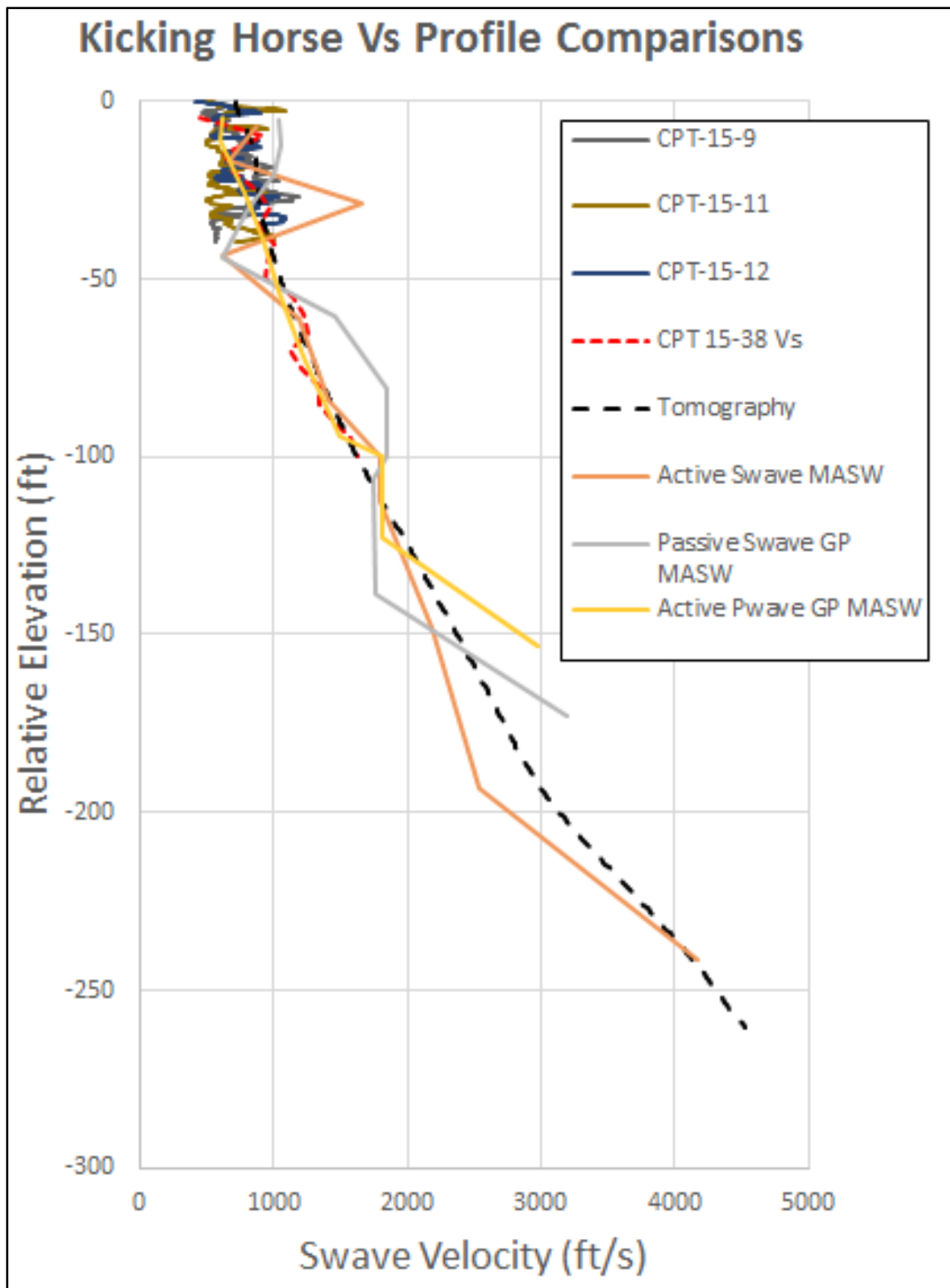
Figure 52 – Comparison of 1D Vs profiles obtained at Kicking Horse Dam using CPT VSP profiling data, estimated Vs from converted CPT data, 2D seismic s-wave tomography, active MASW (Rayleigh wave), active MASW (Love wave), and passive MASW techniques.
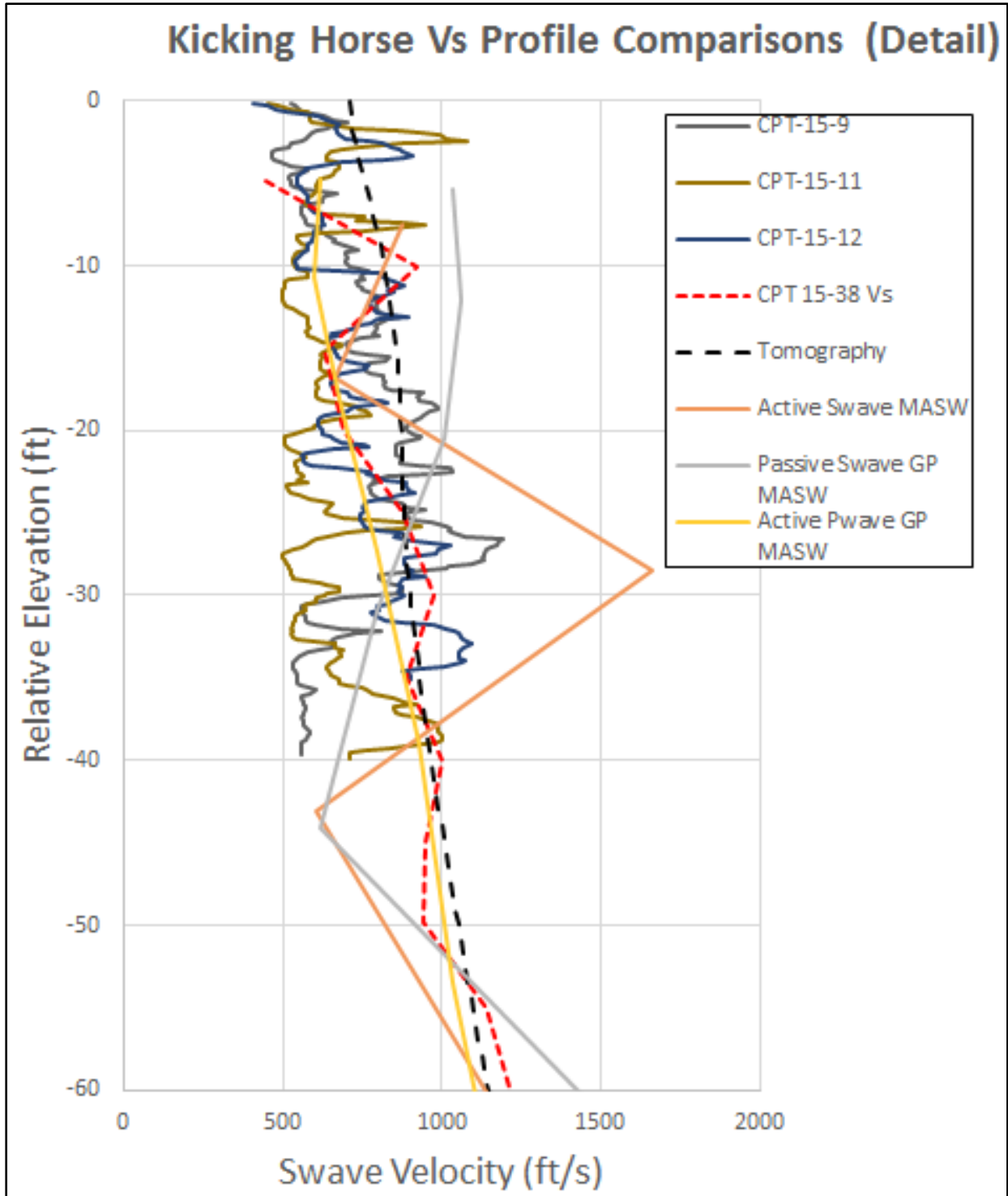
Figure 53 – Detailed comparison of the various 1D Vs profiles at Kicking Horse Dam.

K. American Falls Dam: Example of Geologic Correlations for Estimation of Vs30

An example of implementing geologic correlations to s-wave velocity for sake of estimating a Vs30 value is taken from a 2017 TSC study at American Falls Dam, Idaho (Rittgers 2017a). In this case, no nearby and representative seismic surveys had previously been performed by Reclamation in the Central Idaho region, yet a geologic log from a recent exploratory borehole named DH-201 was available (Lockhart and Link 2003). Therefore, one of the best remaining options for estimation of Vs30 values at the site was to utilize local geologic log data to infer seismic velocity versus depth at the site, and to correlate each material type/depth interval to published values for shear-wave velocities as measured in similar material types.

A general literature review was performed to find a range of published values typical for various geologic materials encountered and recorded in the available geologic log. The materials in question include the following: 1) unconsolidated and interbedded sandy silt with some cobbles/boulders, 2) moderately vesicular/highly fractured basalt, and 3) partially welded yet hard tuff (Little Creek Formation), and fully-welded yet highly fractured obsidian tuff (Walcott Tuff). According to Weghorst (2012), a set of assumed Vs30 values used in a previous seismic hazard analysis study conducted for the nearby Minidoka Dam (located 32 miles west-south-west of American Falls Dam) was published by Wong and Dober (2010). Minidoka Dam is underlain by very similar geology (Little Creek and Neeley formations), and is also located immediately downstream in the Snake River valley.

Sources ultimately chosen for the Vs30 estimation mainly included velocity data from terrestrial-based boreholes/studies, however one velocity from leg 16 of the Deep Sea Drilling Project was used to define the high-end velocity value plausible for intact/massive basalts (Christensen 1973). Primary sources for data from published studies include Toksöz, and Johnson (1981), Bourbié et al., (1987), and Carroll (1994). Additionally, one Reclamation Vs30 study recently conducted at Boca Dam within similar/relevant geologic materials was used to provide additional estimates for velocities in similar materials (Carroll 1994). See citations in Table 9 and corresponding references at the end of this report for a list of all sources utilized.

For the sake of attempting to match site-specific properties of these materials with assumed high/low-end Vs values (specifically the basalt and tuff materials), descriptive properties included in the geologic (e.g., notes on extent of welding, hardness, extent/orientation of fracturing) were accounted for in selecting low/high-end Vs estimates for each depth interval uniquely described in the DH-201 geologic log. This step in estimating representative velocities based on geologic conditions can have a significant impact on the accuracy of the approach, as exemplified by seismic refraction velocity tomography results from El Vado Dam presented in Figure 54 (Rittgers 2016). Here, we see a strong correlation between modeled s-wave velocity distributions and various material properties observed in nearby and coincident boreholes. In Figure 54, overlain stick-logs clearly show that material type, fracture density, amount of weathering, and hardness are all strongly correlated with vertical distributions of seismic s-wave velocity.

Table 10 and Figure 55 present the various shear-wave velocity values published for a given material type that were used for this study. The final estimated range of plausible Vs30 values

for American Falls Dam vary between 2669 ft/s to 7378 ft/s, with a mean of 5023 ft/s. This estimated Vs30 range is in very good agreement with assumed Vs30 values published by Wong and Dober (2010) for the nearby Minidoka Dam: 3775 ft/s, 4430 ft/s, and 4920 ft/s (Wong and Dober 2010).   The close match between the two sets offers relevant validation of the Vs30 range estimated for American Falls Dam.

Beyond this reasonable match with previous estimates for the nearby Minidoka Dam study site, this estimated range indicates that the Vs30 at American Falls Dam is most likely above the informal threshold of 2000 ft/s. Here, subsequent seismic loading predictions and PSHA analysis results become relatively constant and insensitive to variations in Vs30 values above this approximate threshold (Wood 2018). Therefore, any errors in a Vs30 selected from this range (i.e., relative to crosshole data that could otherwise be collected to provide a more accurate site-specific value) would likely have limited impacts on subsequent calculations (e.g., seismic moment magnitude, ground motion time histories, SA, PGA/PHA, etc).
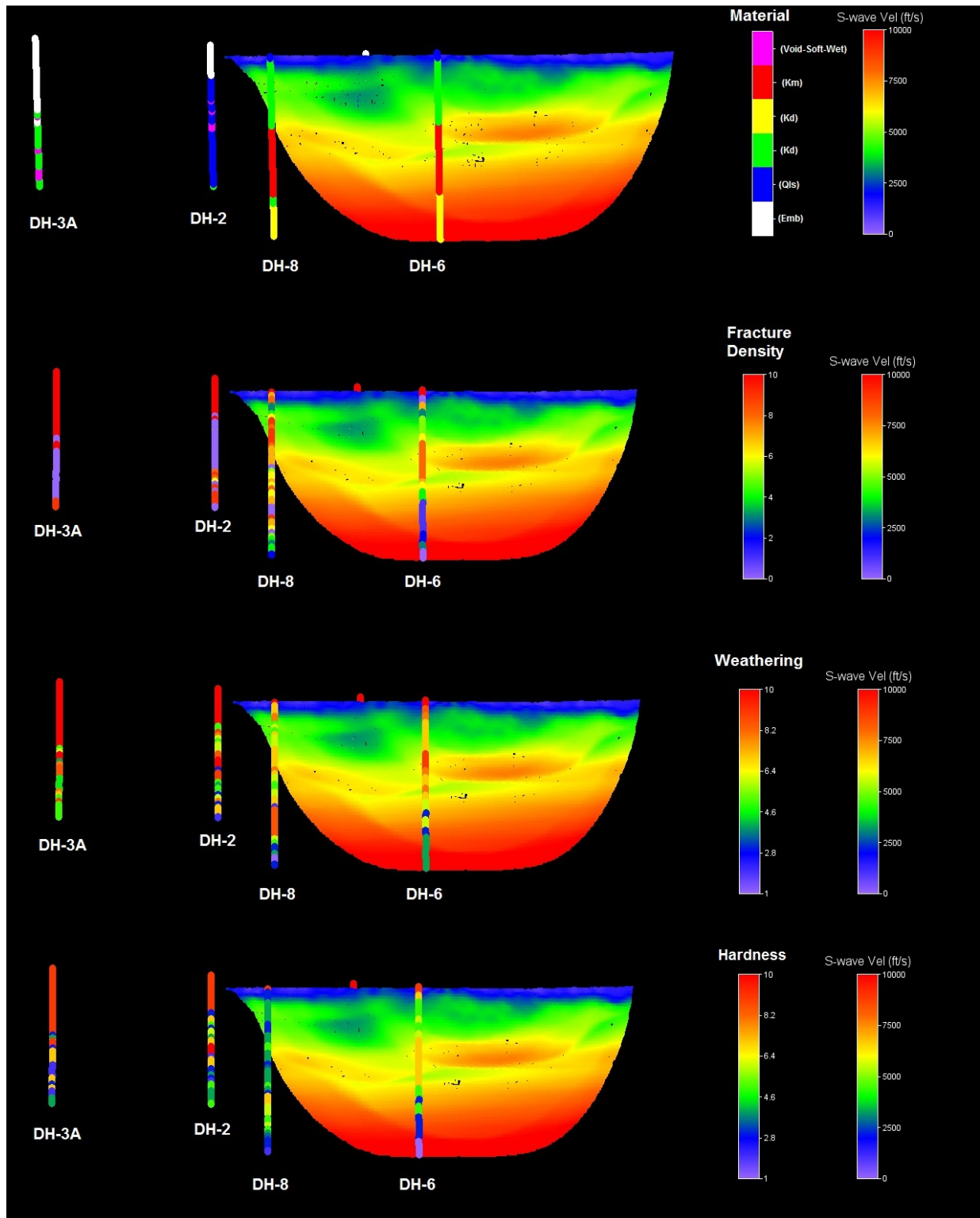
Figure 54 – Example seismic s-wave velocity tomograms with borehole data overlain to depict the strong correlations between seismic s-wave velocity and various material types (top plot), rock fracture density (second plot), level of weathering (third plot), and rock hardness (bottom plot). Figure taken from Rittgers (2016).

Table 9 Published Vs Values for various material types encountered in DH-201

Published Velocities (m/s)										Low (m/s)	High (m/s)	Mean (m/s)
Tuffs:	1400[7]	1100[7]	760[10]	1500[10]						**760**	**1500**	**1190**
Basalts:	3545[12]	2800[6]	3400[6]	3000[12]	1642[8]	2497[8]				**1642**	**3545**	**2594**
Sandy Silts:	100[6]	290[9]	750[11]	400[6]	600[6]	800[11]	1002[8]	1208[8]	1181[8]	1255[8]	**100**	**1255**	**665**

[6] Bourbié et al., (1987)
[7] Carroll (1994)
[8] Rittgers (2014)
[9] Brocher (2005)
[10] BSSC (2004)
[11] Odum (2007)
[12] Christensen (1973)

Table 10 Layer interface depths/absolute elevations, corresponding unique descriptions, and corresponding estimated low/high-end Vs values for each material type, as based on a geologic log from American Falls Dam, Idaho.

Layer #	Depth interval (ft)	Material/Descriptions from DH-201 Log	Estimated High Vs (m/s)	Estimated Low Vs (m/s)
1	0 – 5.8	Sandy Silt/Gravels, basalt frags	1255	100
2	5.8 - 12.5	Basalt (soft/dull)	2594	1642
3	12.5 - 63.4	Basalt (hard/ringy)	3545	2594
4	63.4 - 68.7	Basalt (soft/dull)	2594	1642
5	68.7 - 70.7	Basalt (hard/ringy)	3545	2594
6	70.7 - 77	Partially welded Tuff (Little Creek Formation) soft/granular	1190	760
7	77 - 79.5	Welded/Hard/Dense Tuff (Walcott Tuff Formation) Seams of orange silt/ash ~ a hardness of 1-2 moh's scale	1500	1190
8	79.5 - 98.5	Welded yet Perlitic/friable/highly fractured Obsidian Tuff	1500	760
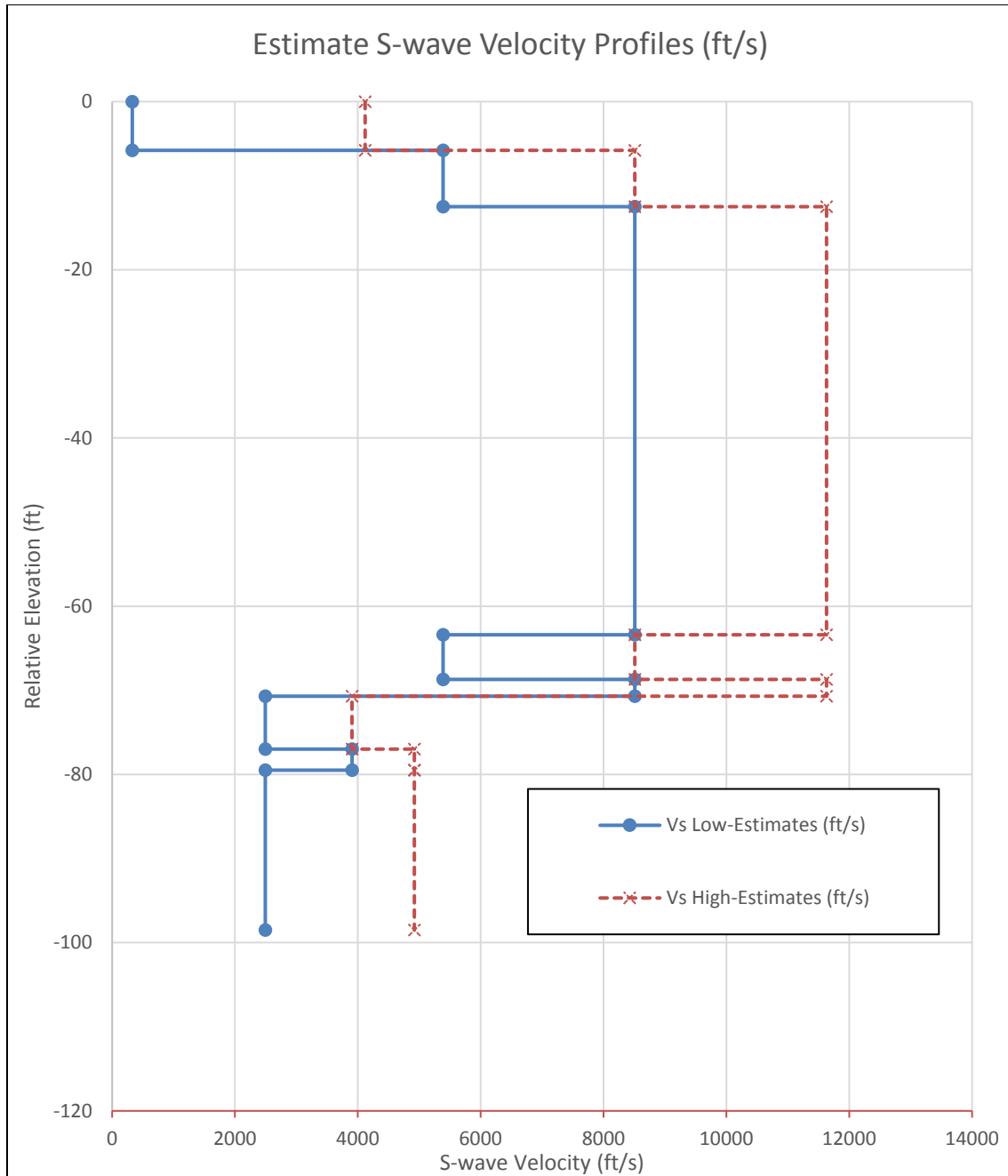
Figure 55 - Low-end (blue) and high-end (red) synthetic s-wave velocity profiles (in units of ft/s) calculated for DH-201 at American Falls dam, estimated from geologic correlations between DH-201 geologic log and published values for typical velocities observed for similar materials. Vs30 values were calculated separately for both low-end and high-end estimates, as well as the average of the two for each layer.

VI. Results

As a part of this Dam Safety Program Technology Development study, a review of the various direct measurement and indirect estimation techniques currently available for the purpose of providing Vs30 values for Reclamation seismic risk studies is provided. During this study, extensive code has been developed to extend and improve the accuracy and reliability of various seismic data processing and modeling techniques applicable to Vs30 estimation. Quantitative and qualitative evaluations and comparisons of the various techniques are provided in the form of several case studies presented in this report. In some cases, seismic surveying data were collected specifically in support of this study, and interagency collaborations with the USACE made other co-located datasets available for use in this study (e.g., Hills Creek Dam).

Overall, this study has verified that any of the various site-specific seismic surveying techniques are valid candidates for obtaining a sufficiently accurate Vs30 value, if appropriate techniques are selected for expected site conditions (e.g., topography and ground surface material) and a given site's geologic setting. Each of these seismic surveying techniques are only adequate if implemented carefully, in order to assure sufficient data quality and adequate depth of investigation (e.g., by means of survey design). Site-specific seismic surveying techniques for obtaining a Vs30 are always preferred, and should be used whenever practical. In terms of accuracy and reliability of these techniques for obtaining a Vs30 value, direct surveying techniques can be ordered from best to worst as follows:

1. 1D cross-hole s-wave seismic profiling
2. Suspension logging
3. 1D surface-to downhole VSP
4. 2D surface-based s-wave refraction tomography
5. 1D/2D MASW or ReMi
6. 1D SASW
7. Alternative seismic data collection and analysis techniques (e.g., seismic reflection analysis, HVSR, alternative non-tomographic refraction analysis techniques, etc.)

When site-specific measurements are not available, the various indirect Vs30 estimation techniques are potential options. These indirect techniques include correlations between Vs and predictor data types such as surface geology and borehole geologic logs, *in situ* penetration test data, undrained shear strength lab testing data, and local topographic slope data. Indirect Vs30 estimation techniques reviewed in this study can be ordered from best to worst as follows:

1. CPT data correlations
2. SPT/BPT data correlations
3. Borehole geologic log data correlations
4. Surface-based geology correlations (e.g. estimation of subsurface structures)
5. Topographic slope correlations

New or otherwise updated Vs30 values are provided in Table 11 for the various Reclamation facilities incorporated in this study, where applicable (some Reclamation sites used to evaluate various data collection and analysis techniques for this study are not immediately applicable to

providing Vs30 value estimations, such as the crosshole data collected within the Prosser Creek Dam embankment materials):

Table 11 – Vs30 values obtained for various Reclamation facilities utilized in this study, where applicable.

Embankment	Vs30	Technique(s) Used	Top of Vs30 Interval
American Falls Dam	5023 ft/s	Geologic Correlation	Ground Surface
Huntington North Dam	3833 ft/s	FWS, Crosshole	Top of Bedrock
Boca Dam	2102 ft/s	Refraction, Crosshole, FWS, MASW	Top of Bedrock
Ochoco Dam	1462 ft/s	Crosshole	Top of Bedrock
Granby Dike 3	1156 ft/s	Refraction, MASW, Crosshole, Reflection	Ground Surface/Foundation Contact
Kicking Horse Dam	1047 ft/s	SCPT, Refraction, MASW, CPT Correlation	Ground Surface

VII. Conclusion and Discussion

Direct (e.g., site-specific) seismic surveying techniques are always preferred for obtaining a Vs30 value, as the various indirect methods presented in this study will inherently introduce greater uncertainty in the estimated Vs profile and/or resulting Vs30 value. In order to better understand the uncertainty in estimated Vs30 when direct measurement techniques are not available or practical, it is recommended to use multiple indirect techniques for estimating Vs30 when possible. Judgment should also be used to assess the quality of input predictor data, agreement between indirect techniques, the size and nature of project or subsequent needs for a Vs30 value, and the potential impacts of under-predicting or over-predicting Vs30 on seismic site response.

The various direct and indirect Vs30 techniques listed in the Results section above are ordered from "best" to "worst" solely based on the evaluated accuracy of these options for estimating Vs30, and this ordering does not necessarily represent practical aspects of specific projects or scenarios that should also be considered. For example, because a nominal threshold of 2000 ft/s Vs30 value has been identified above (i.e., variations in Vs30 values above this threshold do not result in significant variations in the outcomes of subsequent analysis results such as ground motion predictions or PSHA analysis results), initial site visits may offer an opportunity to reasonably determine that site-specific surveys are not necessary. In this example, visual observation of surface geology most likely associated with a Vs30 value that is well above this 2000 ft/s Vs30 threshold value (e.g., a "hard rock site" or "intermediate site" with shallow bedrock of known composition and hardness) could be sufficient to avoid the need for further testing with direct techniques. However, assumptions in the example above would need to be carefully considered, and the assumptions made should be agreed upon by geophysicists, seismologists, and engineers. The validity of such assumptions normally depends on project-

specific needs of seismologists, the planned subsequent analysis steps to be performed by engineers, and the overall risk levels associated with underestimating seismic site responses.

To further build upon this 2000 ft/s threshold, there are very few scenarios where it becomes justified to install one or more boreholes 100 feet into hard rock for the main purpose of evaluating a Vs30 value. In the case of shallow hard rock, the use of a surface-based survey technique would most likely produce an adequately accurate Vs30 value. In the case of intermediate to large depths to top of this hard bedrock unit, partial penetration (far less than 100 feet) of a single hole (or crosshole doublet) would suffice for sake of producing an accurate average Vs value. Extrapolation can also be used to provide a Vs30 value. Essentially, the only scenario where it is justified to spend the required resources to install a borehole this far into hard rock would be to assess specific detailed features at depth, such as fracture densities and orientations (e.g., perform borehole televiewer surveys), or to verify the location of a suspected fault trace or underlying soft material (e.g. a thrust fault structure with hard rock overlaying softer sediments or rock units). Other direct or indirect techniques can likely help to avoid the need for hard-rock coring for the explicit sake of providing a Vs30 value.

Also, as discussed above, each direct surveying technique comes with its own set of practical and technical benefits and limitations, and the validity of each technique should be considered based on all available existing information. Also, the need for information that extends beyond a single Vs30 value should be considered for selection of an ideal technique. For example:

- Do seismologists also need an average velocity of bedrock for estimation of Mw, and is bedrock likely too deep to be accurately imaged using a surface-based technique instead of a borehole technique?
- Is there a specific thin-bed of concern for liquefaction potential that is too thin or deep to be detected using certain techniques?
- Are there difficult site conditions that would prevent efficient or effective implementation of one or more techniques (e.g., extreme topography, complex geologic structure, rough or paved ground surfaces, or insufficient physical access at a given testing location, high levels of background seismic noise)?

Another aspect of the various direct measurement techniques that should be considered is the direction of s-wave propagation and associated directions of particle displacements excited or otherwise utilized by each technique. Here, most seismic studies assume earthquake loading is characterized by vertically propagating waves with horizontal particle displacements. In highly anisotropic materials (e.g., highly foliated/layered shale or highly fractured rock with one or more dominant fracture-set orientations), there could be upwards of a 30% difference in vertical versus horizontal s-wave propagation velocities (Wair et al., 2012).

In this case, techniques such as crosshole or refraction tomography surveys rely on predominantly vertically polarized and horizontally propagating s-waves, and these techniques may overestimate the Vs30 value in highly anisotropic materials (e.g., flat-laying shale beds). In this scenario, the FWS logging and downhole VSP survey techniques predominantly measure s-waves that are horizontally polarized and vertically propagating, and could therefore be more representative techniques for the phenomenon being considered. It should be noted here, that while this aspect of each direct measurement technique should be considered given a particular

geologic scenario or unit, no significant and systematic differences were observed between the various methods that utilize horizontal versus vertically propagating waves.

A.   Vs30 Technique Selection Guidelines

Below, Figure 56 through Figure 58 each present flowcharts that depict generalized approaches to Vs30 technique selection for "soft soil" sites, "intermediate" sites, and "hard rock" sites, respectively. These scenarios each assume that the initial steps of the overall risk analysis workflow presented in Reclamation (2015) have already been completed, and it has been determined that Vs30 is required but not available from existing data or site-visit information.

In each case, the flowchart covers a very basic set of scenarios while attempting to direct the reader towards the most cost-effective options for a given situation. However, the flowcharts do not necessarily account for all subtleties and complexities that a specific project or survey site might involve. While these flowcharts focus on the selection of direct measurement techniques, indirect estimation techniques could be deemed adequate for a particular site (e.g., if risk of a given failure mode is sufficiently low, or if the estimated Vs30 value is sufficiently high that it avoids a level of risk uncertainty at which point more detailed surveying would be required).

Site-specific details (e.g., noise levels, ground surface conditions, weather, physical access and safety, etc.) and project requirements (e.g., time and budgetary constraints, the need for more information beyond Vs30, level of risk involved and the associated need for accuracy) should always be carefully considered along with the various benefits and limitations of each Vs30 technique. Table 12 provides a summary of the main characteristics of the various Vs30 techniques evaluated for this study. Figure 56 through Figure 58 and Table 12 are by no means intended to be a comprehensive set of rigid guidelines for Vs30 technique selection, but should serve more as a starting-point for engineers and project managers during initial project planning, budget estimations, and communications. It is always recommended that an experienced geophysicist be consulted when making final selection of techniques and survey planning.

Lastly, in the case of an intermediate site with top of bedrock located between 10 and 30 meters below ground surface, the foundation's overburden soil profile is of primary concern. Here, the potentially low velocities of these unconsolidated materials will likely have the largest impact on Vs30 and related site response concerns. In these scenarios, it is always recommended to evaluate the need for detailed surveying of the soil column (e.g., accurately measure Vs of soft layers identified during previous subsurface explorations). If not required, then penetration test correlations or SCPT data could be used if available, or a surface-based survey would most likely be adequate for measuring Vs. However, if borehole techniques are deemed necessary for the soil column, sufficiently accurate bedrock velocities can usually be obtained using either geologic correlation with similar rock types, or by using surface-based techniques (e.g., MASW or refraction).

If geologic correlations or surface-based techniques are deemed inadequate (e.g., bedrock is of unknown type/condition or relatively deep and obscured by shallow fast layers), then borehole techniques may be required within the rock interval. Here, only the top several feet (i.e., approximately 20 feet) of bedrock should be penetrated and tested to provide the required rock Vs value. This ~20-foot penetration will most typically provide adequate depth coverage to

assess the weathering of bedrock, and to help constrain the Vs of underlying unweathered rock. Here, crosshole seismic profiling is the most reliable approach, but will require at least two boreholes extend into hard rock. Alternatively, a very limited FWS/suspension logging profile can be obtained using only one borehole that is extended into hard rock. Downhole VSP can be unreliable in these scenarios, where most of the down-going s-wave energy can be reflected off of the top of bedrock, and little energy is recorded by receivers below this interface.
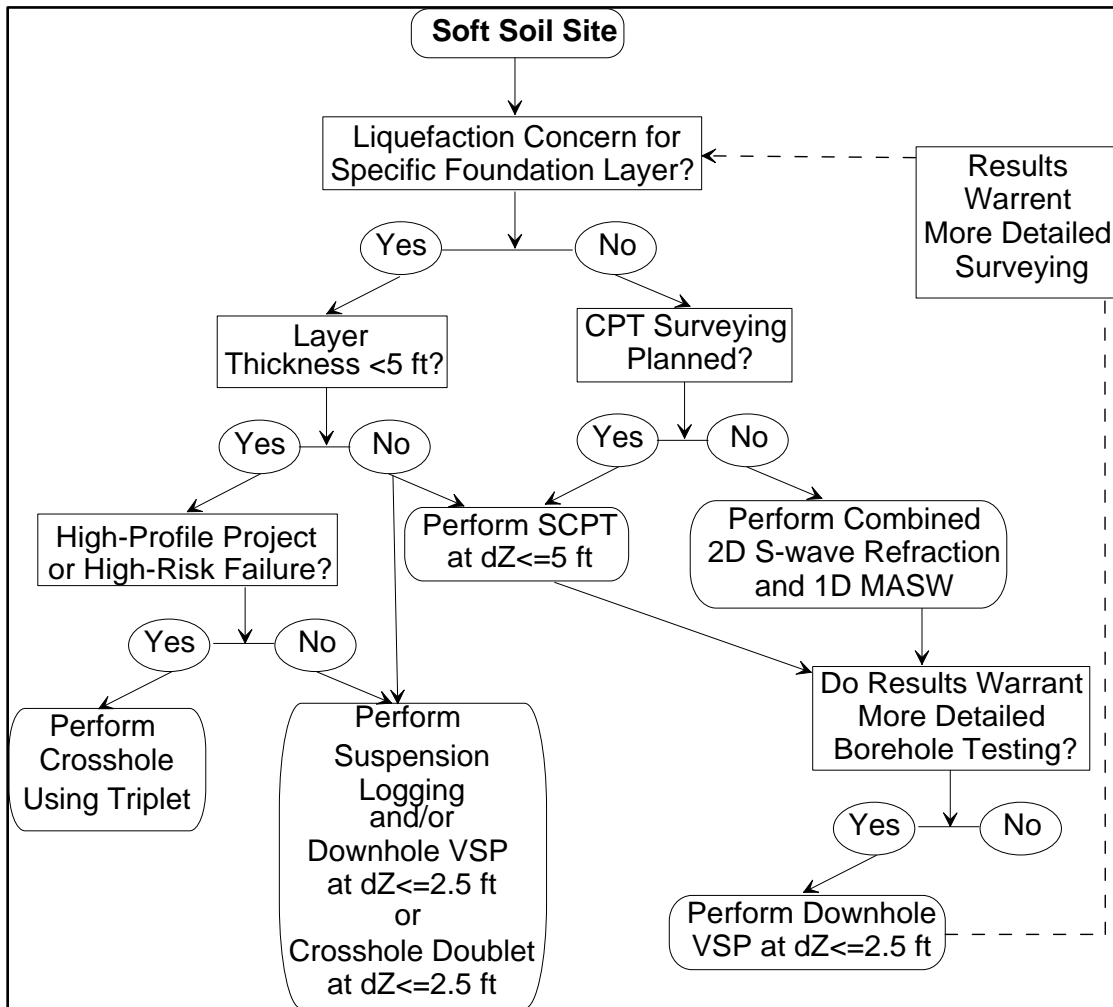
Figure 56 – Flowchart depicting a generalized approach to Vs30 technique selection for "soft soil" sites.
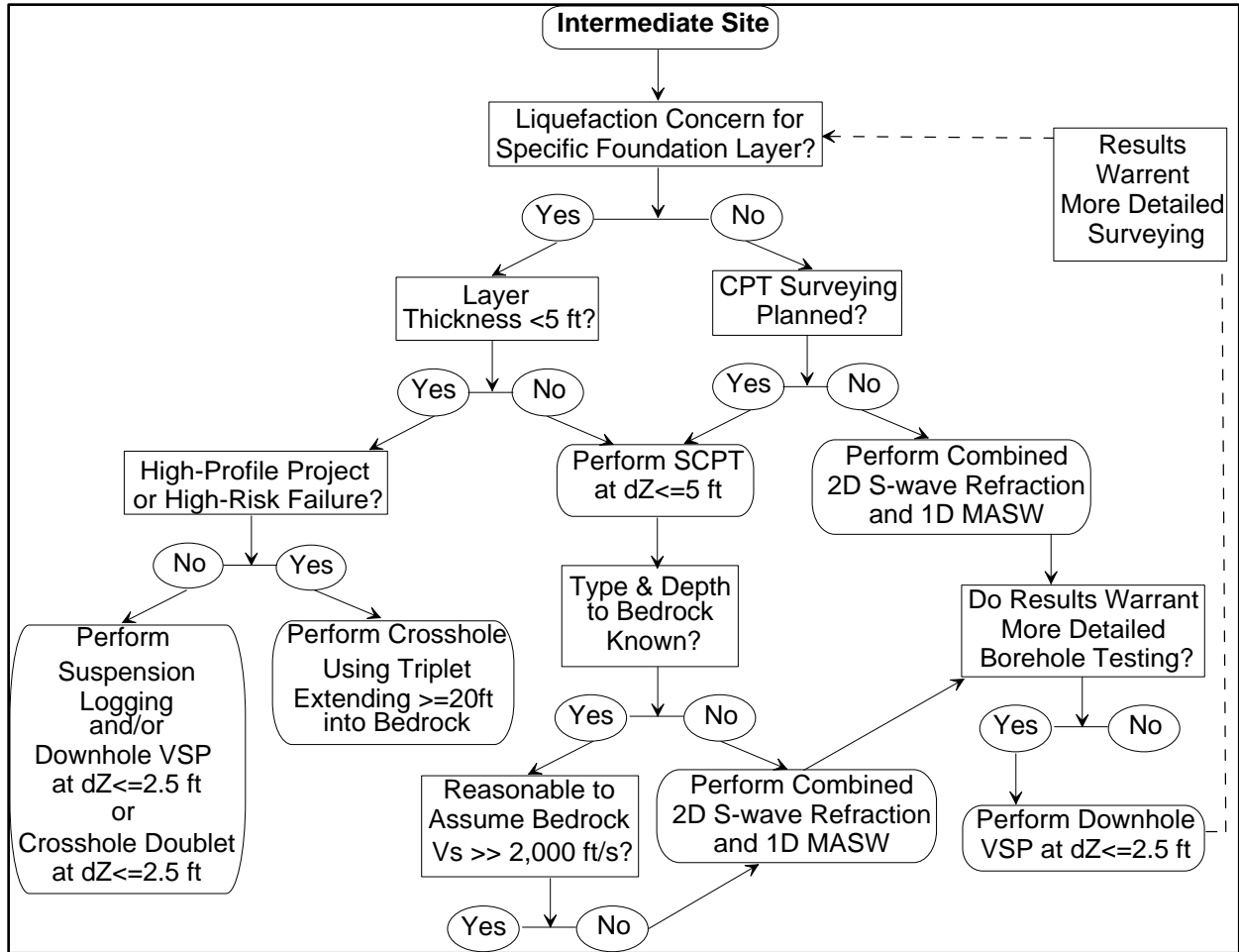
Figure 57 – Flowchart depicting a generalized approach to Vs30 technique selection for "intermediate" sites.
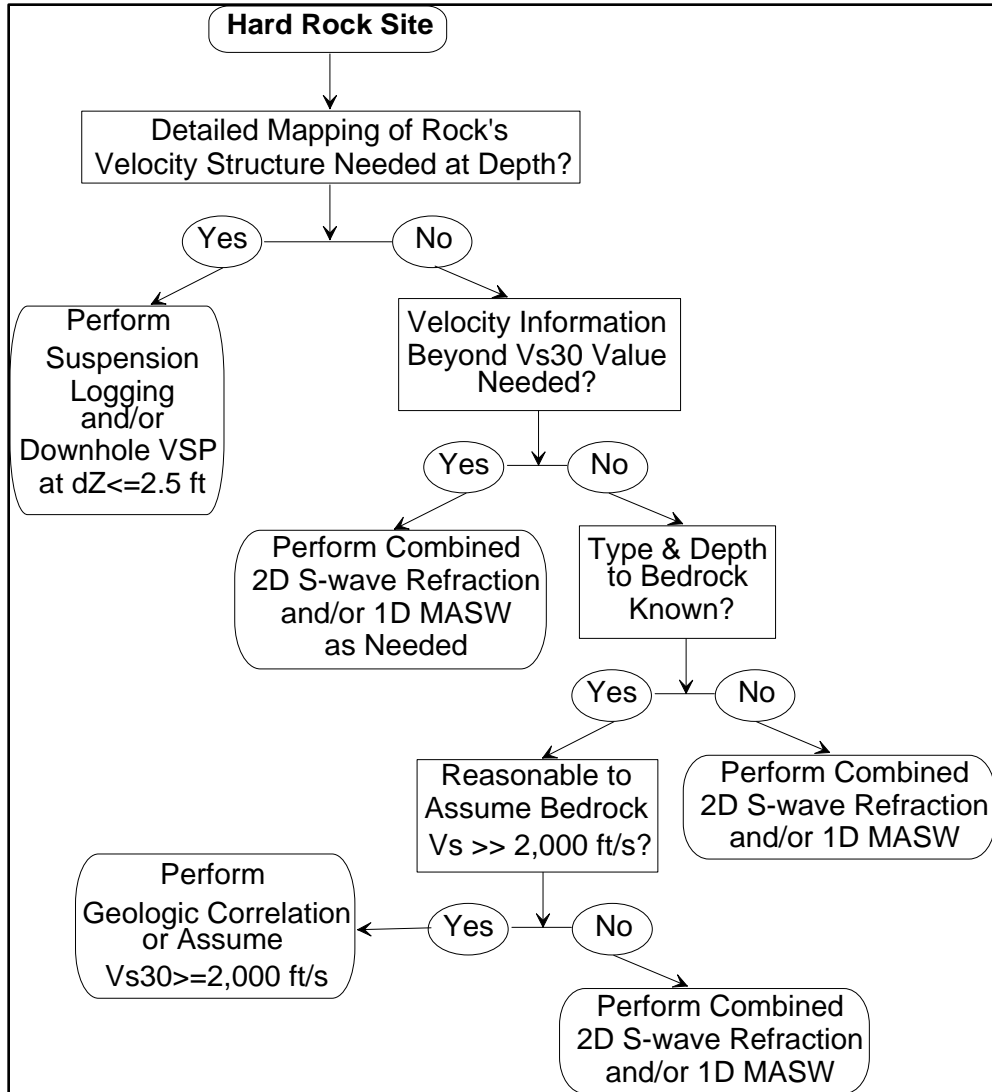
Figure 58 – Flowchart depicting a generalized approach to Vs30 technique selection for "hard rock" sites.

Table 12 - Table modified from Wair et al. (2012) showing a basic overview of qualitative comparisons of various Vs30 techniques.

Relevant Feature or Factor	Direct-Measurement Vs30 Techniques							Indirect Vs30 Estimation Techniques		
	Crosshole	Downhole VSP and SCPT	FWS/Suspension Logging	SASW	MASW	Refraction Tomography	Alternative Seismics: Reflection, HVSR, etc	CPT/SPT/BPT Correlations	Geologic Correlations	Topographic Slope Correlations
# of Boreholes Required	2 or more	1	1	None	None	None	None	1 or more	1 or more for borehole log use, none for surface-based assessments	None
Quality Control and Repeatability*	Excellent	Good	Excellent	Good to fair; complex interpretation required at sites with large velocity contrasts, assumes horizontal-layered geology	Good to fair; complex interpretation required at sites with large velocity contrasts, assumes horizontal-layered geology	Good to fair; s-wave first arrivals can be difficult to distinguish	Good to fair; only works for fairly simple geologic structure with adequate seismic impedance contrasts	Good to fair; quality deteriorates with course-gravel soils	Good to fair for geologic log correlations; poor for surficial assessments	Fair to poor; assumes slope is related to shear strength soils
Thin-Bed Resolution**	Excellent to good; constant with depth	Good to fair; decreases slightly with depth	Excellent; constant with depth, poor within uppermost 3-6m of subsurface	Poor; decreases with depth; provides global average of lateral variations; not robust to velocity inversions or strong velocity contrasts	Poor; decreases with depth; provides global average of lateral variations; more robust to velocity inversions and strong velocity contrasts	Fair to poor; provides global average; assumes monotonic velocity gradient	Poor; provides course global averages; assumes simple layered geology; requires large impedance contrasts	Excellent to good; constant with depth; not available within hard rock or cobbly soil	Excellent to good with geologic logs, poor for surficial assessments	Poor; provides a single Vs30 value
Effects of Large Velocity Contrasts	Problematic; refracted arrivals	Problematic; refracted arrivals can result in infinite or negative velocities; fast layers become sensitive to first arrival picking errors; layered interpretation oftentimes required to average across layers	Can impact seismic coupling of casing if grout doesn't match formation density	Problematic; creates higher modes not accounted for in analysis	Not an issue; higher modes are accounted for in analysis	Can limit depth of investigation, velocity inversions not accounted for	Required for most alternative seismic techniques, except refraction analyses such as slope-intercept and GRM	Can be under-accounted or unaccounted for, based on limitations of penetration tests (e.g., SPT and BPT values capped at 100 blows per foot for refusal)	Can be under-accounted or unaccounted for, based on limitations of available geologic data and physical properties recorded	NA: Geology and corresponding velocities at depth not accounted for by this technique
Can Handle Velocity Inversions	Yes	Yes	Yes	No	Yes	No (for laterally continuous layers)	Reflection can, HVSR and other refraction analyses can't	Yes	Yes, limited by detail of available geologic data	NA
Predominant Wave Propagation Direction	Horizontal	Vertical	Vertical	Horizontal	Horizontal	Horizontal/mixed	Vertical for Reflection, horizontal for refraction and HVSR	NA	NA	NA
Predominant Particle Motion Direction	Vertical for s-waves; horizontal for p-waves	Horizontal for s-waves; vertical for p-waves	Horizontal for s-waves; vertical for p-waves	Vertical	Vertical	Vertical for p-wave, horizontal for s-wave	Reflection: vertical for p-wave, horizontal for s-wave; vertical for HVSR	NA	NA	NA
Susceptible to Background Vibrational Noise	Mostly near surface, decreases with depth	Mostly near surface, decreases with depth	Mostly near surface, decreases with depth	Yes	Active MASW is; passive MASW/ReMi requires and benefits from strong noise	Yes, can be managed with additional shots to stack out incoherent background noise	Reflection/refraction are negatively impacted; HVSR benefits from strong noise	NA	NA	NA

Requires Flat Topography	No	No	No	Yes	Yes	No	No	No	No	No
Requires Extrapolation	Depends on depth-coverage of boreholes – oftentimes stops at or near hard bedrock	Depends on depth-coverage of borehole – oftentimes stops at or near hard bedrock	Depends on depth-coverage of borehole	Depends on seismic source frequency content/energy and site's geologic structure	Depends on seismic source frequency content/energy and site's geologic structure	Depends on survey geometry and site's geologic structure	No	Depends on depth-coverage of penetration test data	Yes for surficial assessments; depends on depth-coverage of geologic logs	NA
Can Provide both Vs and Vp	Yes	Yes	Yes	Vs is measured, Vp is assumed	Vs is measured, Vp is assumed	Yes	Yes for reflection and refraction, no for HVSR	Vs is estimated, Vp can be assumed from Vs estimates	Yes	NA
Typical Depths of Investigation	Less than 500 ft	Less than 300 ft	Depends on application; can be performed several 1000's of feet deep	100-300 ft	100-300 ft	100-200 ft	Several 1000's of feet for reflection and HVSR, 100-200 ft for refraction	100-200 ft	Depends on depth-coverage of geologic logs	NA; assumes 100ft depth of Vs30 value
Common Challenges or Limitations	Most expensive technique; laborious; refracted arrivals obscure slow layers; borehole deviations; only provides 1D profile at survey location	Expensive; refracted arrivals; first arrivals become increasingly emergent (loss of high-frequency energy) and lower SNR with depth; only provides 1D profile at survey location	Expensive; poor borehole grout or sand backfill creates data quality; borehole must be water-filled; s-wave can be hard to "see" in data, cased holes are difficult to measure unbiased formation velocities; only provides 1D profile at survey location	Assumes horizontally-layered geology; requires flat ground; grossly averages large volumes of material properties; higher modes from velocity inversions/high-contrasting layers; laborious data collection; only provides 1D profile at survey location	Assumes horizontally-layered geology; requires flat ground; grossly averages large volumes of material properties; higher modes from velocity inversions/high-contrasting layers can still cause issues; only provides 1D profile at survey location; 2D is laborious and realistic only for flat smooth ground surfaces	Susceptible to background noise; laborious data collection and analysis; smooth velocity models are typical; doesn't capture velocity inversions; depth of investigation can be limited by shallow fast layers	Alternative refraction analysis assume horizontally-layered geology; HVSR only provides 1D profile at survey location, reflection is expensive; require adequate seismic impedance contrasts; HVSR requires three-component data; grossly averages large volumes of material properties; HVSR requires depth to bedrock to be known	Can fail in rocky/cobbly soils; not available in hard rock materials; requires penetration testing vehicle access; SPT and BPT testing limited to pre-determined "refusal" value of 100 blows per foot	Lack of detailed geologic logs; lack of available Vs data for nearby or representative materials; physical properties of materials (e.g., fracture density) can have significant effects on actual Vs; surficial assessments assume subsurface geologic structure	Very course estimates; does not account well for flat-laying rock sites (e.g., horizontal basalt flows, consolidated sedimentary rock units, glacial erosion of hard rock)
Other Considerations and Factors	Highly reliable; each measurement independent of other depths or measurements; ; requires inverse modeling to obtain velocities; enables crosshole tomographic imaging surveys; provides Vp and Vs	Penetration data also obtained with SCPT; provides both Vp and Vs; only requires one borehole; vertical resolution is mostly maintained with depth; requires inverse modeling to obtain velocities	Well suited for deep borehole testing; method assumes p-waves and s-waves propagate through undisturbed media surrounding borehole; susceptible to borehole effects; doesn't require inverse modeling to obtain velocities	Portable; can be performed by one person; assumes flat-layered geology; can be used to provide direct estimate of Vs30 without need for inverse modeling; requires flat topography over a large distance	Laborious; can be used to provide direct estimate of Vs30 without need for inverse modeling; requires flat topography over a large distance; assumes flat-layered geology; can be implemented for 2D profiling; 1D soundings can be performed quickly using a refraction sensor array	Well suited for screening large areas by means of long 2D surveys or large 3D surveys; provides both Vp and Vs; can handle complex topography, rough terrain, and complex geologic structures; requires inverse modeling to obtain velocities	None-ideal techniques, alternative options are almost always inferior to more standard approaches; reflection data is extremely expensive	Penetration data also provides detailed soil profile data; requires vehicle access; not available for rocky soils or below hard rock intervals	Requires access to geologic data or assumes subsurface geology based on adjacent/surficial assessments; leads to large range of possible values	Should be considered a last resort for course estimation of Vs30; doesn't cost anything if regional digital elevation data is available for site

* **Good quality depends on use of good equipment and procedural details, and good interpretation techniques for all methods listed**
** **Resolution depends on test spacing/survey geometry for all methods listed**

B.   Future Work and Recommendations

The next logical steps for better understanding the levels of Vs30 accuracy needed by Reclamation will involve formal sensitivity analysis efforts for quantifying how Vs30 errors propagate and affect the outcomes of subsequent Seismotectonics studies (e.g., variances in predicted time histories, PSHA products, SA values and risk analysis workflows that utilize these analysis products). This should be done by performing seismotectonic analyses for various ranges of Vs30 values that represent a reasonable confidence interval for Vs30, with an initial focus on soft soil and intermediate sites. Also, a better integration of surface-based geophysical surveying with field exploration will potentially help to inform placement of boreholes, test pits and trenches for the sake of targeting specific features (e.g., low velocity zones identified in 2D velocity tomograms). Future work should also investigate the use of strong motion sensor installations at particular dams for seismic site characterization and Vs30 estimations. Lastly, collection and integration of all historic geophysical and geological data into a single queryable GIS database platform such as Reclamation's Tessel platform will make future studies more robust, and will enable geophysicists and engineers to evaluate the use of nearby datasets for cost-effective and reliable Vs30 studies.

VIII. References

AAPG, 2018. AAPG WIKI: Full waveform acoustic logging, accessed September 1st, 2017. Available at: http://wiki.aapg.org/Full_waveform_acoustic_logging.

Allen, T. I., and Wald, D. J., 2009. On the use of high-resolution topographic data as a proxy for seismic site conditions (Vs30), Bulletin of the Seismological Society of America, 99, no. 2A, 935-943.

Andrus, R.D., and K.H. Stokoe II. 2000. "Liquefaction Resistance of Soils from Shear-Wave Velocity," Journal of Geotechnical and Geoenvironmental Engineering, Vol. 126, No. 11, pp. 1015-1025.

Arias, A. 1970. "A Measure of Earthquake Intensity," R.J. Hansen (ed.), *Seismic Design for Nuclear Power Plants,* MIT Press, Cambridge, Massachusetts, pp. 438-483.

Asten, M.W., and Boore, D.M., eds., 2005. Blind comparisons of shear-wave velocities at closely spaced sites in San Jose, California: U.S. Geological Survey Open-File Report 2005-1169. Available at http://pubs.usgs.gov/of/2005/1169/.

Bailey, M., 2018. Hills Creek Project (NID OR00014) Phase 2 Site Exploration Methods and Results, USACE, Verbal and Written Correspondence.

Baker, J. 2011. "Conditional Mean Spectrum: Tool for Ground-Motion Selection*," Journal of Structural Engineering*, Vol. 137, Special Issue: Earthquake Ground-Motion Selection and Modification for Nonlinear Dynamic Analysis of Structures, pp. 322-331.

Boore, D.M., 2004. Estimating VS(30) (or NEHRP Site Classes) from shallow velocity models (depths < 30m), Bull. Seismo. Soc. Am., 94(2):591–597.

Bourbié; T., Coussy; O., Zinszner, B., 1987. Acoustics of Porous Media, Gulf Publishing, Houston.

Bozorgnia, Y., and 30 others. 2014. "NGA-West2 Research Project," *Earthquake Spectra*, Vol. 30, No. 3, pp. 973-987.

Bray, J.D., and T. Travasarou. 2007. "Simplified Procedure for Estimating Earthquake-Induced Deviatoric Slope Displacements," *Journal of Geotechnical and Geoenvironmental Engineering,* Vol. 133, No. 4, pp. 381-392.

Brocher, T.M., 2005. Compressional and Shear Wave Velocity Versus Depth in the San Francisco Bay Area, California: Rules for USGS Bay Area Velocity Model 05.0.0, USGS Open File Report 05-1317, pp. 25.

Brown, L.T., 1998, Comparison of VS profiles from SASW and borehole measurements at strong motion sites in Southern California, Master's thesis, University of Texas at Austin.

Brown, L.T., Diehl, J.G., and Nigbor, R.L., 2000a, A simplified procedure to measure average shearwave velocity to a depth of 30 meters (VS30), Proceedings of the 12th World Conference on Earthquake Engineering, Auckland, New Zealand, February 2000.

Brown, L.T., Diehl, J.G., and Nigbor, R.L., 2000b, A simplified procedure to measure average shearwave velocity to a depth of 30 meters (VS30), Proceedings of the 6th International Conference on Seismic Zonation, Palm Springs, California, November, 2000.

BSSC (Building Seismic Safety Council) 2004. National Earthquake Hazard Reduction Program (NEHRP): Recommended Provisions for Seismic Regulations for New Buildings and Other Structures, Washington DC: BSSC, FEMA 450.

Burke, Lauri, 2011. Digital signal processing and interpretation of full waveform sonic log for well BP-3-USGS, Great Sand Dunes National Park and Preserve, Alamosa County, Colorado: U.S. Geological Survey Scientific Investigations Report 2010–5258, 4 p.

Carroll, R. D., 1994. Measurement of Seismic P- and S-Wave Attenuation in Volcanic Tuff, Rainier Mesa Tunnels, Nevada Test Site, USGS Open File Report 94-618, pp. 7-11.

Christensen, N. I., 1973. Compressional and shear wave velocities in basaltic rocks, Deep Sea Drilling Project, Leg 16, pp647-648, doi: 10.2973/dsdp.proc.16.124.1973

Delgado, J., López Casado, C., Giner, J., Estévez, A., Cuenca, A., and Molina, S., 2000, Microtremors as a geophysical exploration tool: Applications and limitations, Pure and Applied Geophysics, v. 157, p. 1445-1462.

Electrical Power Research Institute, 1991. Standardization of the Cumulative Absolute Velocity, Report No. EPRI TR-100082-T2, EPRI, Palo Alto, CA.

GEOVision, 2018a. A new approach to the Vs30 Method, white-paper accessed October 20th, 2018, available at: http://www.geovision.com/PDF/App%20Note-Method-V30.doc.pdf.

GEOVision, 2018b. Suspension P-S Velocity Logging Method, white-paper accessed October 20th, 2018, available at: http://www.geovision.com/PDF/App%20Note%20-%20P-S%20method.pdf

Kanamori, H. 1983. "Magnitude Scale and Quantification of Earthquakes," *Tectonophysics*, Vol. 93, No. 3-4, pp. 185-199.

Kayen, R., R.E.S. Moss, E.M. Thompson, R.B. Seed, K.O. Cetin, A. Der Kiureghian, Y. Tanaka, and K. Tokimatsu, 2013. "Shear-Wave Velocity-Based Probabilistic and Deterministic Assessment of Seismic Soil Liquefaction Potential," J. Geotechnical and Geoenvironmental Eng., Vol. 139, No. 3 pp. 407-419.

Kim, D., Bang, E., Kim, W., 2017. Evaluation of Various Downhole Data Reduction Methods for Obtaining Reliable VS Profiles, Geotechnical Testing Journal, Vol. 27, No. 6, Paper ID GTJ11811.

Kramer, S., 1996. *Geotechnical Earthquake Engineering*, Simon & Schuster.

Kramer, S.L., and R.A. Mitchell. 2006. Ground Motion Intensity Measures for Liquefaction Hazard Evaluation, *Earthquake Spectra*, Vol. 22, No. 2, pp. 413-438.

Lane, J.W., Jr.; Liu, Lanbo; Chen, Yongping; and White, E.A., 2007. Near-surface site characterization using a combination of active and passive seismic arrays: EOS Transactions, American Geophysical Union, v. 88, no. 52, Fall Meeting Supplement, Abstract H13M-04.

Lane, J.W., Jr., White, E.A., Steele, G.V., and Cannia, J.C., 2008, Estimation of bedrock depth using the horizontal-to-vertical (H/V) ambient-noise seismic method, *in* Symposium on the Application of Geophysics to Engineering and Environmental Problems, April 6-10, Philadelphia, Pennsylvania, Proceedings: Denver, Colorado, Environmental and Engineering Geophysical Society, 13 p.

Liechty, D. J., 2018. Geophysical Surveys: Surface-Based Compressional and Shear Wave Seismic Refraction Tomography & Crosshole Shear Wave Profiling for Vs30 Site Characterization, Granby Dike #3, Colorado-Big Thompson Project, US Bureau of Reclamation Technical Memorandum TM-85-833000-2018-14.

Liu, Lanbo; Zhu, Lieyuan; and Lane, J.W., Jr., 2007. Analysis of the two-dimensional effect in the H/V spectral ratio method for bedrock depth estimation on bedrock depth estimation by the H/V seismic method [abs]: EOS Transactions, American Geophysical Union, v. 88, no. 52, Fall Meeting Supplement, Abstract H21A-0187.

Lockhart, A. C., Link, R., 2003. Summary Report on 1996 Geologic Investigations for Modification Decision Analysis, Safety of Dams Program, American Falls Dam, Minidoka Project, Idaho. Geology, Exploration & Instrumentation Group, Boise Idaho, Appendix A.

Martin ,A., J. and Diehl, J. G., 2004. Practical Experience Using A Simplified Procedure To Measure Average Shear-Wave Velocity To A Depth Of 30 Meters (Vs30), 13th World Conference on Earthquake Engineering, Paper No. 952, accessed October 20th, 2018, available at: https://www.iitk.ac.in/nicee/wcee/article/13_952.pdf

NEHRP, 2003. NEHRP Recommended Provisions for Seismic Regulations for New Buildings and Other Structures (FEMA 450), 2003 Edition, Part 1: PROVISIONS, Prepared by the Building Seismic Safety Council for the Federal Emergency Management Agency, accessed September 1st, 2017. Available at: https://www.nehrp.gov/pdf/fema450provisions.pdf

Nakamura, Y., 1989. A method for dynamic characteristics estimations of subsurface using microtremors on the ground surface, Quarterly Report, RTRI, Japan, v. 30, p. 25-33.

NCEER. 1997. *Proceedings of the NCEER Workshop on Evaluation of Liquefaction Resistance, Salt Lake City, 1996*. National Center for Earthquake Engineering Research, Technical Report 97-0022.

Odum, J.K., Williams, R.A., Stephenson, W.J., et al., 2007. Near-Surface Shear Wave Velocity Versus Depth Profiles, Vs30, and NEHRP Classifications for 27 Sites in Puerto Rico, USGS Open File Report 2007-1174, variously paged.

Park, C.B., Miller, R.D. and J. Xia, 1999. Multichannel analysis of surface waves, Geophysics, Vol. 64 No. 3, p. 800-808.

Park, C. B., Miller, R. D., & Xia, J., 1998. Ground roll as a tool to image near-surface anomaly, SEG Technical Program Abstracts, Pages 874-877.

Park, C. B., 2017. ParkSEIS 3.0 User Guide, Back-Scattering Analysis (BSA) and Common-Offset (CO) Sections.

Pierce, K. S., 2012. Geophysical Surveys – Cross-hole Shear-Wave Surveys & Geophysical Borehole Logging, Huntington North Dam, Emery County Project, Utah Upper Colorado Region, US Bureau of Reclamation Technical Memorandum TM-85-833000-2012-21

Reclamation, 2015. Design Standards No. 13, DS-13(13)-8, Phase 4: Final, Embankment Dams, Chapter 13: Seismic Analysis and Design. May 2015.

Rittgers, J. B., 2011. Follow-up Crosshole Shear-Wave Data Analysis Phase II Investigations, Ridgeway Dam, Colorado, Ridgeway Dam, Colorado, Dallas Creek Project, US Bureau of Reclamation Technical Memorandum TM-86-68330-2011-33.

Rittgers, J. B., 2014a. Geophysical Surveys – Full-wave Sonic Logging (Vs30), Safety of Dams Corrective Action Study, Boca Dam, Truckee Storage Project, Mid-Pacific Region, California, US Bureau of Reclamation Technical Memorandum TM-85-833000-2014-07.

Rittgers, J. B., 2014b. Geophysical Surveys – Cross-Hole Seismic and Full-wave Sonic (FWS) Logging (Vs30), Safety of Dams Corrective Action Study, Ochoco Dam, Crooked River Project, Pacific Northwest Region, Oregon, US Bureau of Reclamation Technical Memorandum TM-85-833000-2014-21.

Rittgers, J. B., 2016. Geophysical Surveys: Void Detection and Seepage Characterization- El Vado Dam, Middle Rio Grande Project, Upper Colorado Region, New Mexico, US Bureau of Reclamation Technical Memorandum TM-85-833000-2016-12.

Rittgers, J. B., 2017a. Geophysical Analysis: Approximation of Vs30 from Geologic Log Correlations, AMERICAN FALLS DAM, Minidoka Project, Pacific Northwest Region, Idaho, US Bureau of Reclamation Technical Memorandum TM-85-833000-2017-04.

Rittgers, J. B., 2017b. Geophysical Analysis – Seismic Profiling and Vs30 Site Characterization, Hills Creek Dam, Hills Creek Project, USACE Portland District, Norwest Division, Middle Fork Willamette, Oregon, US Bureau of Reclamation Technical Memorandum TM-85-833000-2017-09.

Rittgers, J. B., 2017c. Geophysical Surveys: 1D Crosshole Seismic Profiling, and 2D Crosshole Seismic Tomography, Prosser Creek Dam, Washoe Project, Mid-Pacific Region, California, US Bureau of Reclamation Technical Memorandum TM-85-833000-2017-18.

Rittgers, J. B., 2017d. Geophysical Surveys – 2D Seismic S-wave Refraction Tomography and Site Vs30 Characterization, Foster Dam, Foster Lake Project, USACE Portland District, Norwest Division, South Santiam River, Oregon, US Bureau of Reclamation Technical Memorandum TM-85-833000-2017-20.

Rittgers, J. B., 2018. Geophysical Surveys – Downhole Seismic Profiling, Cougar Dam, Cougar Project, USACE Portland District, Norwest Division, Willamette River Basin, South Fork McKenzie River, Oregon, US Bureau of Reclamation Technical Memorandum TM-85-833000-2018-09.

Robertson, P.K., D.J. Woeller, and W.D.L. Finn. 1992. Seismic Cone Penetration Test for Evaluating Liquefaction Potential Under Cyclic Loading, Canadian Geotechnical Journal, Vol. 29, No. 4, pp. 686-695.

Robertson, P.K., Cabal K.L., 2012. Guide to Cone Penetration Testing for Geotechnical Engineering, Gregg Drilling & Testing, Inc., 5t h Edition.

Robertson, P.K., 2009. Interpretation of Cone Penetration Tests - a unified approach. Can. Geotech. J. 46(11): 1337–1355

Sheriff, R.E., 1984. Encyclopedic dictionary of exploration geophysics: Society of Exploration Geophysics, 323 p.

Stokoe, K.H.,II, Wright, S.G., Bay, J.A. and J.A. Roesset, 1994. Characterization of geotechnical sites by SASW method, Geophysical Characterization of Sites, Technical committee for XIII ICSMFE, A.A. Balkema Publisher, Rotterdam, Netherlands, pp. 785-816.

Sturm, J., 2017. Geologic Data Package – May/June 2017 Sod Field Investigations – Prosser Creek Dam, In Geology Files, Reclamation Technical Service Center, Denver, Colorado.

Toksöz, M. N., and Johnson, D. H., 1981. Seismic wave attenuation, Society of Exploration Geophysicists, variously paged.

US Army Corps of Engineers (USACE), 2018. Cougar Dam, Phase 2 IES PROPOSED FIELD INVESTIGATION PROGRAM PLAN (FIPP) overview PowerPoint, USACE Portland District, Northwest Division, Portland, Oregon.

USGS, 2018. USGS Slope based Vs30 Map Viewer, an online data portal accessed on 7/6/2018, available at: http://usgs.maps.arcgis.com/apps/webappviewer/index.html?id=8ac19bc334f747e486550f32837578e1.

Wair, B. R., DeJong, J.T., and Shantz, T., 2012. Guidelines for Estimation of Shear Wave Velocity Profiles, PEER Report 2012/08, Pacific Earthquake Engineering Research Center, Headquarters at the University of California, December 2012.

Wald, D. J., and Allen, T. I.,2007, Topographic slope as a proxy for seismic site conditions and amplification, Bulletin of the Seismological Society of America, 97, no. 5, 1379-1395.

Weghorst, K., 2012. "Seismic Hazard," subsection from "Comprehensive Facility Review (CFR) Report for Minidoka Dam – Safety Evaluation of Existing Dams (SEED) and Review of Operation and Maintenance (RO&M) Programs – Minidoka Project, Idaho, Reclamation Dam Safety Office.

Wong, S. O., and Dober, M., 2010. Probabilistic Seismic Hazard Analysis for Minidoka Dam, Minidoka Project, South-Central Idaho, URS Corporation, Oakland, California, unpublished report for Bureau of Reclamation, Denver Colorado.

Worden, C. B., D. J. Wald, J. Sanborn, and E. M. Thompson, 2015. Development of an open-source hybrid global Vs30 model, Seismological Society of America Annual Meeting, 21-23 April, Pasadena, California.

Yong, A., Thompson, E.M., Wald, D., Knudsen, K.L., Odum, J.K., Stephenson, W.J., and Haefner, S., 2015. Compilation of Vs30 Data for the United States: U.S. Geological Survey Data Series 978, 8 p.

IX. Appendix A

Below, a series of nine appendix sections (A.1 through A.9) taken directly from Chapter 13 of Reclamation's 2015 *Design Standards No. 13: Embankment Dams* document are presented. These sections provide a detailed overview of typical workflows, products and the applications of seismotectonic studies performed at Reclamation:

A.1 Introduction

This appendix of Chapter 13, "Seismic Analysis and Design," of *Design Standards No. 13 – Embankment Dams* provides a brief introduction to the earthquake loadings that may be required for analysis of embankment dams or that may be encountered in reports of earlier analyses or field performance. The required scope of seismotectonic studies for a specific dam depends on the analyses that are likely to be performed. Some analyses may require only very simple inputs, such as peak ground surface accelerations; others may require synthetic or modified earthquake ground-motion records tailored to a specific site.

In current Bureau of Reclamation practice, the Technical Service Center's Seismotectonics and Geophysics Group provides the required loadings for the analyses, including probabilistic seismic hazard analyses (PSHA), maximum credible earthquakes (MCE) (rarely), acceleration time histories, uniform-hazard response spectra (UHS), etc. Therefore, this appendix contains only descriptive information for the benefit of the engineering analyst, not the methodology for developing the loadings, which is covered by other publications.

At present (2015), Reclamation's dam-safety practice is primarily "risk-informed," which means that decisions are made with a consideration of probabilistic risk analysis that considers the annual probability of seismic loading (or other type of loading), the likelihood of dam failure should various levels of loading occur, and the consequences of dam failure. This risk-informed practice contrasts with deterministic analysis and decision making, in which a dam is required to have, for example, some minimum factor of safety against slope instability when subjected to the MCE for the site. Therefore, *Design Standards No. 13 – Embankment Dams*, Chapter 13, "Seismic Analysis and Design," is intended primarily to guide geotechnical analysis in support of probabilistic risk analysis.

The characteristics of the dam and the expected use of the seismotectonic investigation; i.e., what analyses are expected, should be communicated to the seismologists as early in the process as possible. This will help to ensure that their work will meet the needs of the analysis without wasted effort or delays caused by adding more studies.

A.2 Products of Seismotectonic Studies

Depending on the level of analysis, seismotectonic studies for a given dam could include any or all of the following:

- Identification of seismogenic sources, both identifiable faults (which do not necessarily have surface expression but may have been identified through geophysical exploration or

previous activity), or zones of seismicity without identified causative faults. This is the foundation for all other seismotectonic studies.

- Estimated MCEs for the site, generally expressed in terms of magnitude and distance. While these are generally no longer part of current Reclamation practice, this information may be encountered in older reports and other sources.

- Hazard curves that give the annual exceedance probability for values of the peak horizontal acceleration at the ground surface (PHA, also called PGA), or other parameter, such as the spectral acceleration (SA) for a particular response period, or the Arias intensity, which incorporates both the acceleration peaks and the duration of the peaks as an index of seismic energy at the site (Arias, 1970; Kramer and Mitchell, 2006).

- Uniform-hazard response spectra, showing the SAs associated with a given exceedance probability, plotted as a function of the period of oscillation. For embankment dams, UHS is primarily used to identify appropriate earthquake ground motions for a particular analysis.

- Earthquake ground-motion time histories associated with specific scenarios, such as rupture of some particular fault, or with some annual probability of exceedance, considering all seismogenic sources. These are required for numerical analysis of deformation and cyclic stresses.

- Identifying potential for coseismic fault rupture in the foundation of the dam or for displacement of the reservoir basin that could cause destructive waves.

Seismogenic sources can be either identified faults or other structural features, or zones of seismicity without identified causative faults. Evaluation of fault sources usually includes general geologic information, fault geometry (length, strike, dip, and down-dip extent), style of slip (i.e., strike-slip fault versus thrust fault versus normal fault), fault segmentation, and rate of slip. When feasible, the rate of slip and activity of a fault are evaluated using paleoseismic studies, such as trenching across fault traces, to locate and age-date soil horizons that have been disrupted by fault movement, historic seismicity (including "microseismicity"), and surface deformation data (global positioning system [GPS], geodetic surveys, etc.). Source zones without identified fault sources are evaluated primarily from statistical analysis of historic seismicity; however, if there is reason to suspect the existence of a significant fault that is obscured by overlying strata, it can sometimes be identified from a combination of historic seismicity, surface deformation from aseismic fault creep, and geodetic measurements. Reclamation has used geophysical data obtained from petroleum exploration by others to clarify the geometry of faults and other structures.

Source characterization is a significant source of uncertainty in dam-safety evaluation, especially in the western U.S., where relatively little is known about active faults outside of major population centers. Reclamation dams are frequently located in rural parts of the West, where there is only basic understanding of fault activity and earthquake hazards. For dam safety risk analysis, it is often necessary to gain a better understanding of earthquake hazards than can be obtained from existing information. In fact, much of what is known about earthquake hazards outside of population centers in the western U.S. was developed for Reclamation's dam-safety program.

It can be tempting to simply default to conservative estimates for ground motions, material properties, etc., instead of addressing the uncertainty. However, this can lead to a design that is

unnecessarily conservative, or a decision to modify a dam that creates only modest risk. PSHAs sometimes address this by developing 16th- and 84th-percentile curves (or similar) for the annual probability of exceedance for some index of loading, in addition to mean and median hazard curves. This can be valuable for assessing the need for additional seismotectonic studies. If, for example, calculating risk assuming the 16th-percentile loadings, instead of the mean, gives a different overall outcome (such as whether an existing dam should be modified), confidence in the result would not be very high. Additional seismotectonic investigation may help clarify the situation and increase confidence in the decision.

Ground-motion parameters can be developed for a specific scenario, such as the MCE from a given fault, or in a probabilistic study that considers the frequency of occurrence and magnitudes from all sources in the general area of the dam. The most commonly used parameters for embankment dams are PHA, earthquake magnitude, acceleration response spectrum, and acceleration time histories. Acceleration response spectra (discussed below) are not used directly in analyses of embankment dams the way they sometimes are in structural analysis. They are, however, used to indicate the frequency content of ground-motion records to determine whether a given record is appropriate for a dam site. PHA and response-spectrum values can be expressed as point estimates for a single earthquake scenario, or as hazard curves showing the relationship between parameter values and annual probability of occurrence. Vertical accelerations are frequently included in seismotectonic studies and numerical analysis, although their importance for embankment dams is typically fairly minor compared to the horizontal motions.

To estimate any ground-motion parameter for use in an engineering application, it is necessary to have a clear understanding of the site geology and dynamic characteristics, both shallow and deep. There are significant differences in ground motions between rock and soil sites. It is important to perform the calculations of ground motions using assumptions about site conditions that are consistent with the engineering analyses. Furthermore, for numerical response and deformation analysis, it is necessary to use acceleration time histories that are consistent with the depth where the ground motions will be applied to the model. In other words, if the ground motions will be applied to a finite-element model at its base 50 feet below the ground surface, the input ground motions must be what would happen 50 feet below ground, not on the surface. Surface records can be adjusted numerically (deconvolved), but clear communication between the engineers and the seismologists is vital, so that all of them understand how the records will be applied in the numerical model.

A.3 Earthquake Magnitude

Earthquake magnitude is an index of the amount of energy released by an earthquake (Kanamori, 1983). On its own, magnitude indicates very little about the severity of loading at a particular site; however, when combined with the distance from the source to the site, it can be used to estimate other measures of loading, including the peak ground acceleration (horizontal and vertical) and SA. Magnitude correlates fairly well with the duration of strong shaking or the number of strong cycles of shaking, so it is used as a proxy for the number of cycles in liquefaction triggering analysis and in some simplified deformation analyses. Magnitude is generally abbreviated as "M," usually with a subscript to indicate how it was calculated (as described below).

The Richter scale (sometimes abbreviated M_L for "local magnitude") was the first practical method to quantify the overall energy release from an earthquake. Originally developed in the 1930s by C.F. Richter, the Richter scale is based on the response of a specific instrument (Wood-Anderson torsion seismograph) at a specific epicentral distance (100 kilometers [km]). It has no real physical meaning and is simply a rough index for comparing sizes of earthquakes. Richter magnitude is seldom used now (except in countries of the former Soviet Union), but the term "Richter scale" persists in the popular media, and occasionally in technical publications, even when other magnitude scales are actually being reported. The Richter scale is generally not useful for magnitudes above about 6.5 because the scale "saturates;" that is, increases in energy release do not produce consistent increases in the response of the Wood-Anderson seismograph. Hence, it cannot, for example, distinguish very well between 7.0 and 7.5. It was not intended to be used for earthquakes more than about 1,000 km away. Other magnitude scales have been proposed since then, based on the intensity of specific types of waves or on the perceived level of shaking at different distances. Most magnitude scales have been "calibrated" to coincide with Richter magnitude, to the extent practical, for consistency and ease of comparison.

The moment magnitude, M_w, is the preferred scale in most of the world because it has a physical basis and does not saturate at large magnitudes. It is based on the seismic moment, which is an index of the strain energy released by the earthquake.

The moment, M_O, is a function of fault area, fault displacement in the earthquake, and the shear modulus of the bedrock. M_w is a function of the seismic moment:

$$MW = 2/3 \log(MO) - 6.0 \qquad \text{Equation A1}$$

The seismic moment, M_O, is defined as:

$$MO = \mu A s \qquad \text{Equation A2}$$

where μ is the shear modulus, A is the area of the causative fault (or of the causative segment), and s is the average displacement. (M_O has the same units as energy, dyne-centimeters, and it is roughly proportional to the energy released.) Equation A1 indicates that an increase of 1.0 in M_w corresponds to a 32-fold increase in energy M_O.

M_w can also be estimated from the Fourier spectra of recorded acceleration time histories, allowing comparison between magnitudes predicted from fault characteristics and magnitudes that have occurred.

For fault sources, the estimate of maximum magnitude is usually based on fault parameters, such as rupture dimension, and displacements in previous events. For source zones, analyses of historical data, physical constraints on rupture dimensions in features lacking surface expression, dimensions of zones of concentrated historic seismicity, and analogies to other regions are used. Maximum magnitude estimates should include estimates of uncertainty. Magnitude is used in selecting appropriate loadings for dam analysis (such as peak ground acceleration and acceleration time histories). Many simplified analyses of settlement and liquefaction potential use the magnitude as a proxy for the number of cycles of strong loading.

A.4 PHA and SA

The PHA is frequently an input in seismic analyses, including liquefaction triggering and dynamic deformation. (Peak vertical acceleration is seldom a major consideration for embankment dams, although vertical acceleration time histories are often included in response or deformation analysis.) Peak accelerations are predicted from empirical ground motion prediction equations (GMPE), also called attenuation curves, which give PHA (or other parameter) as a function of earthquake magnitude and distance from the site to the fault rupture surface. GMPEs are updated periodically as new earthquakes provide additional data. For the western and central U.S., the most recent GMPEs are provided by the Next Generation Attenuation West2 (NGA-West2) models (Bozorgnia et al., 2014). Different parts of the U.S. require different attenuation relationships; for some sites, it may be necessary to use more than one GMPE because it is not always obvious which one should be used. For a given magnitude and distance, earthquakes in the eastern and central U.S. generally yield higher PHAs. Most of Reclamation's dams are located in the Rockies, or farther west, and would require GMPEs for the western U.S., and dams on the Great Plains usually require GMPEs for the central and eastern U.S. PSHAs for dams near the interface between the mountains and the plains may need to incorporate both (for example, those in the Colorado Front Range). Predicted ground motions also depend on the characteristics of the site, usually represented by Vs30, which is the time-weighted mean, shear-wave velocity in the top 30 meters (m) (98 feet [ft]). (The time-weighted mean is equal to 30 m divided by the travel time for a shear wave to travel upward through the top 30 m, rather than the mean velocity weighted by layer thickness.) Sites with soft bedrock or deep soil profiles may require geophysical investigations to determine Vs30.

The SA provides a general indication of how strongly a structure would respond to a particular earthquake motion. For a given earthquake record and a given period of oscillation, the SA is equal to the calculated peak acceleration of a one-degree-of-freedom oscillator driven by the acceleration record. For embankment dams, the SA is mainly used to select appropriate ground-motion records for dynamic response or deformation analysis, so they are realistic for the source and would excite the structure at the frequencies of greatest concern. (The SA has other uses in structural engineering.) Usually, the SA is calculated for a wide range of fundamental periods, ranging from zero to several seconds, and plotted as a function of period to obtain the response spectrum, which is unique to each earthquake record. In general, the more energy the record contains at a particular period of oscillation, the greater the SA will be at that period. If the earthquake record contains primarily long-period motion (for example, 0.5 second or longer), it would produce a greater response when applied to a structure with a similar period than it would when applied to a structure with a shorter period, like 0.05 second. For the special case of a rigid oscillator, whose fundamental period is zero, the SA is equal to the PHA of the earthquake record.

Like peak accelerations, SA values for fundamental periods other than zero can be estimated from magnitude and fault distance using empirical GMPEs. Most empirical attenuation relationships that are used to predict parameters like PHA and SA apply to either bedrock outcroppings or stiff soils. Additional calculations are required if the engineer needs the peak acceleration or other quantity at the surface of a soft soil, or at some depth below the surface. In particular, the Seed-Lee-Idriss simplified procedure for liquefaction potential requires PHA at the soil surface, not at a bedrock outcropping (NCEER, 1997). The difference is very important

because the acceleration on a level soil surface is commonly 80 to 200 percent of what the same earthquake would produce on a bedrock outcrop. Nonlevel ground (a dam embankment, for example) can cause even greater amplification. The peak acceleration at the interface between bedrock and the overlying soil would be somewhat lower than on exposed bedrock. Therefore, there needs to be clear communication on what location an estimate of a parameter like PHA or a ground-motion record is to be applied in the analysis, such as at a bedrock outcropping, 40ft below the top of bedrock in the embankment foundation, etc. The specific needs of the investigation should be conveyed to the seismologists in advance, and the seismologists should explicitly label hazard curves and other products with the locations at which they are applicable.

A.5 MCEs

In earlier Reclamation practice, dams were typically evaluated for MCEs and required to withstand that loading. The MCE is literally the largest earthquake that could credibly be produced by an identified source (fault or fold), or by a zone of historic seismic activity. A dam that might not survive the MCE would have been considered deficient, and some sort of corrective action would be required. For each potential source, the peak acceleration and other parameters for the MCE were estimated by attenuation curves that are functions of distance from the source.

For an identified fault source, the MCE is usually determined by the dimensions and characteristics of the fault, and how far it could slip in a single event. Where the source is a zone of seismicity, rather than an identified fault, the MCE is sometimes defined by an annual probability of exceedance of 1/5,000 to 1/20,000 (with the precise value being somewhat arbitrary because the MCE has no probability associated with it). This is sometimes referred to as a "random" or "floating" MCE. A particular annual probability does not define one particular earthquake scenario, so the random MCE for a site could, for example, be a magnitude 5.5 earthquake within 20 km from the site, a magnitude 6.0 earthquake within 45 km, or a magnitude 6.25 earthquake within 70 km, all of which would have the same annual probability. Therefore, the random MCE for a site is often expressed as several pairs of magnitude and distance, and there can also be fault-related MCEs in the same analysis. It may not be obvious which of those earthquakes actually represents the worst loading for a particular structure. It depends on earthquake magnitude, distance from the site, the nature of the structure and its foundation, and the type of analysis being performed. For some analyses; e.g., liquefaction potential, the earthquake producing the highest peak acceleration is not necessarily the most severe loading, because larger magnitude earthquakes tend to produce more cycles of strong acceleration, even if the peak is lower. Sometimes, engineering analysis is required to determine which potential load case is most severe.

Typically, PSHAs provide hazard curves for outcroppings of bedrock or stiff soil. The peak acceleration on a soft soil surface or on a dam embankment can be somewhat lower, or as much as double the acceleration on bedrock. Similarly, ground-motion time histories are usually developed for motion at the surface of a rock outcropping, although modern computational techniques permit development of acceleration or shear stress records that would apply at some depth in the bedrock or a thick layer of soils above bedrock, so they can be applied at the base of a response model (finite-element or finite-difference).

Although the "deterministic" MCE approach has been superseded in Reclamation's dam-safety practice, it is still commonly required among regulatory agencies and dam owners outside Reclamation; some have specific requirements for the level of conservatism in selecting the MCE ground motions, such as using the 84th percentile. Although the MCE is no longer part of typical Reclamation dam engineering practice, it is frequently referred to in older documents.

A.6 PSHA and Risk Analysis

In current practice at Reclamation, dam-safety decisions are generally based on the amount of risk a dam poses to public safety. For probabilistic risk analysis, it is necessary to know probabilities associated with different levels of loading, not just the maximum loadings considered possible at a site. This requires a PSHA, which yields curves of PHA values (and other parameters, such as 1-second SA) versus the annual probability of each value being exceeded. (Strictly speaking, these are frequencies of exceedance, rather than annual probabilities, but for practical purposes, they can be treated as probabilities for earthquakes of interest for dam safety.) PSHA is fundamentally an accounting method that combines earthquake recurrence information for all sources directly with earthquake energy-propagation models (attenuation curves). Figure A1 shows typical hazard curves, which give the mean annual probability that the peak ground acceleration or SA would exceed a particular value, along with confidence bounds. For example, the probability that the PHA would exceed 0.6 g (very severe loading) in any year is about 1.7×10^{-4} or 1/6,000, as indicated by the heavy dashed lines. The heavy red curve in figure A1 represents the sum of the hazards from a number of sources, with different activity rates, maximum potential magnitudes, and distances from the site. For this particular site, the great majority of the PHA hazard results from two major faults located nearby, each capable of producing earthquakes with magnitude M_w up to about 7 (the solid blue and black curves). Note that the summation occurs in the vertical direction, adding the exceedance probabilities for a given value of PHA (or other parameter), not in the horizontal direction.
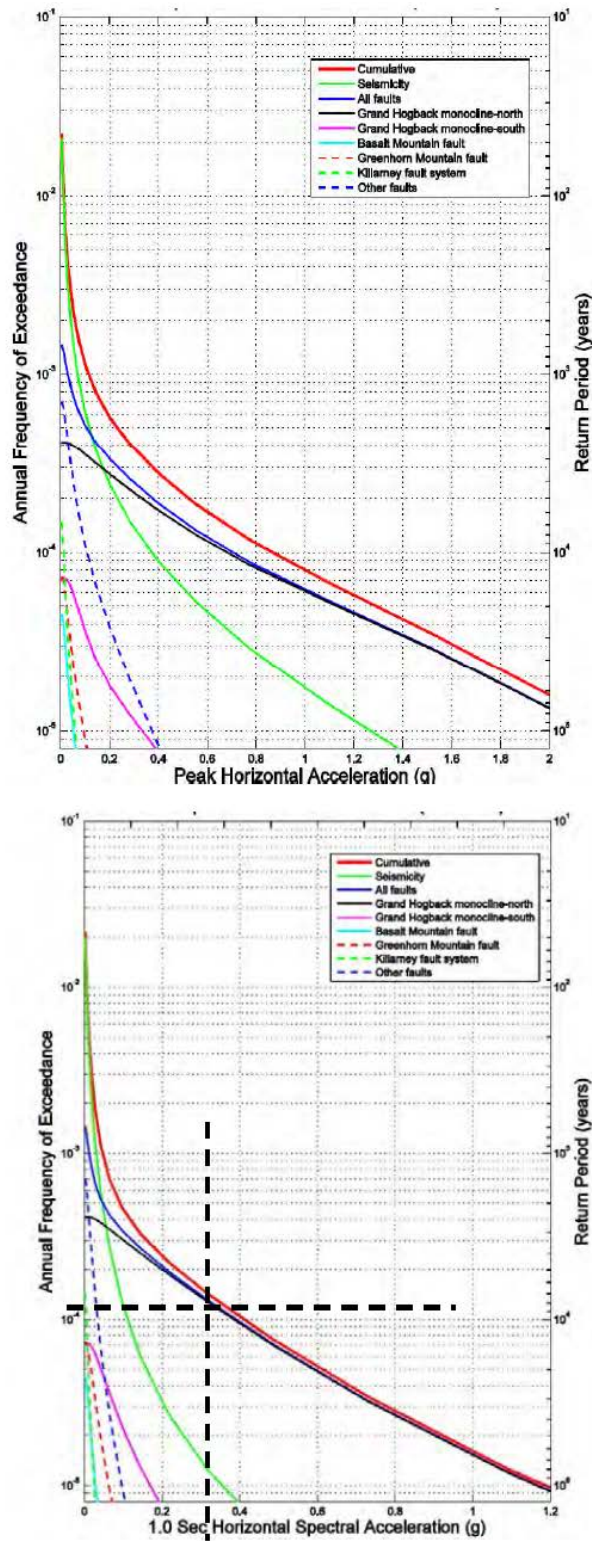
Figure A1 - Typical hazard curves giving probability of exceedance for PHA and for 1-second SA.

As mentioned above, the PHA does not, on its own, provide a complete description of the loading. For simplified liquefaction triggering analysis, one needs, at minimum, PHA at the ground surface and the earthquake magnitude, Mw. (The magnitude is used as a proxy for the number of cycles of strong motion because magnitude and duration correlate fairly well.) Numerical analyses of response and deformation require ground-motion records (time histories) with durations and frequency contents that are realistic for the earthquake source and the return period.

The widely used Seed-Lee-Idriss simplified method of liquefaction triggering analysis uses cyclic shear stresses estimated as a function of PHA and depth, via the factor rd, which is a function of depth. (See the main text of this chapter.) Therefore, a risk analysis based primarily on the simplified analysis may require hazard curves only for PHA (with some indication of the average earthquake magnitude to associate with a value of PHA). However, other analyses may require different indices of loading and, therefore, different hazard curves. For example, Bray and Travasarou's simplified deformation analysis (2007) uses the SA for a period equal to 1.5 times the fundamental period. Pseudostatic analysis of appurtenant structures, such as intake towers or spillway gate piers, may use the SA for the structure's fundamental period directly in the calculations. In these cases, the main index of loading in a risk analysis would be something other than the PHA.

Numerical analyses of response (including cyclic shear stresses) and deformation are sensitive to the frequency content of the ground motions; they require ground-motion records that are suitable for the specific source of the earthquake, including magnitude, distance, and style of faulting. Selecting suitable records therefore requires hazard curves for SA over a wide range of periods (further discussed below).

In contrast to embankments, concrete structures generally have shorter fundamental periods, and they are unable to tolerate as much momentary yield and permanent deformation as an embankment. Like concrete dams, appurtenant structures, such as spillway retaining walls, may have "brittle" failure modes, so yield needs to be avoided, unlike embankment dams where yield is expected to occur with fairly modest PHA values and can often be tolerated (within limits). Short-period hazard curves (including PHA) are required for stiff structures.

In seismic risk analysis of an embankment dam, the first entries of the event tree are commonly the earthquake loadings, although the first event can also be conditions that exist prior to the earthquake, such as reservoir level or foundation properties. Usually, the input loadings are either ranges or "bins" of PHA (or a related parameter) within which generally similar behavior is expected, or they are earthquake ground motions that could plausibly represent earthquakes with a particular return period.

If the risk analysis will be based on a simplified liquefaction analysis with the cyclic stress ratio (CSR) proportional to the surface PHA, the loading would be divided into PHA ranges with, to the extent practical, similar probability of liquefaction. The probability of each PHA range is simply the probability of exceeding the lower limit, but not exceeding the upper limit. If the range of interest is 0.3 to 0.5 g, figure A1 indicates the annual probability of a PHA in that range to be 3.9×10^{-4} minus 2.1×10^{-4}, or 1.8×10^{-4}.

If, instead, the risk analysis will be based on more detailed analysis, whether site response to calculate the CSR directly (rather than using the simplified equation with rd) or some type of numerical deformation analysis, the inputs would generally be ground motions to represent particular return probabilities. For example, the dam may have been analyzed with motions representing 1/500-, 1/1,000-, 1/5,000-, and 1/20,000-year loadings. In this case, the response or deformation using the 1/5,000-year earthquake might be assumed to represent all ground motions with return periods of 1/3,000 to 1/7,000 years. The probability of that range of loadings is also the annual probability of exceeding the lower limit, but not exceeding the upper limit. In this case, the load probability is 1/3,000 minus 1/7,000, or 2×10^{-4}.

The PSHA begins with identifying the sources, determining the recurrence characteristics of each source, and then applying empirical ground-motion prediction equations (GMPEs) to determine how events at each source would affect the dam site. The characteristics each source and the GMPEs are used to develop an individual hazard curve, giving the annual probability of exceedance for PHA or other parameter at the dam site contributed by each source. The individual probabilities are then summed as shown in figure A1.

In a region where no active faults have been identified, the earthquake hazard is based primarily on historic seismicity. Rates of occurrence are calculated from historic accounts and any available seismograph recordings. This can be complicated by the relatively short observation periods in the western U.S., as well as the relative lack of seismometers. In areas that were sparsely populated at the time of important earthquakes, there may be very few eyewitness accounts of the intensity of shaking. Recurrence rates are estimated from historic and recorded seismicity by statistical methods, although interpreting the statistics requires some judgment about site response and the PHA and M_w inferred from historic accounts, etc.

Where active faults have been recognized, the earthquake hazard is based on both historic seismicity and paleoseismicity. Recurrence intervals and the amount of movement from each event, and the variability associated with them, are best estimated from paleoseismologic trenching studies, in which the displacements from individual previous events are measured, and the timing of the events is determined by topsoil development, carbon dating, and other geologic techniques. Even with detailed paleoseismologic data, the uncertainty in frequencies and magnitudes can still be very large. As in every other aspect of seismic analysis of dams, uncertainties in earthquake recurrence need to be estimated and documented for every seismotectonic study.

The value of PHA (or other parameter) having an annual probability of exceedance of 1/1,000, for example, is sometimes referred to as the "1,000-year PHA," and the "recurrence interval" or "return period" is said to be 1,000 years. These are both somewhat misnomers because they appear to imply that the ground motion would occur once every 1,000 years. The probability of the 1/1,000-year PHA being exceeded in a given millennium is actually 1-[(1-1/1,000)1000] or 0.63 (assuming each year to be an independent "trial," with no periodicity). While "recurrence interval" and "___-year earthquake" are convenient and familiar terms, they are sometimes misunderstood and need to be used carefully. Referring to the "1/1,000-year earthquake" may be less confusing.

Empirical GMPEs are available for both the PHA and the SA for longer periods, which allows hazard curves to be produced for both PHA and SA at longer periods that could be of importance for a dam. The hazard for the full range of periods of oscillation can be shown on a single plot showing the UHS for different return periods, including zero, which corresponds to the PHA. Each curve on figure A2 corresponds to the SA having a given exceedance probability, as a function of oscillation period. In effect, the PSHA has generated hazard curves for SA for periods of 0.01 to 5 seconds. The UHS curves are a plot of, for example, the 1/10,000-year value from each of those hazard curves. For embankment dams, the main use of UHS is in selecting ground motions for numerical analysis of response or deformation. The shape of the curves can vary with the characteristics of the source. For example, if the primary source is a large distant fault, the UHS would generally be higher at long periods, compared to local "random" seismicity of smaller magnitudes, even if the closer, smaller earthquakes would give higher peak acceleration.

The major benefit of the PSHA is that it combines the hazard from all potential sources to provide a more complete picture of the earthquake hazard for the dam site. However, many types of analysis require more than one parameter, so a unified PHA hazard curve cannot portray the probability for all "components" of the loading. For example, the simplified Seed-Lee-Idriss empirical liquefaction analysis (like the many methods that grew out of it) requires the earthquake magnitude as a proxy for the number of cycles of loading, in addition to the PHA (NCEER, 1997). However, a particular value of PHA or SA could result from a small, nearby earthquake, or a very large one distant from the dam site. Combining all of the earthquake sources into a single PHA hazard curve obscures the contribution from particular sources, and it may not be clear what magnitude to apply in the liquefaction analysis, or what duration of strong motion a record for deformation analysis should have. Therefore, it would be necessary to disaggregate the PSHA results into the contributions from the various sources.

Figure A3 portrays this in a three-dimensional plot of magnitude and distance in the horizontal plane, and relative contributions to the total hazard (exceedance probability) on the vertical axis. As shown in figure A3, the hazard is dominated by sources within 10 km of the dam (primarily represented by the solid blue and black curves in figure A1). It is also apparent that the hazard comes from earthquakes with a wide range of magnitudes. This information needs to be accounted for in the geotechnical and risk analyses because liquefaction potential and dynamic deformation are both strongly dependent on the number of cycles of shaking, not just the peak acceleration. The number of cycles is generally much larger with larger-magnitude earthquakes, and the frequency content tends to be different.
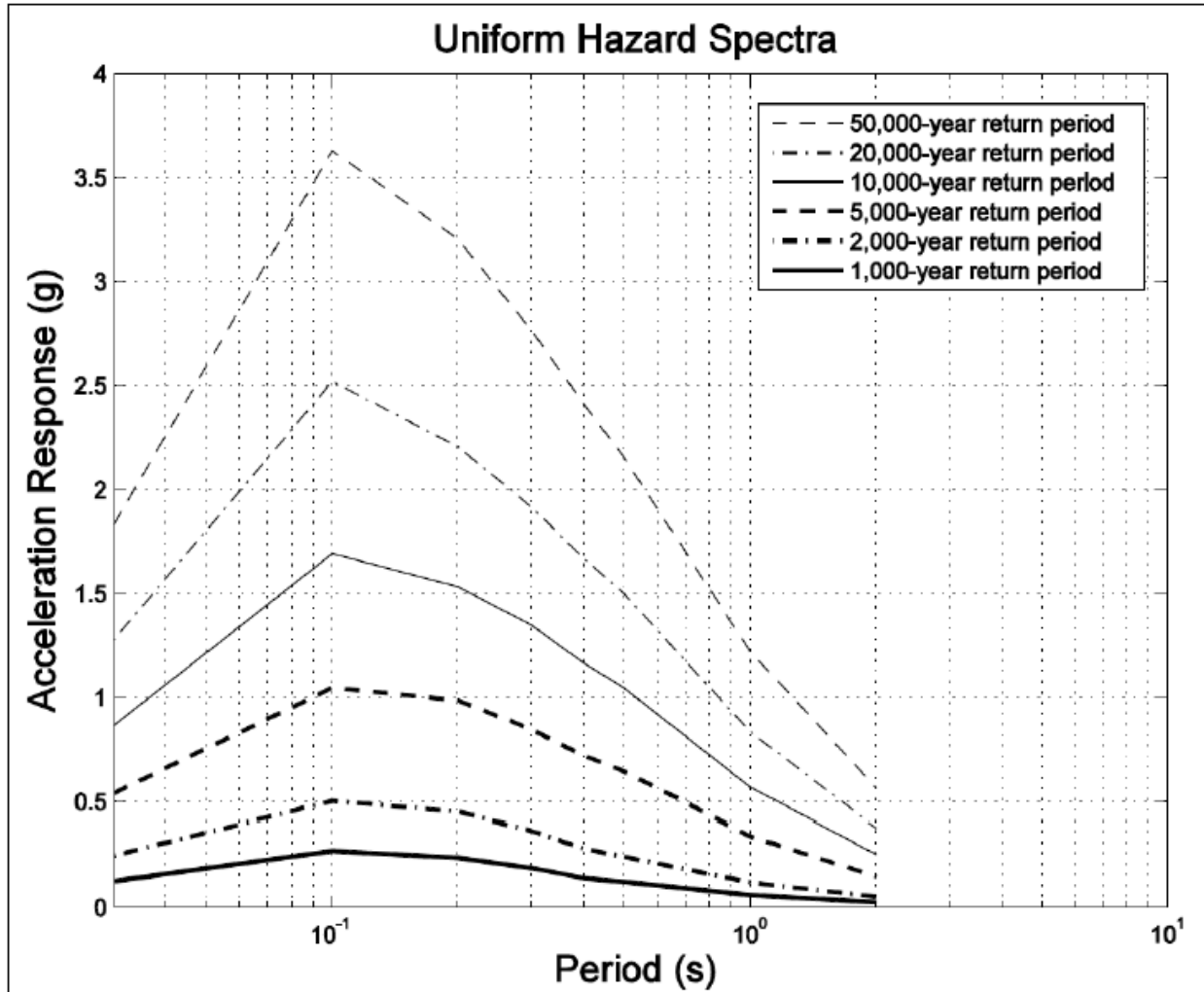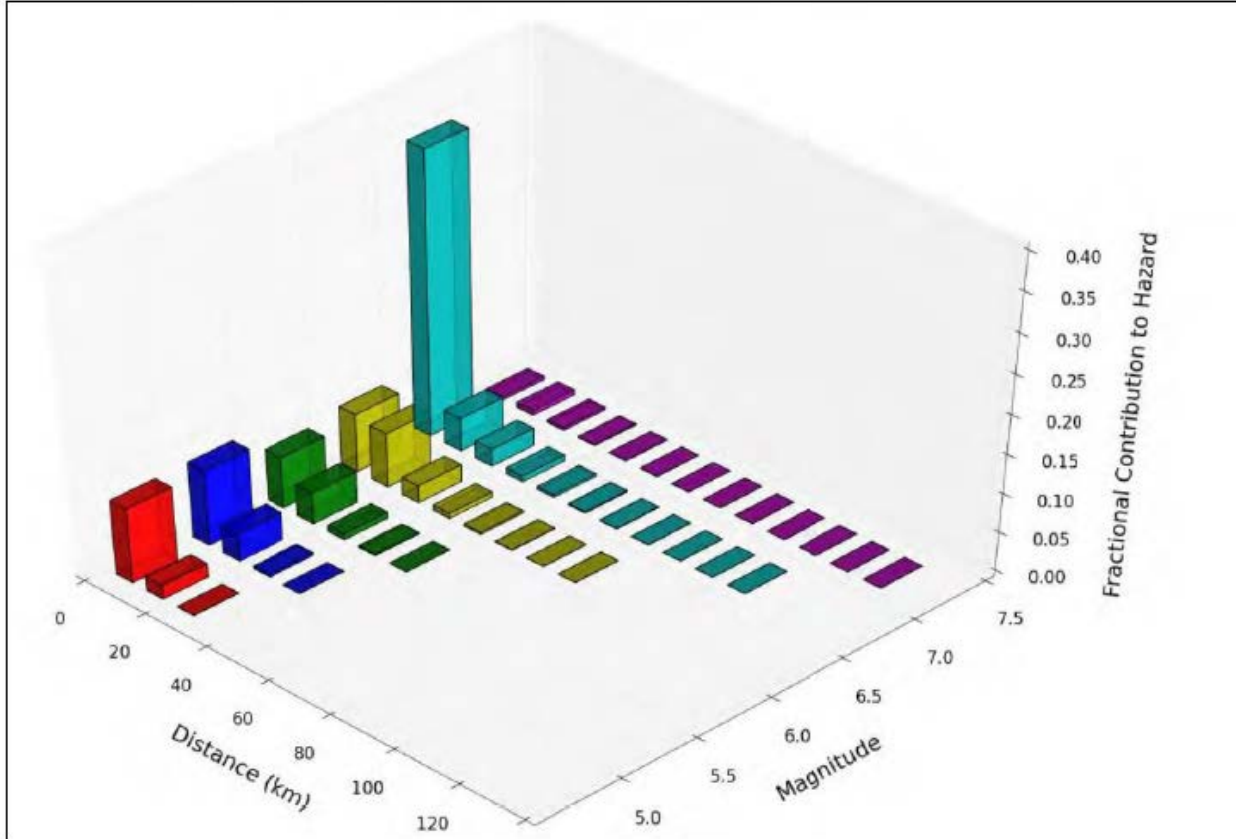
Figure A2 - Example UHS. Each curve indicates the SA with a particular exceedance probability, plotted as a function of oscillation period.

Figure A3 - Example 1/10,000-year PHA hazard disaggregated to show relative contributions from different sources.

A.7 Earthquake Ground Motions for Response and Deformation Analysis

Analyses of dynamic response, cyclic stresses, and deformation may require more information than just peak acceleration and magnitude. The analyses may also require records of ground acceleration as a function of time, so that dynamic responses (accelerations, shear stresses and strains, deformation, etc.) can be calculated as functions of time. (Sometimes, ground motions are input as shear stress at the base of a finite-element or finite-difference model, rather than as acceleration, but the same considerations apply.) Ground motions can be developed for a specific scenario, such as the MCE or 1/5,000-year earthquake from a particular fault, or to represent ground motions with a particular probability of exceedance, considering the frequency of occurrence and magnitudes from all sources in the general area of the dam.

Deformation of a dam embankment is generally not very sensitive to high-frequency shaking with periods less than 0.2 second. Instead, it is much more sensitive to longer periods, such as 1 second. Beginning with a record that is rich in long-period shaking then numerically filtering out the portion with periods less than 0.2 second, the PHA could be reduced significantly but there may not be much difference between the deformations predicted with the original and filtered records. If the PHA exceeds 0.2 g, most embankments would experience momentary yield and plastic deformation, which can typically, but not always, be tolerated, aside from any effect it

would have on appurtenant structures. If the ground motion consists predominantly of very short periods, the duration of each occurrence of intermittent yield would be very short, and, therefore, the amount of deformation would be small. If the strong shaking predominantly consists of longer periods, the duration of each yield event and the permanent deformation could be much greater. There is also some effect from the elastic response of the embankment, which can magnify the acceleration, particularly if the record contains a large amount of energy near the fundamental period of the embankment. Thus, ground motion records must both be realistic for the earthquake sources, and be selected according to the hazard curves for the most critical periods for the dam. The critical period can be significantly different from the fundamental period of the embankment. Also, when response analyses are performed for liquefaction analysis, the computed CSR is strongly influenced by the long-period portion of a record's response spectrum, not just the PHA. For these reasons, PSHAs for embankment dams need to include hazard curves for parameters that reflect long-period shaking, such as 1-second SA, along with the PHA. Periods as long as 3 seconds may need to be considered in selecting ground motions for deformation analysis of a high dam.

Time histories for analysis can be existing strong-motion recordings or computed synthetic records. (Details of generating synthetic records and modifying existing records are not presented here because, at Reclamation, seismologists usually perform this work, rather than engineers.) Ground-motion time histories are selected with consideration of style of faulting, earthquake magnitude, source distance, and the specified return period, as well as the nature of the structure to be analyzed. A large embankment dam may respond most strongly to vibration with a period on the order of 1 second (depending primarily on its height and the stiffness and strength of the embankment materials). In contrast, a concrete dam might respond more to vibration with a period of 0.1 second. The response of soils is highly nonlinear, and the shear modulus decreases markedly with increasing strain, so the fundamental period at very low strains may have little relationship to how the dam responds under large accelerations with large strains. There is, unfortunately, no simple way to compare two acceleration records and determine which one constitutes more severe loading, without actually doing the response analysis and comparing results. Whether for a deterministic analysis with a design-basis earthquake or as input for a probabilistic risk analysis, a number of different plausible earthquake time histories need to be used for each scenario or return period.

Although the UHS is a useful tool for looking at the general severity of loading as a function of probability, it would not match the response spectrum for a particular recorded earthquake or earthquake scenario. Actual earthquake response spectra usually have one or two main peaks at particular oscillation periods, with the remainder of the spectrum being lower than the UHS. The 1/1,000-year UHS is an envelope for all possible earthquake ground motions that can be considered to have 1/1,000 annual probability of exceedance. A response spectrum only needs to touch the 1/1,000-year UHS at one oscillation period to be considered a 1/1,000-year loading. It is quite unlikely that an actual earthquake would touch the UHS at numerous different oscillation periods.

Therefore, ground motions for analysis should not be forced to match the UHS for the full range of periods because that would be unnecessarily conservative. For a 1/1,000-year earthquake, for example, that would require the ground motions to match the 1/1,000-year PHA, the 1/1,000-year 0.1-s SA, the 0.2-s SA, the 1.0-s SA, etc. This is much less probable than an earthquake that

fits the 1/1,000-year UHS in a small range of periods. At some sites, the short-period portion of the UHS (including the PHA) is governed by small nearby earthquakes, and the long-period portion is governed by distant, large-magnitude earthquakes. Ground motions matching the whole UHS would, therefore, require simultaneous occurrence of two earthquakes! The example disaggregation plot in figure A3 shows that the PHA hazard is distributed over a wide range of magnitudes, and a response or deformation analysis would require ground motions representing two or three different magnitudes, with the PHA probability distributed among them. Whether for deformation analysis or liquefaction triggering, it is not always obvious which source really governs the risk until the analysis is performed. (This needs to be allowed for in budgets and schedules.)

When response analyses are required, to produce shear stress, deformation, etc. as inputs for risk analysis, but suitable records for a particular earthquake scenario do not exist, available records can be modified to fit the scenario. Simple proportional scaling of recordings to match some specific parameter, such as peak acceleration or spectral response at a particular period, should be avoided, except when the adjustment is small, because the results can be unrealistic. There are preferred techniques for numerically adjusting available records to match the UHS at a particular oscillation period of interest. One such technique is the conditional mean spectrum (CMS) (Baker, 2011). It is not always obvious which period is most critical for a particular dam, so the preferred practice is to apply CMS to several existing records, each with two or more potentially critical oscillation periods. The resulting modified records are used in the response or deformation analysis to determine the most critical oscillation period; subsequent response and deformation analyses can then be focused on records matched to that period. With nonlinear behavior expected for embankments, the most critical period is often longer than the fundamental period of the embankment.

Typical Reclamation practice is for the Technical Services Center (TSC)'s Seismotectonics and Geophysics Group to provide several sets of ground motion records for each return period requested (with each set consisting of two horizontal components and the vertical component). These records may all be adjusted to fit the UHS for one particular oscillation period, or to fit several different periods, depending on the anticipated behavior of the embankment and/or other structures. By design, each of these records is equally likely because each matches the UHS at one particular period or range of periods. It is, therefore, unnecessarily conservative to base a risk analysis only on the records and the polarity that give the worst results in response analysis. If only one or two out of six sets of records "tested" indicate severe distress to the dam, ignoring the results of the other records, which are equally likely, would cause the risk to be overstated by a significant factor. Carrying more sets of ground motions through the engineering analysis would significantly increase the labor cost, but that may be necessary so that the full range of results is available for the risk analysis. The "default" assumption in preparing project budgets and schedules should be that several ground motions will be used for each permutation of return period and material assumptions, not just the single record identified as the worst.

It is important that ground motions also fit the location at which they are applied to a numerical model. Typical ground-motion attenuation relationships and historic earthquake records are provided for bedrock outcroppings or the surface of stiff soil. However, in finite-element or finite-difference response and deformation analysis, the motions are usually input as records of acceleration or shear stress at the base of the model. This requires them to be numerically

adjusted or "deconvolved" to find the acceleration time history that would occur at the depth of interest. Typically, this is done beginning with an outcrop record and using a simple response-analysis program like SHAKE to modify it. Refer to *Design Standard No. 13 – Embankment Dams*, Chapter 13, "Seismic Analysis and Design," Section 13.5.3, "Seismic Loading."

A.8 Required Scope of Seismotectonic Studies

There is no single scope of work that is universally applicable to all dams and all levels of analysis. The level of effort required depends on the seismotectonic setting of the dam, the nature of the foundation soils and embankment, appurtenant features, and the possibility of coseismic movement of foundation faults.

At minimum, a risk analysis that is based on simplified methods for liquefaction triggering and slope-stability analysis would require a hazard curve for PHA, and an indication of appropriate magnitudes to apply in the liquefaction analysis. As discussed above, it is not strictly correct to use a single value of magnitude for a single value of PHA, let alone for all values of PHA because the hazard comes from a range of magnitudes, although, in some cases, it may be a reasonable approximation to use an average magnitude without much loss of precision. However, in many other cases, it is necessary to distribute the disaggregated hazard between smaller, nearby earthquakes and larger, distant earthquakes with different magnitudes applied in the liquefaction triggering analysis, and with different ground motions applied in response and deformation.

For nonlinear deformation analysis performed to support a probabilistic risk analysis, hazard curves are required for the full range of periods from 0 to 3 seconds, and possibly more. These hazard curves are needed to select or create ground motions that are appropriate to the magnitude, distance, and style of faulting for each source. It is suggested here that five or more sets of records be provided for each return period to be analyzed (each set consisting of two horizontal and one vertical). These records should be selected to match the UHS at oscillation periods selected for the particular dam under study. For two-dimensional analysis, this would create 20 combinations of horizontal and vertical motion, with 2 horizontal components from each of 5 earthquakes, and each horizontal component applied both upstream-downstream and downstream-upstream (different polarity). From these twenty, it may be feasible to identify two to four records that would portray the full likely range of results. Sometimes, one of the horizontal components is obviously much less severe than the other, and the effect of changing the polarity of a horizontal motion is typically small.

A.9 Summary

Reclamation's dam-safety program is largely guided by probabilistic risk analysis. In addition to knowing the behavior of dams under various levels of earthquake loading, this requires probabilities to be associated with the different levels of loading. Deterministic seismic hazard methodologies, such as the MCE, have been superseded by the PSHA in Reclamation's practice. The PSHA combines the annual exceedance probabilities for some measure of earthquake loading, such as the PHA, from all known seismic sources into unified hazard curves for different measures of earthquake loading, including the PHA and SAs for oscillation periods of interest. Depending on the level of analysis, the hazard curves may suffice, or they may need to

be used in a more detailed analysis to develop suitable ground motions for numerical analysis of embankment response and deformation.

Even for simplified analyses of deformation and liquefaction potential, the relationship between PHA and probability does not provide enough information. The PHA hazard may require disaggregation, so that pairs of PHA and magnitude can be associated with both probability of their occurrence and probability of liquefaction if they do occur.

Earthquake records for numerical analysis must be appropriate for the structure, the seismic source, and the location at which the records will be applied to the numerical model. Records to represent earthquakes of a particular return period should be selected according to the SA hazard for the critical oscillation period(s) that most affect the behavior of the dam. Therefore, the response spectrum of a suitable 1/10,000-year record would preferably meet the 1/10,000 UHS curve only at the oscillation period of main interest. The CMS is a technique for adjusting the UHS to create a target response spectrum that a suitable ground motion would resemble. The most important period(s) may not be the same as the fundamental period of the embankment, and it may not be obvious what the most important periods are without performing preliminary numerical analyses with different records. The duration of the ground motion must also be realistic for the source, because liquefaction potential and deformation are both more severe with more cycles of shaking. Hazard curves may, therefore, need to be disaggregated into the contributions from different earthquake magnitudes, because magnitude is a good predictor of the number of cycles. Finally, the selected records may need to be numerically deconvolved, so it can be applied to the model at some depth, rather than on an outcropping.

Changes in PSHA results over time reflect the constantly evolving understanding of earthquakes. In the western U.S., measurements and observations of newer earthquakes continually supplement the understanding of earthquake mechanisms and the resulting ground motions. In a similar way, understanding of prehistoric earthquakes is constantly changing, as new faults are discovered and studied. As more earthquakes are recorded with improving instrumentation, GMPEs and attenuation relationships will continue to evolve. Therefore, any given PSHA is considered a "snapshot in time" of the best available information. As new information becomes available, PSHAs may require adjustment to reflect the current state of knowledge.